Ben Mills

AEDC-TR-79-1

Store Separation Testing Techniques at the Arnold Engineering Development Center

Volume II
Description of Captive Trajectory Store Separation Testing in the Aerodynamic Wind Tunnel (4T)

J. B. Carman, Jr., D. W. Hill, Jr., and J. P. Christopher
ARO, Inc.

June 1980

Final Report for Period October 1, 1978 – September 30, 1979

Approved for public release; distribution unlimited.

ARNOLD ENGINEERING DEVELOPMENT CENTER
ARNOLD AIR FORCE STATION, TENNESSEE
AIR FORCE SYSTEMS COMMAND
UNITED STATES AIR FORCE

NOTICES

APPROVAL STATEMENT

This report has been reviewed and approved.

ALVIN R. OBAL, Captain, CF
Project Manager
Directorate of Technology

Approved for publication:

FOR THE COMMANDER

MARION L. LASTER
Director of Technology
Deputy for Operations

REPORT DOCUMENTATION PAGE

READ INSTRUCTIONS BEFORE COMPLETING FORM

1. REPORT NUMBER	AEDC-TR-79-1, Vol. II
2. GOVT ACCESSION NO.	
3. RECIPIENT'S CATALOG NUMBER	
4. TITLE (and Subtitle)	STORE SEPARATION TESTING TECHNIQUES AT THE ARNOLD ENGINEERING DEVELOPMENT CENTER, VOLUME II: DESCRIPTION OF CAPTIVE TRAJECTORY STORE SEPARATION TESTING IN THE AERODYNAMIC WIND TUNNEL (4T)
5. TYPE OF REPORT & PERIOD COVERED	Final Report, Oct. 1, 1978 - Sept. 30, 1979
6. PERFORMING ORG. REPORT NUMBER	
7. AUTHOR(s)	J. B. Carman, Jr., D. W. Hill, Jr., and J. P. Christopher, ARO, Inc., a Sverdrup Corporation Company
8. CONTRACT OR GRANT NUMBER(s)	
9. PERFORMING ORGANIZATION NAME AND ADDRESS	Arnold Engineering Development Center/DOT Air Force Systems Command Arnold Air Force Station, TN 37389
10. PROGRAM ELEMENT, PROJECT, TASK AREA & WORK UNIT NUMBERS	Program Element 65807F
11. CONTROLLING OFFICE NAME AND ADDRESS	Arnold Engineering Development Center/DOS Arnold Air Force Station, TN 37389
12. REPORT DATE	June 1980
13. NUMBER OF PAGES	133
14. MONITORING AGENCY NAME & ADDRESS (if different from Controlling Office)	
15. SECURITY CLASS (of this report)	UNCLASSIFIED
15a. DECLASSIFICATION/DOWNGRADING SCHEDULE	N/A
16. DISTRIBUTION STATEMENT (of this Report)	Approved for public release; distribution unlimited.
17. DISTRIBUTION STATEMENT (of the abstract entered in Block 20, if different from Report)	
18. SUPPLEMENTARY NOTES	Available in Defense Technical Information Center (DTIC).
19. KEY WORDS (Continue on reverse side if necessary and identify by block number)	Aerodynamic Wind Tunnel (4T) captive trajectory applications program CTS systems operation CTS hardware store separation

20. ABSTRACT (Continue on reverse side if necessary and identify by block number)

This report describes the current captive trajectory support (CTS) hardware, systems operation, and the captive trajectory applications program for the Aerodynamic Wind Tunnel (4T). Also included are brief descriptions of additional CTS applications and some guidelines for potential users of the system.

PREFACE

The work reported herein was conducted by the Arnold Engineering Development Center (AEDC), Air Force Systems Command (AFSC), at the request of the AEDC/DOT. The AEDC Project Manager was Mr. A. F. Money. The results of the research were obtained by ARO, Inc., AEDC Division (a Sverdrup Corporation Company), operating contractor for the AEDC, AFSC, Arnold Air Force Station, Tennessee, under ARO Project Number P32E-39D. The manuscript was submitted for publication on December 17, 1979.

This report is the second in a series of four volumes entitled "Store Separation Testing Techniques at the Arnold Engineering Development Center." Subtitles of these volumes are as follows:

Volume I	An Overview
Volume II	Description of Captive Trajectory Store Separation Testing in the Aerodynamic Wind Tunnel (4T)
Volume III	Description and Validation of Captive Trajectory Store Separation Testing in the von Kármán Facility
Volume IV	Description of Dynamic Drop Store Separation Testing

CONTENTS

ILLUSTRATIONS

TABLES

APPENDIXES

Figure | Page

1.0 INTRODUCTION

In the Arnold Engineering Development Center (AEDC) Aerodynamic Wind Tunnel (4T), store separation testing with the Captive Trajectory Support (CTS) mechanism was initiated in 1968. A description of the initial CTS hardware and the separation trajectory applications program are contained in Ref. 1. In the ensuing years, numerous improvements to the operating system and applications program have been implemented as a result of experience accumulated with repeated use of the system. The purpose of this report is to document the current CTS hardware, the systems operation, and the present trajectory applications program. In so doing, this volume will automatically supersede Ref. 1. This document is the second in a series of four volumes which describe store separation capabilities at the AEDC. Volume I gives an overview of the various store separation techniques, Volume III describes store separation testing in the AEDC Supersonic Wind Tunnel (A), and Volume IV covers dynamic drop testing capabilities for all AEDC wind tunnels.

2.0 APPARATUS

2.1 TEST FACILITY

The Aerodynamic Wind Tunnel (4T) is a closed-loop continuous flow, variable density tunnel in which the Mach number can be varied from 0.1 to 1.3 and can be set at discrete Mach numbers of 1.6 and 2.0 by placing nozzle inserts over the permanent sonic nozzle. At all Mach numbers, the stagnation pressure can be varied from 300 to 3,700 psfa. The test section is 4 ft square and 12.5 ft long with perforated, variable porosity (0.5- to 10-percent open) walls. It is completely enclosed in a plenum chamber from which the air can be evacuated, allowing part of the tunnel airflow to be removed through the perforated walls of the test section. A more complete description of the test facility may be found in Ref. 2.

During captive trajectory testing, two separate and independent support systems are used. The Captive Trajectory Support (CTS) and the wind tunnel main pitch sector are used to support the store and aircraft models, respectively. The aircraft model is supported on an adapter sting assembly mounted to the boom of the main pitch sector.

The store model is supported on a sting assembly mounted to the CTS rig. An isometric drawing of a typical store separation installation is shown in Fig. 1, along with a block diagram of the computer control loop used with the CTS. A schematic showing the test section details and the location of typical models in the tunnel is shown in Fig. 2. A photograph showing a CTS test installation with multiple positions of the released store is shown in Fig. 3. Further description of the CTS rig can be found in Ref. 2.

2.2 CAPTIVE TRAJECTORY SUPPORT SYSTEM

2.2.1 General

The CTS is used primarily for the trajectory analysis of air-launched stores as a separation simulator which uses the wind tunnel as a six-degree-of-freedom function generator for the aerodynamic coefficients of the store. The CTS hardware consists of a six-degree-of-freedom store model support with a closed-loop, analog-control positioning system for each degree of freedom and interface equipment to provide communications with the AEDC Propulsion Wind Tunnel Facility (PWT) computer. The CTS model support and positioning systems were designed and built by General Dynamics, Convair Division. The interface hardware and the software required for trajectory generation and data reduction were developed by the AEDC/PWT Instrumentation Branch.

The speed and precision of the CTS position control promote its use for nontrajectory tests also. A sequence of positions can be rapidly traversed with the desired data collected at each point. Typical uses to date are listed below:

1. Grid test: the store model is located at various positions and attitudes relative to the aircraft model; forces and moments are measured, and aerodynamic coefficients are calculated and displayed.
2. Free-air test: the store model, with no aircraft model present, is rotated in pitch, yaw, and/or roll, and data are reduced as in the grid test.
3. Flow-field survey: a pressure probe mounted on the CTS rig is used to map any region of interest.

2.2.2 Store Model Support

The CTS is an electromechanical system with six degrees of freedom. All axes of motion are contained within a single mechanism that is independent of the aircraft model support. Drive motors located in a housing attached to the tunnel structure above the tunnel diffuser are printed circuit armature, d-c electric motors with extremely fast response. The motors will come up to speed in approximately 0.1 sec. The motors for axial and vertical motion are rated at 780 in.-oz of torque at a speed of 1,060 rpm. For pitch, yaw, roll, and transverse horizontal motion, the motors are rated at 120 in.-oz of torque at a maximum speed of 2,750 rpm. The horizontal, pitch, and yaw maximum velocities have been reduced by a factor of ten to minimize overtravel in the event of aircraft-store fouling (see Section 2.2.5). The resulting linear and angular velocities of the six degrees of freedom are as follows:

Component	Velocity
X_R, Axial	1.7 in./sec
Y_R, Horizontal	0.5 in./sec
Z_R, Vertical	1.1 in./sec down,
	2.2 in./sec up
ν_R, Pitch	2.0 deg/sec
η_R, Yaw	2.0 deg/sec
ω_R, Roll	55.0 deg/sec

The axial, vertical, and horizontal motions are accomplished by driving ball screws. The envelope of translation of the support head is ± 15 in. away from the tunnel centerline in the transverse horizontal and vertical directions. The axial range is ± 18 in. from a reference pitch axis location at tunnel station 133.26. Pitch and yaw motions are accomplished by driving the respective gear sector with a conical worm gear located in the head of the support. The maximum angular range of pitch and yaw motion is ±45 deg. Roll motions are accomplished using a roll shaft driven by an eccentric gear reduction drive with a maximum angular motion of ±360 deg. Zero, 3-in., and 6-in. offset roll mechanisms (Fig. 4) are available for test applications. The sting support and balance hardware for nonrolling stings is shown in Fig. 5.

The axial and vertical motors are connected to their respective ball screws by timing belts. Power for transverse horizontal motion, pitch, yaw, and roll is transmitted to the support head by flexible shafts. Position readout for each degree of freedom is accomplished by the use of precision rotary potentiometers which are driven with a minimum gear reduction between the motion gear and the potentiometer.

2.2.3 Position Control

A schematic of the CTS control system is shown in Fig. 1. Signal-conditioning equipment and position control and monitoring equipment are located on the CTS control console shown in Fig. 6. The control console is located in an instrument room adjacent to the tunnel. The position indicators and some of the components of the control panel, except the manual positioning potentiometers and override switches visible in Fig. 6, are duplicated on a panel of the Tunnel 4T Data Production Console (DPC) for monitoring purposes. The DPC panel also contains command switches, Fig. 7, to the computer for initiating and stopping a trajectory and controlling output trajectory data from the computer. In computer-controlled operation, the CTS position command signals are applied to the summing junctions of operational amplifiers, Fig. 1, by digital-to-analog converters (DAC) which are controlled and updated by the computer. For manual operation, the DAC inputs are replaced by potentiometers for manually positioning the CTS. The controllers respond to the difference between commanded and actual rig positions as computed by the operational amplifiers and drive printed-circuit motors through silicon-controlled rectifier (SCR) bridge circuits. Back-emf of the motors, sampled when the SCR bridges are turned off, provides velocity feedback. Motor velocity is proportional to the position error with maximum speed obtained for a 4-percent error. The threshold for movement corresponds to an error signal of less than 0.05 percent. The controllers provide motor overload protection by electronically limiting the drive currents. For any axis, the overall positioning error including effects of rig misalignment, potentiometer nonlinearity, backlash, power supply drift, and other error sources is less than 0.2 percent of full-scale travel.

2.2.4 Computer-CTS System Interface

A general block diagram of the CTS system and computer interface is shown in Fig. 1. A strain-gage balance located inside the store model detects the aerodynamic forces and moments on the model. The resulting force and moment signals are processed by the Digital Data Acquisition System (DDAS). The Digital Multiplexer and Control System computer (DMACS) obtains the tunnel conditions and the six CTS positions. The CTS positions, aerodynamic data, and tunnel conditions are then input to the facility computer which performs the prescribed trajectory calculations and concludes the cycle by transmitting the six new calculated positions to the six respective digital-to-analog converters (DAC). At the conclusion of rig movement, another data cycle is automatically initiated.

2.2.5 System Safety Provisions

For overtravel protection, a dual limit switch is provided in each direction for each degree of freedom. If the first limit is exceeded, a controller safety circuit is activated which applies dynamic braking to stop the motor. This limit can be overridden to return to a safe position. If a backup limit is exceeded, the motor controller power is shut off, and the motor must be manually cranked back into the operating range.

The CTS system is also electrically connected to automatically stop the CTS movement if the store model or CTS contacts the aircraft model, the aircraft support sting, or the test section walls. Television monitors located in the Tunnel 4T instrument room and on the Tunnel 4T control console are used for visual observation during movement of the store to the starting position and during the controlled positioning of the store in the trajectory.

Additional protection is provided by mechanical brakes which are actuated to prevent horizontal, vertical, or axial movement in case of a power failure. Brakes are not required for the other degrees of freedom since the loads are not large enough to overcome the friction of the drive train.

2.2.6 Store Model Alignment System

In Tunnel 4T, the pylons and racks of the aircraft models contain an optical sensor which enables the store model to be accurately positioned at the carriage position. The optical sensor emits infrared radiation and detects the reflected radiation from the store model. The signal of the reflected radiation is inversely proportional to the distance between the store and the sensor. The sensor is sensitive to store positions both vertically and laterally with respect to the pylon surface. In test peculiar cases, the pylons and racks may be instrumented with spring-loaded plungers (touch wires) which are electrically connected to give a visual indication on the DPC and control console when the store model makes contact with the touch wire.

2.2.7 Store Model-Carriage-Positioning Modes

There are four basic operational modes for positioning the store model for initiating a trajectory. Initially, the store is manually positioned offline in its carriage position and the six coordinates (plus aircraft angle of attack) constituting a "touch point" are recorded by the facility computer. The CTS operator located at the DPC selects one of the four operational modes for positioning the store to its initial position.

The first mode allows the store to be positioned from a safekeeping location (nominally 1 in. away, vertically) by making a series of small movements (sting deflection corrections included) as the store model is automatically driven toward the calibrated position by the facility computer. Movement is terminated when the proper signal is sensed by the optical sensor or the touch wire. The second mode of operation is the same as the first except that the store model is moved to the calibrated spatial coordinates rather than to the preselected signal from the optical sensor or touch wire. The third operational mode allows the store model to be moved to its initial position in one motion (including the necessary sting deflections). The fourth and final operational mode allows the CTS operator to manually move the store model to the desired spatial coordinates or carriage position.

3.0 TRAJECTORY GENERATION PROGRAM

3.1 GENERAL

The Tunnel 4T trajectory generation applications program can be divided into three basic blocks: the open-loop service routine job, the CTS rig control job, and the trajectory generation job. The open-loop service routine can be accessed by the data acquisition panel (DAP) operator at many points and contains all the setup and calibration programs necessary for the conduct of the test. These include recording pre- or postrun instrument readings, loading program constants, initiating the summary program, performing various calibrations, performing CTS and balance instrumentation checks, obtaining store model weight tare values, recording model check loading values, and recording touch points.

The CTS rig control job is accessed by the DAP operator primarily in three ways. First, "Initialize Control" is performed; this transfers control of the CTS rig from manual to computer-controlled operation. Once the CTS is in computer control, the "Reset CTS" or "Set CTS to IP" function may be activated by the DAP operator. When the "Reset CTS" function is chosen, the CTS rig is automatically moved from its present location to the station-keeping position, and the desired aircraft model angle of attack is set. When the "Set CTS to IP" function is used, the store model is automatically moved from the station-keeping position to the initial position (normally carriage), accounting for sting deflections under load on both store model position and attitude. The station-keeping position, aircraft model angle of attack, and store model initial position are all described by the selected touch point. After the store initial position is determined to be within allowable tolerances, the closed-loop trajectory generation process (see flow diagram, Fig. 8) is automatically activated. The new CTS coordinates and attitudes, which are generated from the trajectory equations, are set by the closed-loop module of the CTS rig control job. The closed-loop operation will be continued until an internally defined limit is reached or until external termination. The closed-loop process may be paused and then continued or terminated by the DAP operator at any time. When a store ground, balance static limit, balance dynamic limit, emergency stop, or other limit is encountered, an error flag is set which automatically initiates the return to open-loop operation. A detailed description of the CTS mechanism is given in Section 2, and details of the trajectory generation process are contained in Sections 3.2 through 3.7 and Appendixes A through L.

The general composition of the trajectory generation package, as outlined in the flow diagram of Fig. 8, consists of staging/initialization, input processing, full-scale trajectory calculations, integration/extrapolation, output processing, and closed-loop CTS positioning. When wind tunnel aerodynamic data are utilized in the full-scale trajectory calculations, the store model measured forces and moments are reduced to coefficient form and applied with the proper full-scale store dimensions and flight dynamic pressure. The equations of motion allow for six-degrees-of-freedom movement of the released store and are given in Appendix I (see Fig. 9 for definition of the body-axis system). In addition to free motion releases, the equations include provisions for several modes of staged separation, aircraft accelerated flight (Fig. 10), and aircraft dive or bank maneuvers. Assumptions and techniques used in the development of the motion equations are described in Volume I of this series. The full-scale force and moment equations (Appendix H) include terms to account for aerodynamic damping, weight, thrust, ejector forces, static aerodynamic forces, and external input forces. Integration of the accelerations and velocities is accomplished using the Adams-Moulton (predictor-corrector) algorithm with a Runge-Kutta algorithm to start the process.

The modular structure of the program allows for the implementation of new routines that might be required for a specific test (e.g., autopilot simulation) with a minimum of effort. Requirements for the addition of such routines and for standard program utilization are given in Section 5.

3.2 STAGING/INITIALIZATION

The staging process of the trajectory generation package is accomplished in two steps. The first step is executed by a constants point request during open-loop operation. The program assembles an array of 360 constants from previously stored permanent files; performs calculations such as model reference areas and lengths, transfer distances, CTS rig physical parameters, and full-scale initial position coordinates and attitudes; tabulates the constants and calculated parameters; and stores the constants and calculated parameters in a temporary initialization disk file. Details of the assembly process and the calculation equations are contained in Appendix A. The second step of the staging process is executed in the first-pass loop of the trajectory generation job (see Fig. 8) and consists of reading the temporary initialization and CTS rig position files and storing the values in the common array of the closed-loop program.

Initialization of the trajectory generation job is also carried out in the first-pass loop of the closed-loop program. It includes assigning and initializing the integrators, initializing program control flags and counters, and doing once-only calculations. The standard trajectory package uses only 21 of the 50 available integrators, so the remainder may be used in test peculiar applications. The once-only calculation equations are listed in Appendix A.

3.3 INPUT PROCESSING

The primary functions of the input processing job are to acquire the experimental data, define wind tunnel test conditions, calculate the measured aerodynamic coefficient data, determine angular and linear deflections of the model balance/sting combination under load, and manage and update the extrapolation data base. Secondary functions include data acquisition and tunnel conditions validity checks, deflection change limit checks, and critical moment checks on the CTS sting and/or gears. Sequencing of the input processing events is described in the flow diagram of Fig. 8.

The wind tunnel test conditions are calculated using a standard Tunnel 4T data reduction routine. Balance readings are converted into gross forces and moments using a standard PWT six-component balance data reduction program. The equations which are used to calculate the aerodynamic coefficients and sting deflections from the gross forces and moments are given in Appendix B. If differences in sting deflections between succeeding points exceed allowable tolerances (0.05 in. for linear deflections, 0.15 deg for pitch and yaw, and 1.0 deg for roll), subsequent calculations are bypassed and the model is repositioned using the updated deflections. This check was incorporated because model positioning is always based on the sting deflections calculated for the previous loading condition.

For critical moment checks, the model gross forces and moments are resolved into moment loadings about the CTS pitch and yaw gears. If these moments exceed the maximum allowable of 900 in.-lb, the "critical moment" flag is set and the trajectory is terminated by the output processing job before another rig movement is executed. If either the zero or the 6-in. offset roll mechanism is used in the balance/sting combination, a more stringent moment check is required which is described in the Test Facilities Handbook (Ref. 2). CTS sting or gear moment overloads are not often encountered during testing since the static load capacities of most CTS balances are reached well before critical moments would be obtained.

On each pass through input processing, the extrapolated coefficient values are identified and set equal to the current measured values (see Appendix B) so that the final evaluation of the trajectory equations (before data output) is based on measured aerodynamic data. Two files are maintained for extrapolation purposes, and each file contains three values for each of the identified extrapolation parameters. The tunnel data file retains the current and two previously measured values of each parameter and is updated only during input processing such that (typically):

$$\left(C_N\right)_{i-2} = \left(C_N\right)_{i-1}$$

$$\left(C_N\right)_{i-1} = \left(C_N\right)_{i}$$

$$\left(C_N\right)_{i} = C_N$$

Therefore, when fully established, the incremental full-scale time spacing of the tunnel data file corresponds to the program data acquisition time increment (i.e., values are stored at t = 0, 0.5Δt, Δt, 1.5Δt, 2Δt, 3Δt, 4Δt, . . .). These coefficient stacks are used to generate pseudo data in the multiple-pass integration routine (see Section 3.5).

The extrapolator file is updated on each pass through input processing but is also updated by the pseudo data generated in the multiple-pass integration. When fully established, incremental full-scale time spacing of the extrapolator file corresponds to the program integration time increment (i.e., values are stored at t = 0, 0.5δt, δt, 1.5δt, 2δt, 3δt, 4δt . . .). One absolute and two incremental coefficient values are stored such that (typically):

$$\left(\Delta C_N\right)_{i-2} = \left(\Delta C_N\right)_{i-1}$$

$$\left(\Delta C_N\right)_{i-1} = C_{N,x} - \left(C_{N,x}\right)_{i}$$

$$\left(C_{N,x}\right)_{i} = C_{N,x}$$

The incremental coefficient stacks are used for extrapolation in the corrector loop of the integration algorithm. The basic program uses 6 of the 25 available extrapolators; the remainder may be used in test peculiar applications.

3.4 TRAJECTORY CALCULATIONS

3.4.1 General

In the trajectory calculations routine, the sequence of operations is to update the integration parameter buffers, evaluate the trajectory generation equations, and then update the integrator buffers. The trajectory generation equations are divided into functional modules to facilitate handling. The equations and flow diagrams for each of the functional modules are contained in Appendixes C through I. A brief description of each module in the sequence of evaluation is given as follows.

3.4.2 Conversion Module (Appendix C)

Several diverse functions are performed in the conversion module, including assigning the appropriate positions and velocities to the integrator results, defining the inertial-to-body-axis direction cosine matrix, describing the store position and linear velocity with respect to the inertial-axis system origin, and describing the store attitude with respect to the inertial-axis system coordinate directions. The nonrolling sting restraint is implemented in this module when required (see Appendix L for information concerning this restriction). Additional store-related calculations include body-axis weight components, total velocity (with respect to a space-fixed axis system), dynamic pressure at altitude, angle of attack, sideslip angle, and lanyard length.

3.4.3 Offset Coefficient Module (Appendix D)

The purpose of this module is to define any aerodynamic data inputs which are required in addition to the measured aerodynamic coefficients. The standard offset coefficient module allows for constant coefficient inputs (as might typically be used to correct for reduced-scale model asymmetries) and for a ramp axial-force input (to simulate drogue chute deployment). On a test peculiar basis, specialized modules can be routinely substituted for the standard module when more complex offset aerodynamic coefficient inputs are required (e.g., autopilot simulation).

3.4.4 Total Coefficient Module (Appendix E)

This module sums measured, offset, and aerodynamic damping coefficient contributions.

3.4.5 Thrust Module (Appendix F)

The thrust module defines the values of simulated full-scale thrust forces and moments. For the standard module, one or two fifth-degree polynomial curve fits are used to describe the longitudinal thrust force as a function of time. Only longitudinal thrust forces are considered, and moments arise only through jet-damping coefficient contributions. Module options include thrust force simulation with no delay, onset of thrust forces delayed by a time increment, and onset of thrust forces delayed by a lanyard pull followed by a time increment (see Figs. F-1 and F-2). In test peculiar applications, thrust vector control could be included in this module.

3.4.6 Ejector Module (Appendix G)

The ejector module defines the values of simulated full-scale ejector forces and moments. For the standard module, two independent ejector forces may be input using one or two fifth-degree polynomial curve fits for each to describe the forces as functions of time or displacement (see Fig. G-2). Moment contributions are determined from the relationships of the ejector piston locations with respect to the store center of gravity, and duration of ejector action may be defined in terms of either time or displacement. Module options include the following combinations: ejector forces and cutoff = f(t); ejector forces and cutoff = f(displacement); or ejector forces = f(t) with cutoff = f(displacement).

3.4.7 Full-Scale Force and Moment Module (Appendix H)

The full-scale forces and moments resulting from weight, aerodynamic, thrust, and ejector contributions are summed in this module.

3.4.8 Dynamic Equations of Motion Module (Appendix I)

In addition to unrestrained motion, this module allows for the following three basic types of staged separation: pivot motion, rail launch motion, and ejector-plane motion (see Fig. I-3). For pivot and rail motion, the store is initially constrained to rotate about a point other than the center of gravity. For the pivot case, the rotation center is fixed with respect to the aircraft (a typical fuel tank release), while in the rail case, the rotation center (hook) is allowed to translate with respect to the aircraft (a typical missile rail launch). For ejector-plane motion, the store rotates about the center of gravity but is constrained to translate and rotate only in the plane of the ejectors for the duration of ejector action.

The equations of motion for each option are solved to determine the linear and angular body-axis accelerations, the inertial-axis linear velocities, the inertial-to-body-axis direction cosine derivative matrix, and the hook accelerations for staged release. Each of these terms is then assigned to the appropriate integrator input. Additional module output includes reaction forces and moments required to impose the staged separation. Other restrained motion applications could be incorporated for test peculiar requirements.

3.5 INTEGRATION AND EXTRAPOLATION

Integration of the store velocities and accelerations is accomplished using an Adams-Moulton algorithm with a Runge-Kutta start (Ref. 3 and Fig. 11). The Runge-Kutta process requires four evaluations of the trajectory equations over each integration step and is used for the first three integration time increments. Since the first four passes through the integration module using the Runge-Kutta calculations advance time only in half steps, five passes are required to accomplish the first three integration time steps. At the beginning of the fourth integration step, the required derivative history files have been established and the Adams-Moulton procedure is initiated. The Adams-Moulton process is a predictor-corrector method which requires two evaluations of the trajectory equations for each integration time step. Details of both numerical integration procedures are contained in the flow diagram (Fig. 11).

To permit the trajectory calculations in the corrector loop of the integration process to be made independently of data acquisition, extrapolated values of the aerodynamic coefficients are used in the calculations made after time advance (see Fig. 11). The coefficients are extrapolated using a quadratic fit of the form shown in Fig. 12. The different values of the extrapolation equation constants used during passes 4 and 5 result from the initial uneven time spacing of the coefficient values stored in the extrapolator file (see Section 3.3).

A second extrapolation procedure is employed in the program to allow multiple passes through the integration module for each data acquisition cycle (see flow diagrams of Figs. 8 and 13). This permits data acquisition time to remain large (typically, 10 to 20 msec, full-scale time) while integration time is small (typically, 0.5 to 1 msec, full-scale time). As a result, wind tunnel test time required for each trajectory and errors associated with step functions in the integrated parameters (see Section 3.8) can be minimized. The small penalty extracted by the multiple-pass integration (approximately 20 msec computational time per pass through the integrators) is more than adequately compensated by the acquired advantages.

The extrapolator for multiple-pass integration operates on the tunnel data file using a quadratic fit of the form described in the module flow diagram (Fig. 13) and generates pseudo data which are used to update the extrapolator file. The pseudo-data generated by this routine are used in the trajectory calculations and the integration procedure exactly as if they had been measured. The extensive checking at the beginning of the routine is done to insure compatibility with the Runge-Kutta integration and to set the proper time structure of the tunnel data file. Manipulation of extrapolation equations in passes 4 and 5 results from the initial uneven time spacing of the tunnel data file coefficient values (see Section 3.3).

3.6 OUTPUT PROCESSING

The output processing job is executed in two phases. The first phase is initiated immediately after completion of the trajectory calculations which follow input processing; it consists of calculating additional trajectory parameters, storing pertinent trajectory information in a 768-word engineering-unit-data disk file, tabulating hard copy data (optional), displaying selected trajectory parameters on an alphanumeric cathode ray tube screen, and increasing the data cycle/integration time increments as required (see flow diagram, Fig. 14).

The additional calculations are performed just prior to data output to increase program efficiency since these parameters are useful in interpreting trajectory results but are not required in the trajectory generation process. Additional information calculated includes cg displacement and store attitudes relative to the flight, nonrotating flight, pylon, nonrotating pylon, aircraft, and earth axis system coordinate directions; store nose and tail displacement and store attitudes relative to the flight-, nonrotating flight-, pylon-, nonrotating pylon-, aircraft-, and earth-axis system coordinate directions; store nose and tail displacements parallel to the flight- and pylon-axis coordinate directions; hook displacement parallel to the pylon-axis coordinate directions; and aerodynamic coefficients in the stability, wind, and aeroballistic axes. The standard tabulated summary data printout is shown in Table 1, but any of the information stored in the disk file can be tabulated as required.

The flow diagram for the data cycle/integration interval increase module is shown in Fig. 14. Options are to double the data cycle and integration time increments or double the data cycle time increment only when total store displacement (lanyard length) reaches a prescribed value. However, no increase is allowed regardless of the prescribed displacement value until the derivative, extrapolator, and tunnel data history files have been fully established. This option is exercised to speed up the trajectory generation process after the store has reached a position in the flow field where aerodynamic coefficient gradients are not expected to be large. This completes the first phase of output processing, and integration follows (see flow diagram, Fig. 8).

After integration is completed, the second phase of output processing is begun. It includes advancing the data cycle pass counter, checking the critical moment flag (see Section 3.3) and terminating the trajectory if so required, and calculating the store model position coordinates and attitudes which will be executed by the CTS rig. These coordinates are store model cg displacements with respect to the origin of the flight-axis system (see Fig. 10) and angular displacements relative to the free-stream wind vector for a pitch, yaw, roll movement sequence (including corrections for induced angles resulting from vertical and lateral velocities of the store cg, see Fig. 15). The equations are given in Appendix J.

3.7 CTS CLOSED-LOOP POSITIONING

The primary function of the CTS closed-loop positioning module is to locate the store model at the new set of trajectory coordinates and attitudes obtained from output processing. Secondary functions include travel limit, sidewall clearance, and DAP terminate request checks. The equations and flow diagrams for this module are contained in Appendix K.

Positioning of the store model is accomplished using an absolute tunnel coordinate system, the origin of which is described by the midpoint of travel of the CTS linear positions. After the store model is located at the initial position (by the touch job), the carriage coordinates ($X_{TP,o}$, $Y_{TP,o}$, $Z_{TP,o}$) are calculated by the touch job and stored. The same equations as described in Appendix K are used except that the carriage coordinates rather than rig positions are the unknown quanities.

On the first pass through the module, the carriage coordinates and constant box inputs (ΔY_c, ΔZ_c) are read from the touch file. These values remain constant for the duration of the trajectory. The new set of rig angular positions is calculated by substracting sting deflection and sting bend angle contributions from the absolute store attitude. It should be noted that the sting deflection angles used are calculated from the previous aerodynamic load condition, but experience has shown that deflection changes from point to point are normally small. If changes should become large, corrections are made in input processing (see Section 3.3). The new set of rig linear coordinates is determined according to the contributions resulting from CTS rig geometry, linear sting deflections, the new trajectory coordinates, and constant box inputs. The constant box inputs are included in the calculations as a means for correcting air-off carriage coordinates for air-on conditions when a touch sensor is not located at that particular launch station.

If the new CTS linear positions or angular orientations are calculated to be outside the normal operating limits listed below, the trajectory is automatically terminated before a rig movement is executed.

CTS Position Drives	Design Travel Limits	Normal Operational Travel Limits Positive	Normal Operational Travel Limits Negative	Position Tolerances
Axial, in.	±18	16.9	-17.7	±0.05
Horizontal, in.	±15	14.8	-14.7	±0.05
Vertical, in.	±15	14.7	-14.8	±0.05
Pitch, deg	±45	43.0	-44.3	±0.15
Yaw, deg	±45	44.5	-44.1	±0.15
Roll, deg	±360	359.0	-359.0	±1.0

Similarly, if the new position of the store nose is calculated to be within 2 in. of the tunnel wall, the trajectory is aborted.

After the rig movement has been executed, differences between the command and set positions and angles are calculated. If these differences are within allowable tolerances (see preceding table), the trajectory generation process is continued. If not, the rig is repositioned until the tolerance criteria are met.

3.8 VALIDATION

Verification of the trajectory generation applications program was accomplished in four basic steps. The first consisted of thoroughly checking the computer code to insure accuracy and completeness. During the second step, the outputs of the individual program modules were verified, when feasible. During the third phase, trajectory simulations were performed independently of the wind tunnel for verification of the combined equations. The fourth step consisted of incorporation of the trajectory generation package with the wind tunnel and CTS hardware and software systems for total program verification.

Because of the modular structure of the program, a considerable portion of the verification was accomplished during the second step. Of particular importance was the validation of the integration scheme. Even for such relatively extreme motions as rapidly divergent (30-deg motion in 0.1 sec) and short period sinusoidal (15-deg amplitude with 0.3-sec period), errors in the trajectory results derived from the integration algorithm were determined to be at least an order of magnitude less than errors expected from normal input data scatter. As would be expected, the integration algorithm cannot precisely respond to step functions in the accelerations (e.g., ejector cutoff, staged separation termination). For the worst case, step functions effectively increased (or decreased) the integrated parameter values by one-half integration time increment at the point where the step occurred. Therefore, using a small integration time increment in the trajectory calculations (by multiple pass integration, see Section 3.5) can minimize step function effects.

After the preliminary verification was completed, numerous analytical trajectories were calculated to check out the combined trajectory equations. Typical trajectory results are given in Figs. 16 through 20. For simple gravity releases, the motion of the store was identical to exact solutions of the equations of motion (Fig. 16). For the ejector-augmented gravity release (Fig. 16a), the calculated motion differed only slightly from the exact solution because the small integration time increment used (1 msec) minimized the step function effect.

Although exact solutions could not be calculated for comparison with the pivoting and rail-staged separation trajectories because of the complexity of the motion equations, quantitative verification was established (Figs. 17 and 18). Trends in the trajectory data were consistent with the applied restraints, and termination of the staged separations occurred as expected. Identical trajectories could be obtained with equivalent inputs, and mirror image solutions could be accomplished with sign changes on appropriate inputs. The ejector plane restraint was demonstrated to be valid (Fig. 19), and comparisons of trajectory results for the present and Ref. 1 programs were quite good (Fig. 20). Similarly, experimental trajectories from Tunnel 4T and Tunnel A compared favorably (Ref. 4).

4.0 AERODYNAMIC AND FLOW-FIELD GRID TEST APPLICATIONS

Approximately 75 percent of the CTS grid applications program is common to the trajectory applications program. Only a few changes are necessary in the open-loop service routine, and none are required in the rig control job (see Section 3.1). In the closed-loop portion of the program, all trajectory-related calculations are deleted and simply replaced by the grid-positioning algorithm. In addition, when a flow-field probe (Fig. 21) is substituted for the model/balance combination, the aerodynamic coefficient calculations are replaced by the flow angle calculations.

For grid tests, the store model or flow-field probe is positioned in the aircraft flow field (or free stream) at selected locations and orientations which are preprogrammed into the digital computer. The grid matrix can be defined relative to any coordinate system (e.g., flight axis, pylon axis, aircraft axis), and the choice of origin location and positive coordinate directions is arbitrary. Since the grid program was developed primarily for use in aircraft model-related test applications, translational position parameters are normally output in full-scale feet. However, both model-scale and full-scale positions can be made available in other dimensional units.

Aerodynamic grid coefficient data are normally calculated in the body-axis system, but stability-axis, wind-axis, or aeroballistic-axis coefficients can be made available. Interference coefficient values (flow-field aerodynamics minus free-stream aerodynamics) may also be determined by means of an offline data reduction program. Aerodynamic flow angles are calculated relative to the probe axis and the free-stream wind vector. Standard tabulated summary printouts for aerodynamic and flow-field grid data are given in Tables 2 and 3, respectively.

5.0 REQUIREMENTS FOR TESTS USING THE CTS

5.1 MODEL DESIGN CONSIDERATIONS

In addition to normal design requirements, two special considerations are necessary in model design for test programs which utilize the captive trajectory support mechanism.

First, it is imperative that all models be electrically conductive to insure proper operation of the store ground system (see Section 2.2). If this safety system were to be defeated, extensive damage to balance or test hardware could result in the event of a store/aircraft model collision. Second, sting-supported store models should be designed for minimum weight and with the model mass center located near the balance electrical center. This requirement is imposed to alleviate model/balance dynamic loading problems encountered during some test programs.

5.2 TEST CRITERIA

Unless specified otherwise, the values of the trajectory input parameters compiled in this section are required to be constant throughout a trajectory. However, for specific test applications, selected parameters could be reprogrammed as variables if the functional relationships were defined. Values of the following parameters (as required) must be defined in the test planning:

Store Physical Parameters (Trajectory or Aerodynamic Grid)

λ, A, ℓ_1, ℓ_2, ℓ_3, ℓ, X_{cg}, Y_{cg}, Z_{cg}, hook locations

Grid Matrix Information (Aerodynamic or Flow-Field Grid)

Origin Location
Orientations and positive directions of grid coordinates
Orientation of store with respect to grid coordinates
Definition of grid points

Store Mass Properties (Trajectory)

Wt, I_{XX}, I_{XY}, I_{XZ}, I_{YY}, I_{YZ}, I_{ZZ}

Store Aerodynamic Inputs (Trajectory)

C_{ℓ_p}, C_{m_q}, C_{n_r}, $\Delta X_{m,cg}$, $\Delta X_{n,cg}$, additional aerodynamic coefficient inputs ($C_{A,o}$), etc.)

Trajectory Simulation Parameters

h, N_Z, γ, $\phi_{A/C}$

Ejector Simulation Parameters (Trajectory)

X_{FE}, ΔX_{AE}, ω_m, Z_{E1}, Z_{E2}
(F_{E1}, F_{E2}) versus time (stroke)

Thrust Simulation Parameters (Trajectory)

t_D, Z_L, $F_{T,X}$ versus t, C_{jd_ℓ}, C_{jd_m}, C_{jd_n}

Staged Separation Parameters (Trajectory)

X_o, Y_o, Z_o, $X_{P,1}$, $X_{P,2}$, $\Delta\theta_R$, staged separation mode

Initial Conditions (Trajectory)

For trajectories which are initiated at points other than carriage, the initial trajectory time and store initial positions, orientations, linear velocities, and angular velocities must be defined.

Miscellaneous Information (Trajectory)

If lanyard length calculations are required, attachment coordinates of the lanyard to both store and aircraft should be defined.

Autopilot Applications (Trajectory)

The simulation of trajectories with active guidance and control systems requires a mathematical model of the inertial and/or mechanical response of the systems. Since the mechanisms are unique to each missile, no standard programming exists to describe them. However, the standard trajectory program is capable of dealing with the active control situation by calculating incremental aerodynamic coefficients resulting from the control surface deflections. Information required includes a mathematical algorithm describing the control surface movements as functions of missile acceleration, velocity, position, attitude, etc., and the body-axis aerodynamic coefficient variations resulting from the control surface deflections. Since this requires test-unique program additions, at least eight weeks' lead time should be allowed to permit program preparation and checkout. Sample check calculations should be provided, if available.

5.3 NOMENCLATURE UPDATE

Comparison of nomenclature from Volume III of this series and the present report will disclose differences in the engineering symbols for several terms. Since the publication of Volume III, an extensive effort has been initiated at AEDC to standardize nomenclature among the test facilities and among different types of test programs, and differences are generally a result of this effort. Where terminology differences are noted between the two reports, those given in this report will supersede Volume III as the correct notation.

REFERENCES

1. Christopher, J. P. and Carleton, W. E. "Captive-Trajectory Store-Separation System of the AEDC-PWT 4-Foot Transonic Tunnel." AEDC-TR-68-200 (AD839743), September 1968.

2. *Test Facilities Handbook* (Eleventh Edition). "Propulsion Wind Tunnel Facility, Vol. 4." Arnold Engineering Development Center, June 1979.

3. Henrici, Peter. *Discrete Variable Methods in Ordinary Differential Equations.* John Wiley and Sons, Inc., New York, 1964.

4. Hill, D. W., Jr., Best, J. T., and Tolbert, R. H. "Comparison of Store Trajectory and Aerodynamic Loads, and Model Flow-Field Characteristics Obtained in the AEDC PWT/4T and VKF/A Wind Tunnels at Mach Number 1.63." AEDC-TR-78-45 (ADA065137), February 1979.

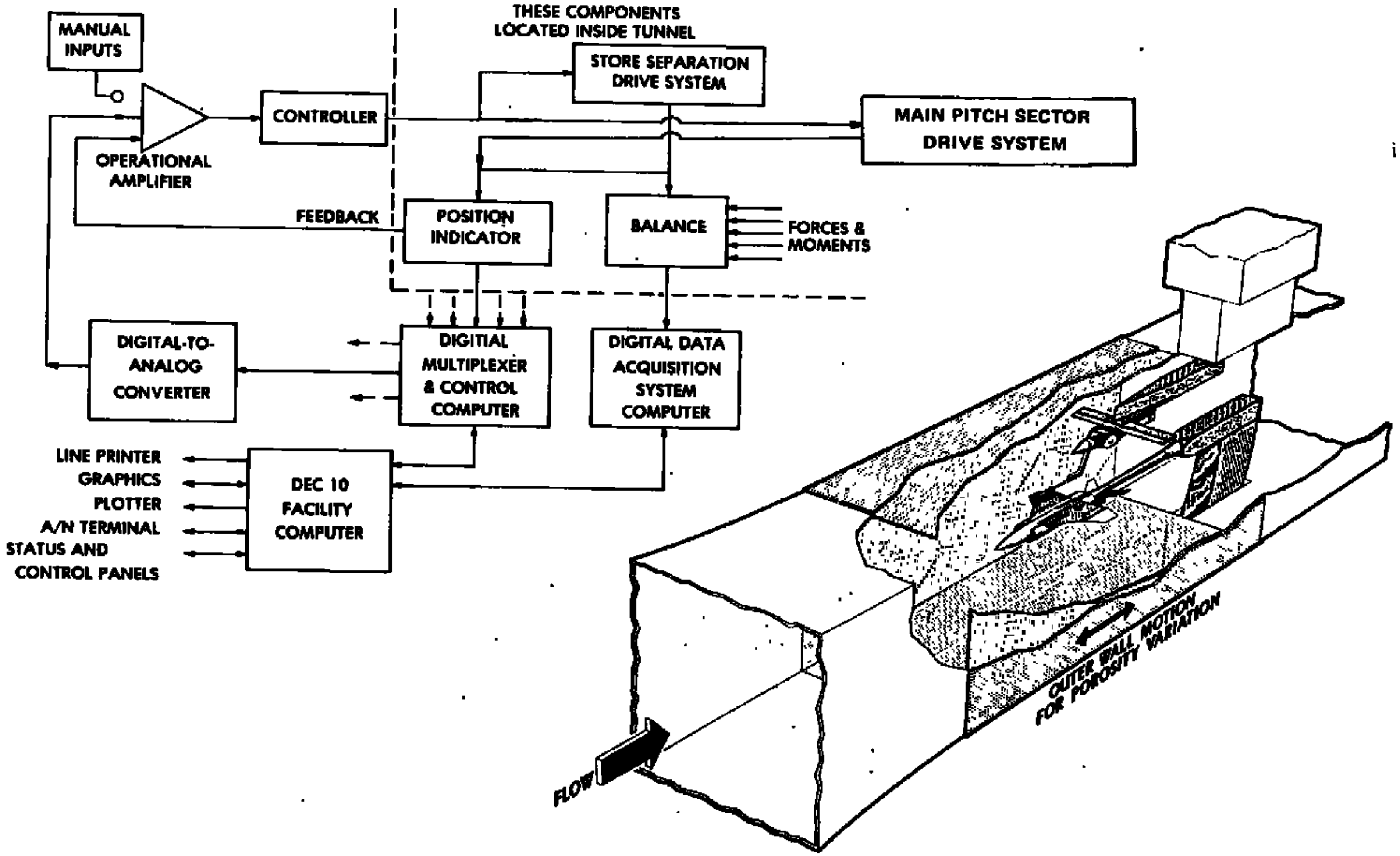

Figure 1. Isometric drawing of a typical store separation installation and a block diagram of the computer control loop.

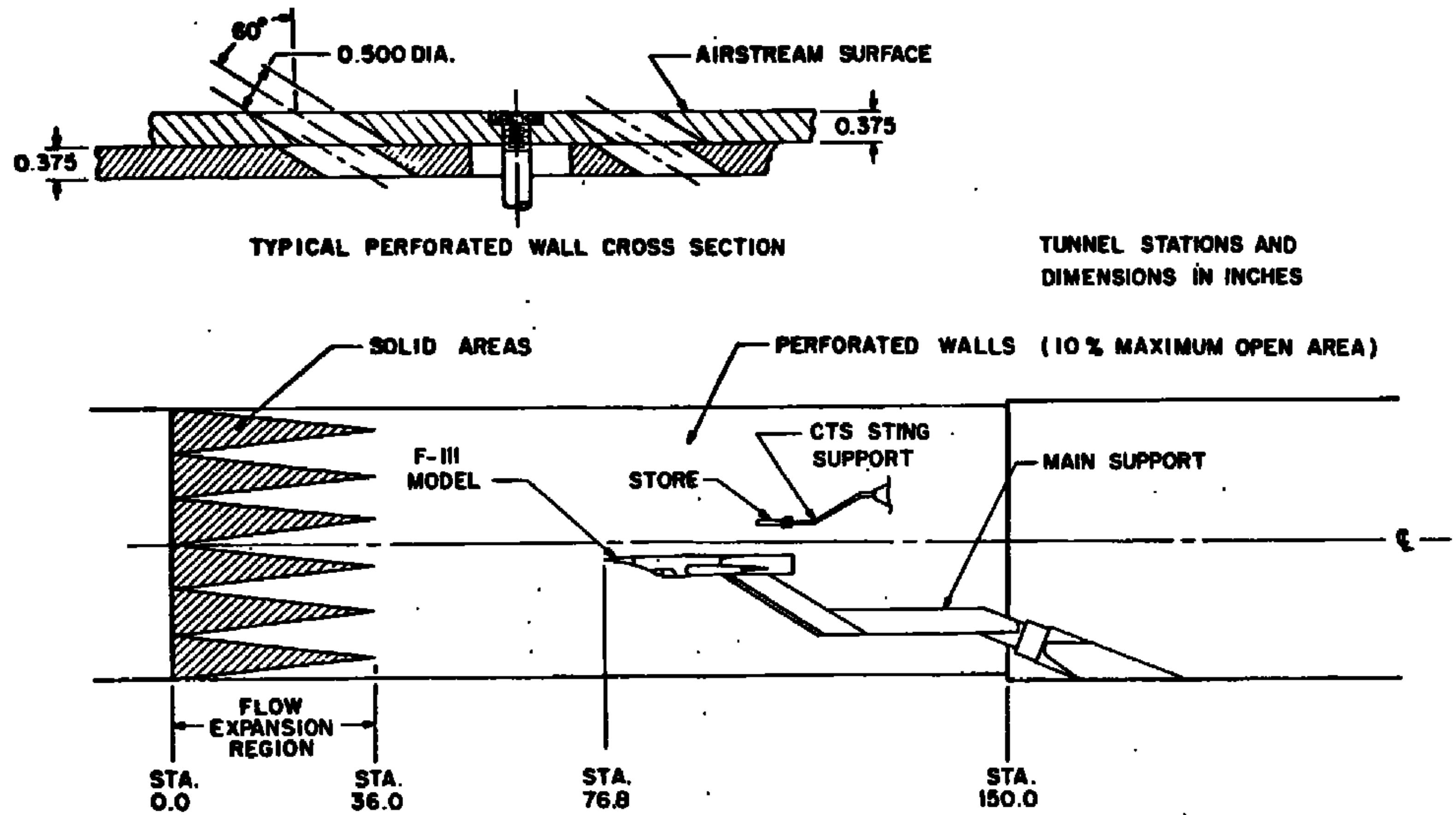

Figure 2. Schematic of the tunnel test section showing typical model locations.

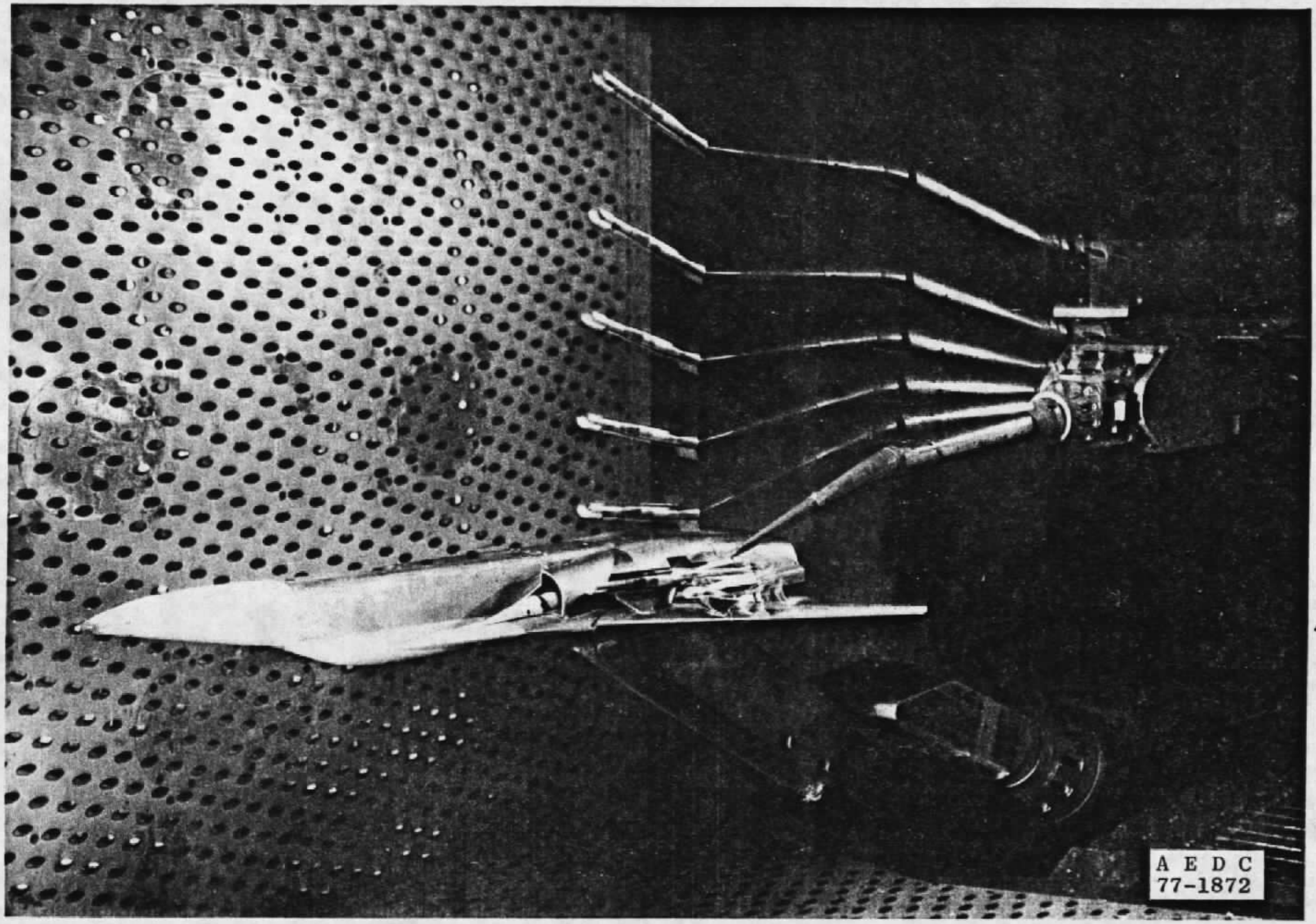

Figure 3. CTS installation photograph showing multiple locations of the released store.

DIMENSIONS IN INCHES

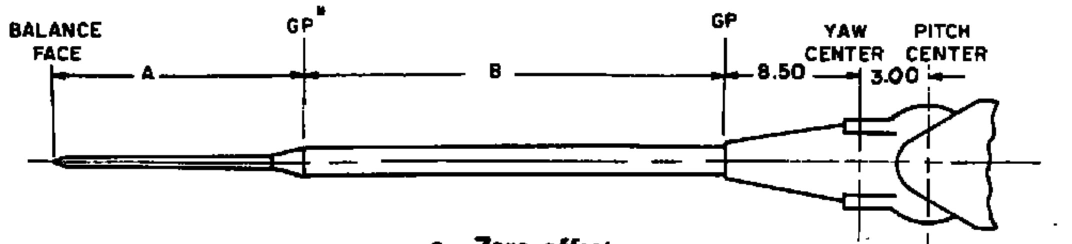

a. Zero offset

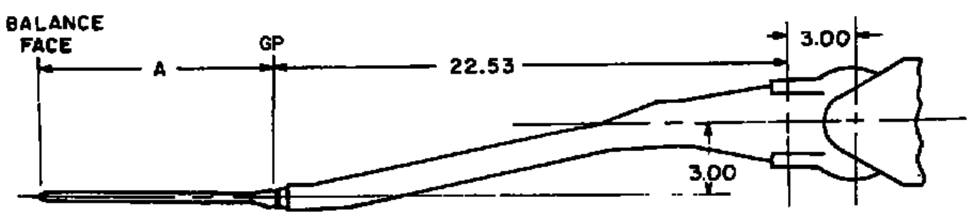

b. 3-in. offset

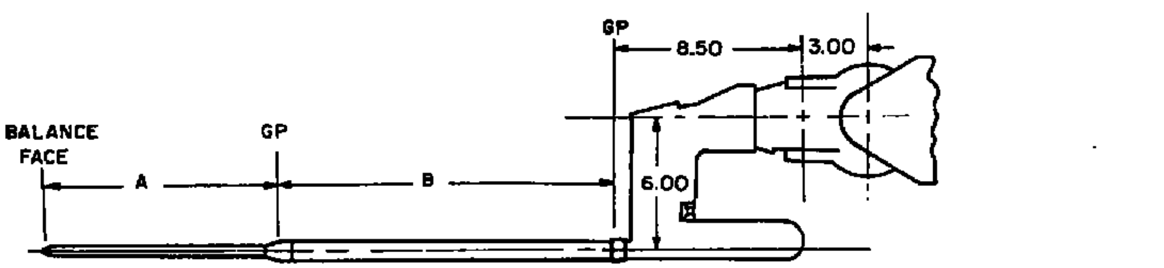

c. 6-in. offset

BALANCE

NAME	NOMENCLATURE	A
0.16" 6.5 lb STRAIGHT BALANCE	5-.16-.0065-.400M	7.98
0.16" 6.5lb SPEC BALANCE	5-.16-.0065-SPEC	11.76**
0.188" 4.0lb SPEC BALANCE	5-.188-.0040-SPEC	11.76**
0.30" 7.2lb SPEC BALANCE	6-.30-.0072-SPEC	7.77**
0.40" 10 lb STRAIGHT BALANCE	6-.40-.010-.40 M	8.03
0.40" 20lb STRAIGHT BALANCE	6-.40-.020-.40M	8.03
0.40" 10lb SPEC BALANCE	6-.40-010-SPEC	9.43**
0.40" 20lb SPEC BALANCE	6-.40-.020-SPEC	9.43**

STING SUPPORT

NAME	NOMENCLATURE	B
8" STRAIGHT EXTENSION	S-.402F-8.00-.402M	8.00
11.25" STRAIGHT EXTENSION	S-.402F-11.25-.402M	11.25
13.50" STRAIGHT EXTENSION	S-.402F-13.50-.402M	13.50

* GP denotes gage point
** Includes spec sting

d. Additional information

Figure 4. CTS roll mechanisms and associated sting/balance hardware.

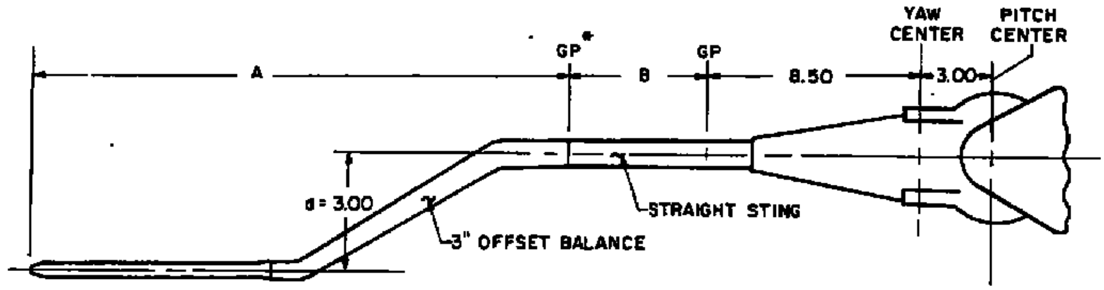

BALANCE INFORMATION

NAME	NOMENCLATURE	A
0.16" 6.5lb OFFSET BALANCE	4-.16-.0065-3" OFFSET-.40 M	16.57
0.40" 10 lb OFFSET BALANCE	5-.40-.010 - 3" OFFSET-.40 M	17.62

FOR STING-SUPPORT INFORMATION (B)
SEE FIGURE 4.

a. Offset balance

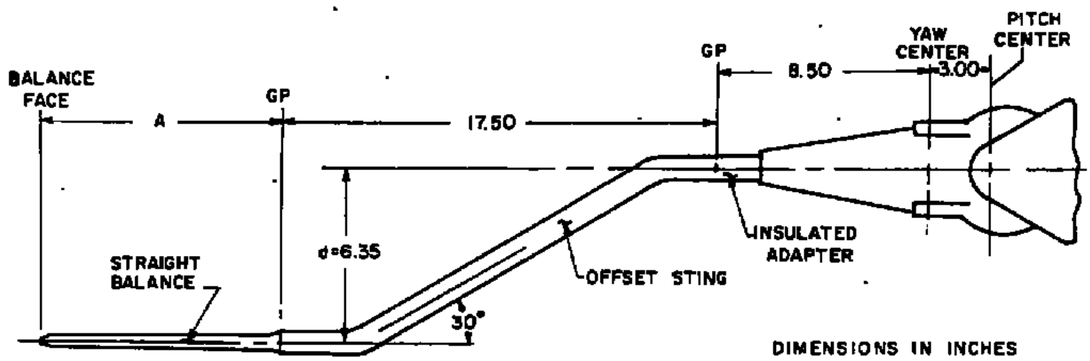

*GP denotes gage point

FOR BALANCE INFORMATION (A)
SEE FIGURE 4.

b. Offset stings

Figure 5. CTS nonrolling sting/balance hardware.

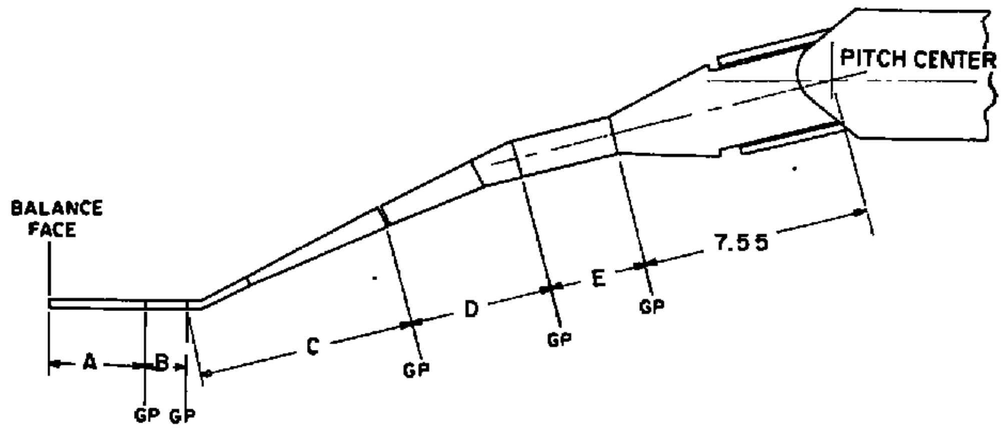

.16" - .30" Balance and CTS Hardware

BALANCES

NAME	NOMENCLATURE	A
.16" 6.5 lb BALANCE	5-.16-.0065-Spec	6.64
.188" 4.0 lb BALANCE	5-.188-.0040-Spec	6.64
.30" 7.2 lb BALANCE	6-.30-.0072-Spec	2.65

SPECIAL STING ADAPTER

NAME	NOMENCLATURE	B
2" ADAPTER	SPA.30SSF-2.00-.30SSF	2.00

BENT SPECIAL STING

NAME	NOMENCLATURE	C
12° BENT STING	BSP.S.-Spec-8.835-12°-.520M	8.58
20° BENT STING	BSP.S.-Spec-8.751-20°-.520M	8.52
27° BENT STING	BSP.S.-Spec-8.765-27°-.520M	8.43

.40" Balance and CTS Hardware

BALANCES

NAME	NOMENCLATURE	A
.40" 10 lb BALANCE	6-.40-.010-Spec	3.76
.40" 20 lb BALANCE	6-.40-.020-Spec	3.76

SPECIAL STING ADAPTER

NAME	NOMENCLATURE	B
2" ADAPTER	SPA.40SSF-2.00-.40SSF	2.00
3.5" ADAPTER	SPA.40SSF-3.50-.40SSF	3.50

BENT SPECIAL ADAPTER

NAME	NOMENCLATURE	C
12° BENT STING	BSP.S.-Spec-9.30-12°-.520M	8.95
20° BENT STING	BSP.S.-Spec-9.23-20°-.520M	8.87
27° BENT STING	BSP.S-Spec-9.14-27°-.520M	8.77

BENT STING ADAPTER

NAME	NOMENCLATURE	D
12° ADAPTER	BSA-.520F-5.125-12°9'-1.120M	4.38

CTS ADAPTER

NAME	NOMENCLATURE	E
3.5" ADAPTER	SA-1.120F-3.50-1.120M	3.50
10.0" ADAPTER	S-1.120F-10.00-1.120M	10.00

c. Modular stings & balances
Figure 5. Concluded.

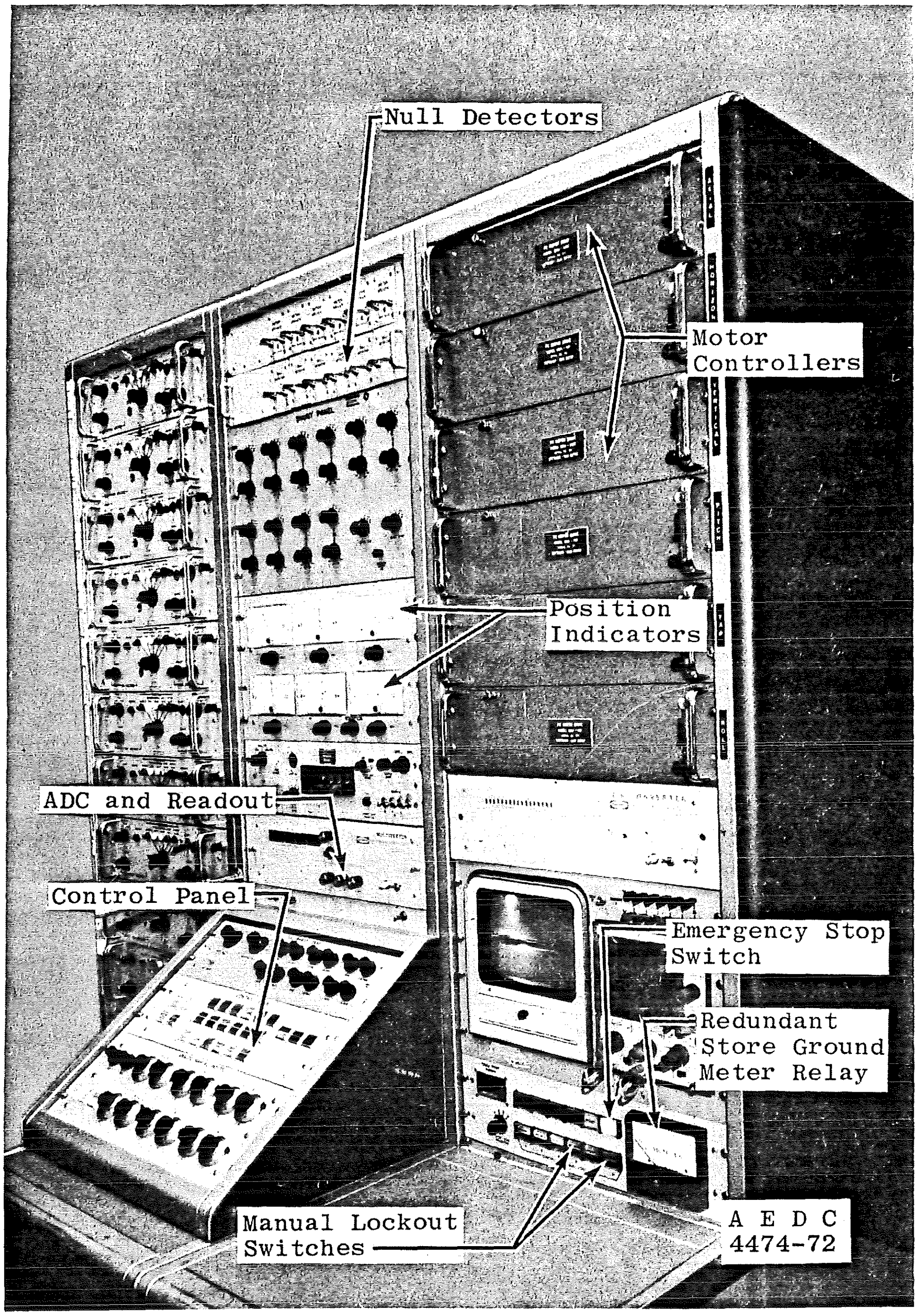

a. Control console components
Figure 6. Photographs of the CTS control console.

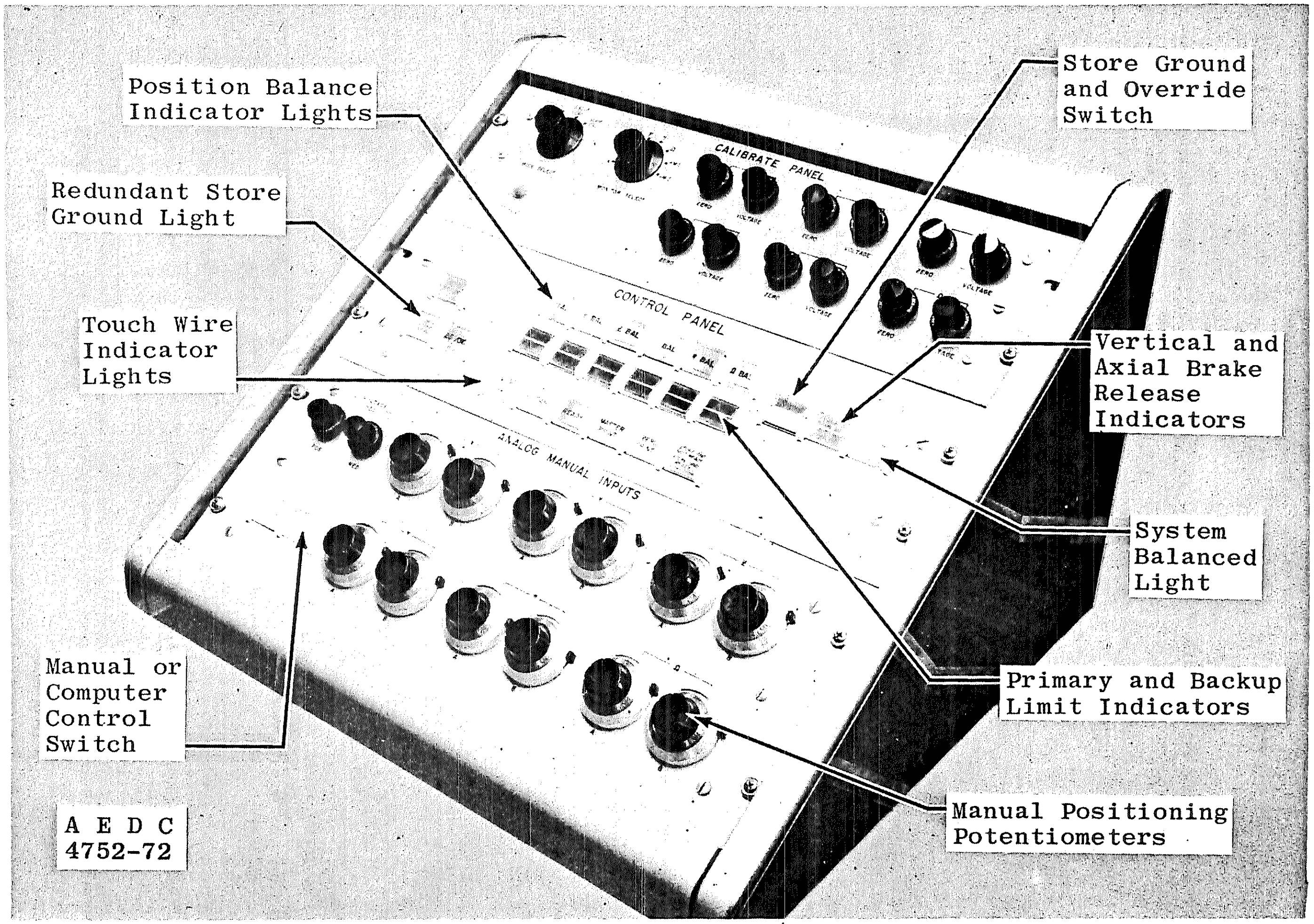

b. Control panel components
Figure 6. Concluded.

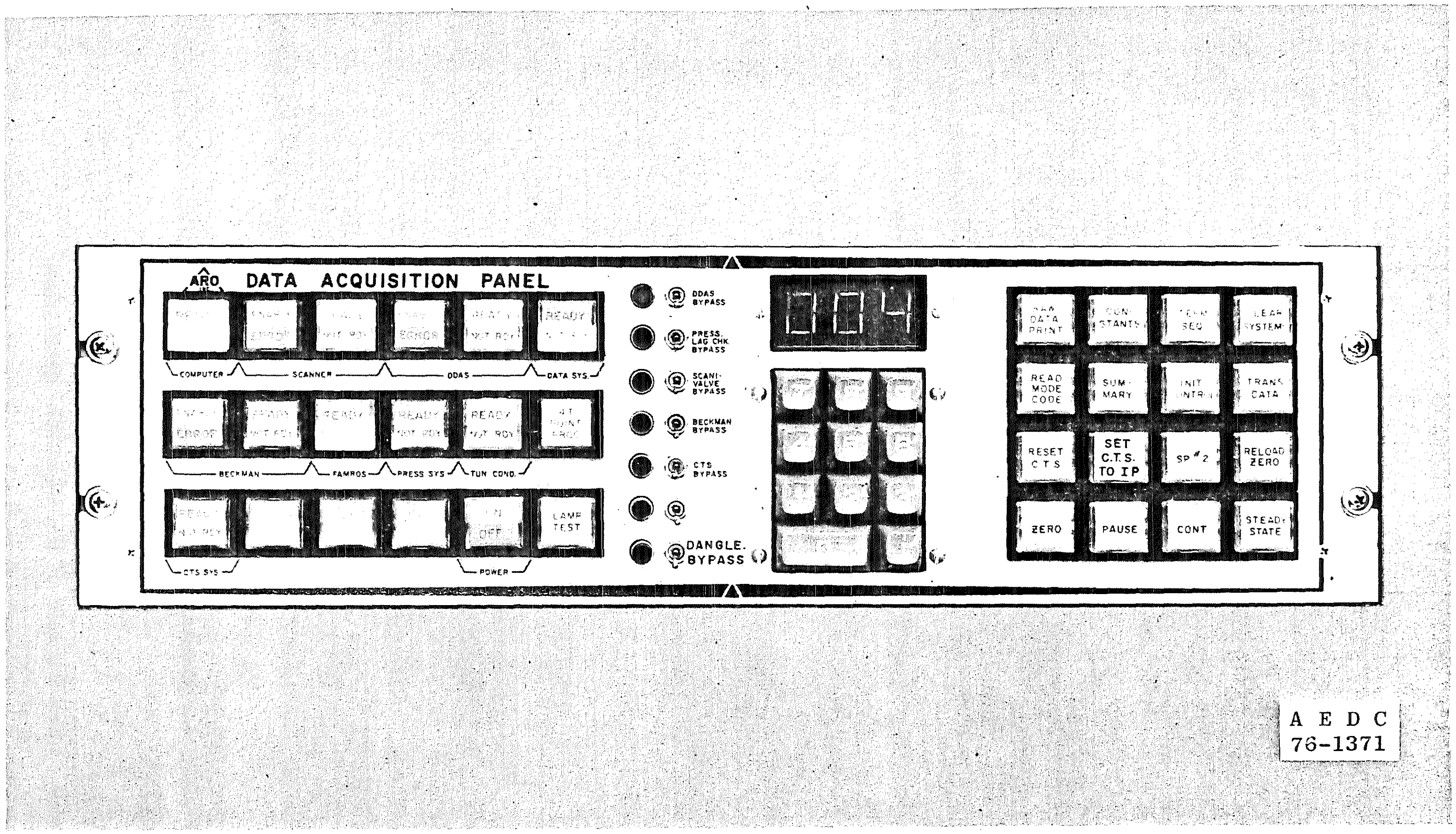

Figure 7. Photograph of the data acquisition panel (DAP) located on the tunnel 4T data production console (DPC).

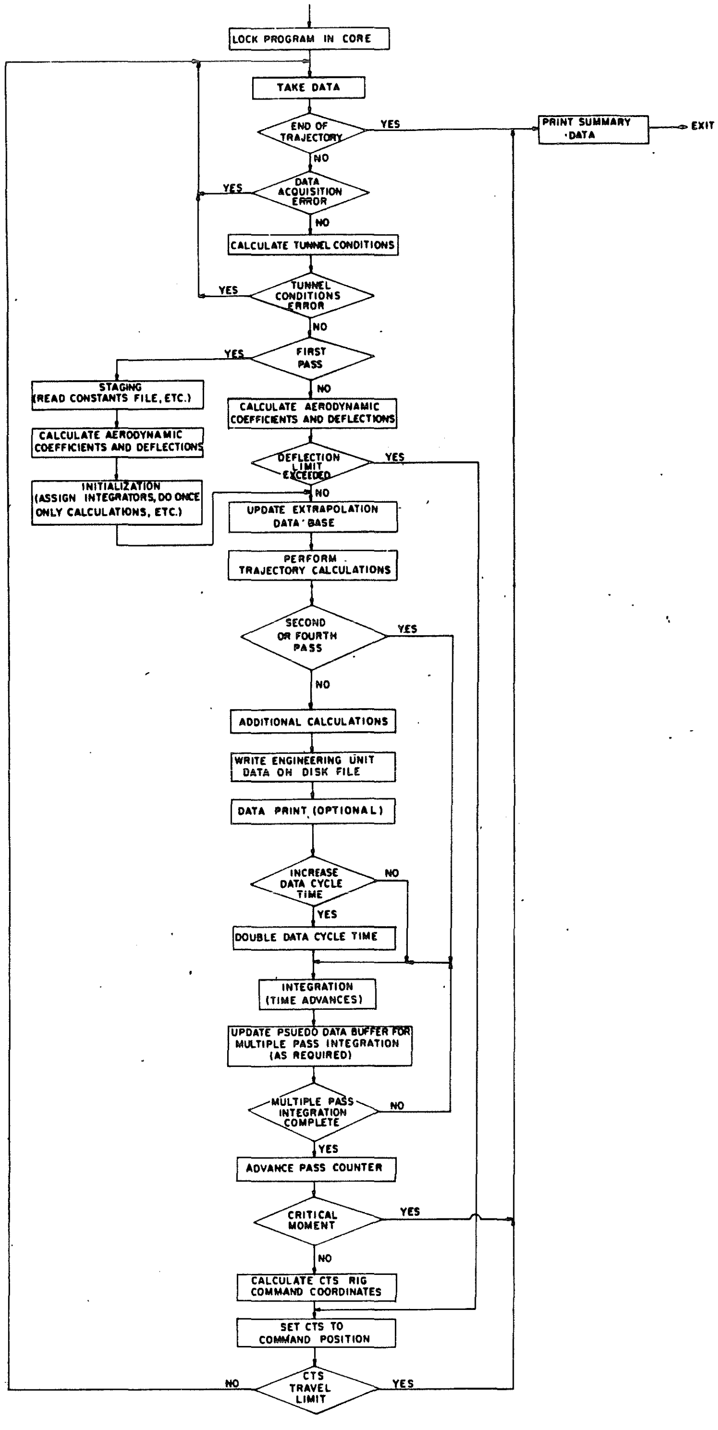

Figure 8. Flow diagram of the trajectory generation closed-loop program.

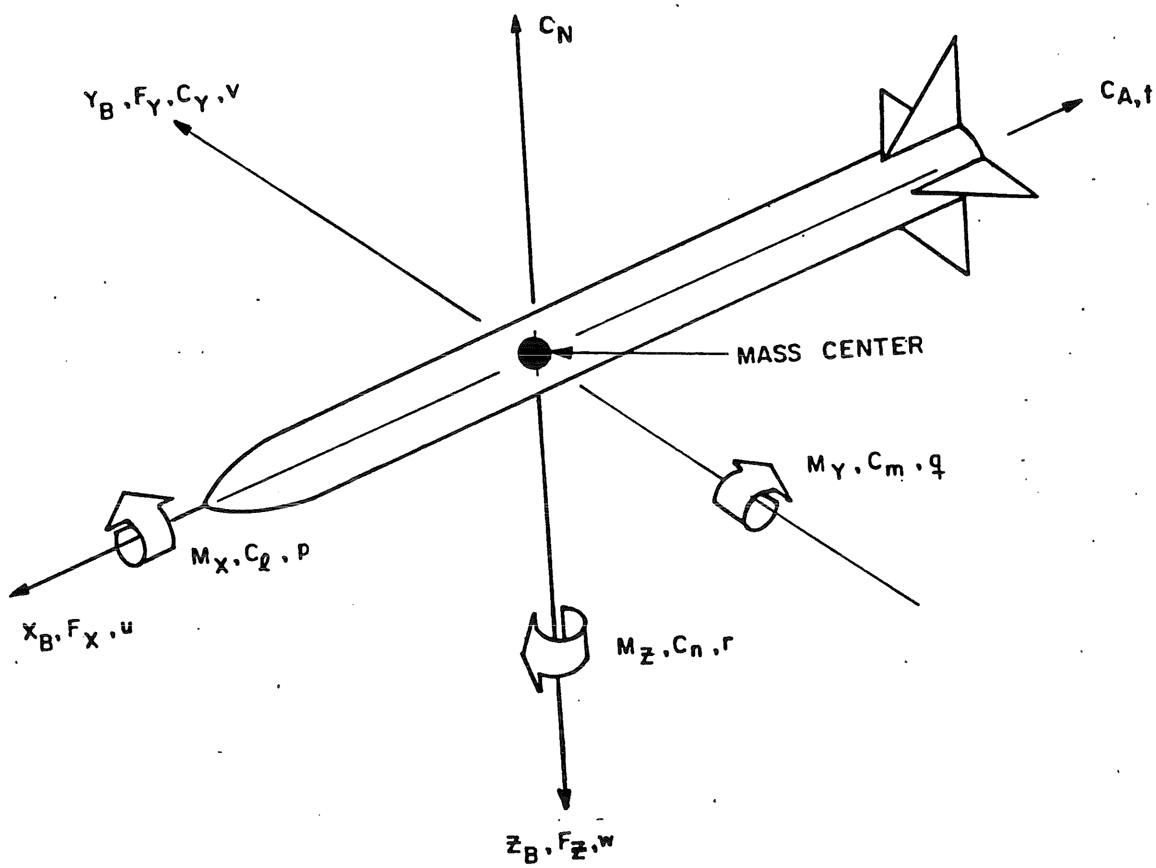

Figure 9. Positive directions for the body-axis coordinate system.

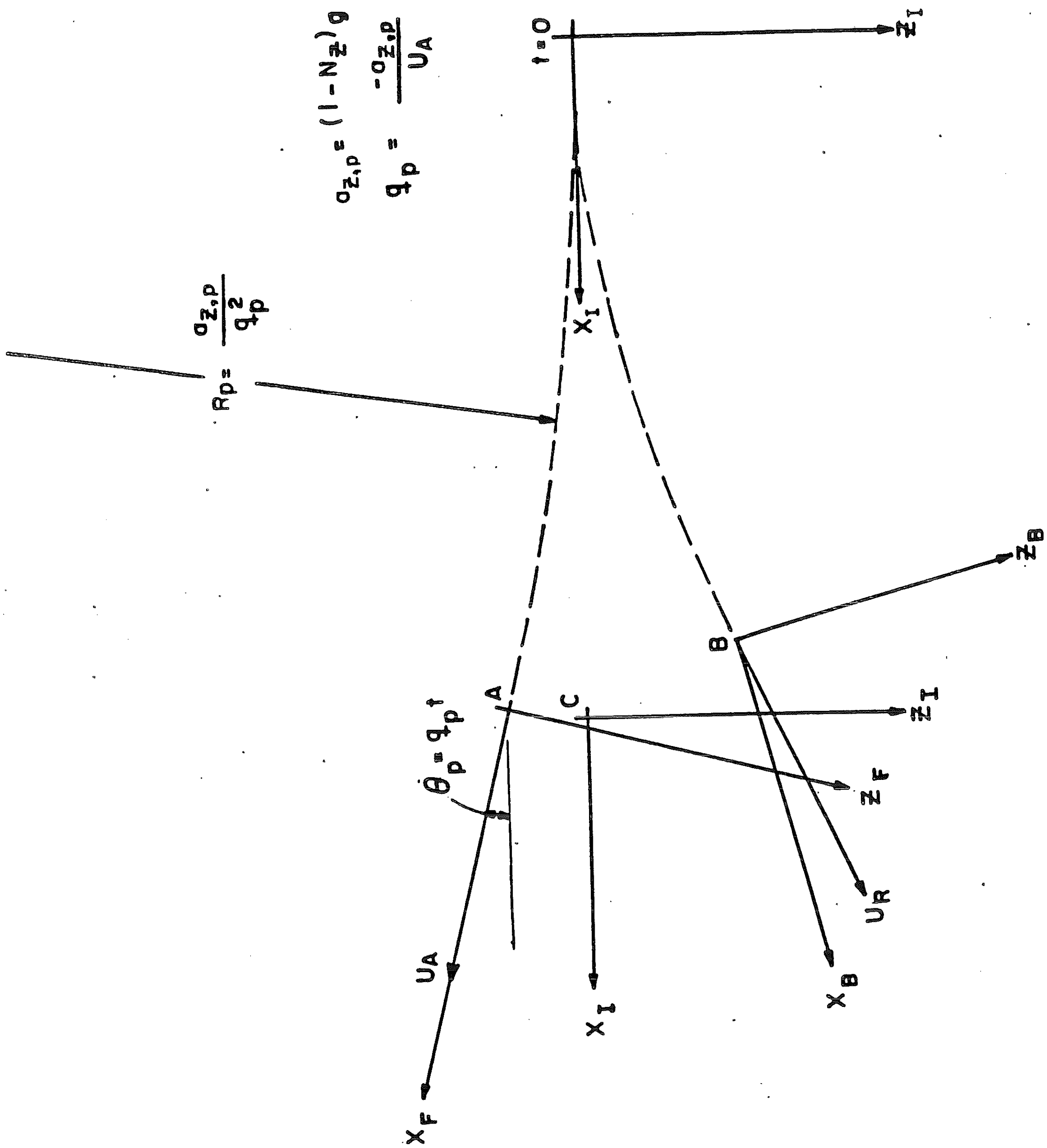

Figure 10. Body/inertial/flight-axes directions for an aircraft pullup/pushover maneuver.

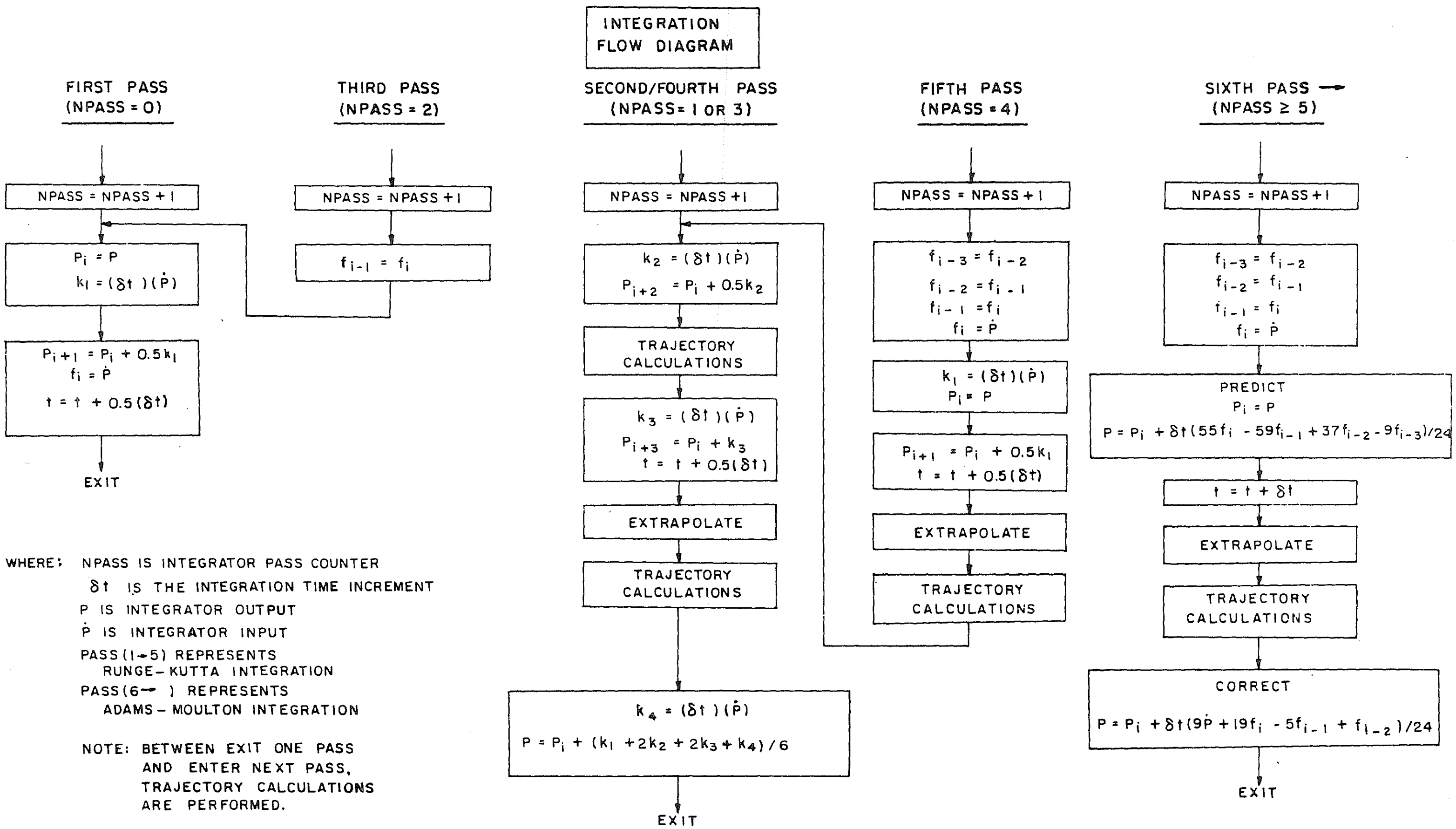

Figure 11. Flow diagram for the integration module.

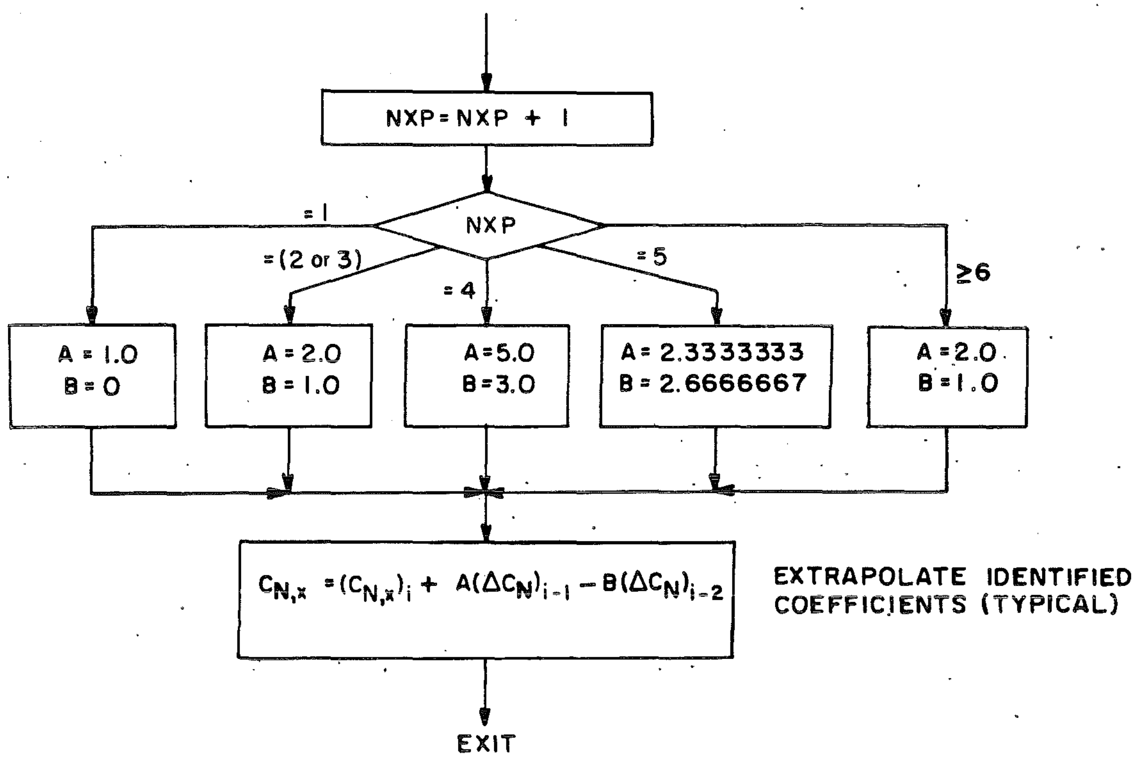

NOTE: NXP IS THE EXTRAPOLATOR PASS COUNTER

Figure 12. Flow diagram of the quadratic extrapolation routine.

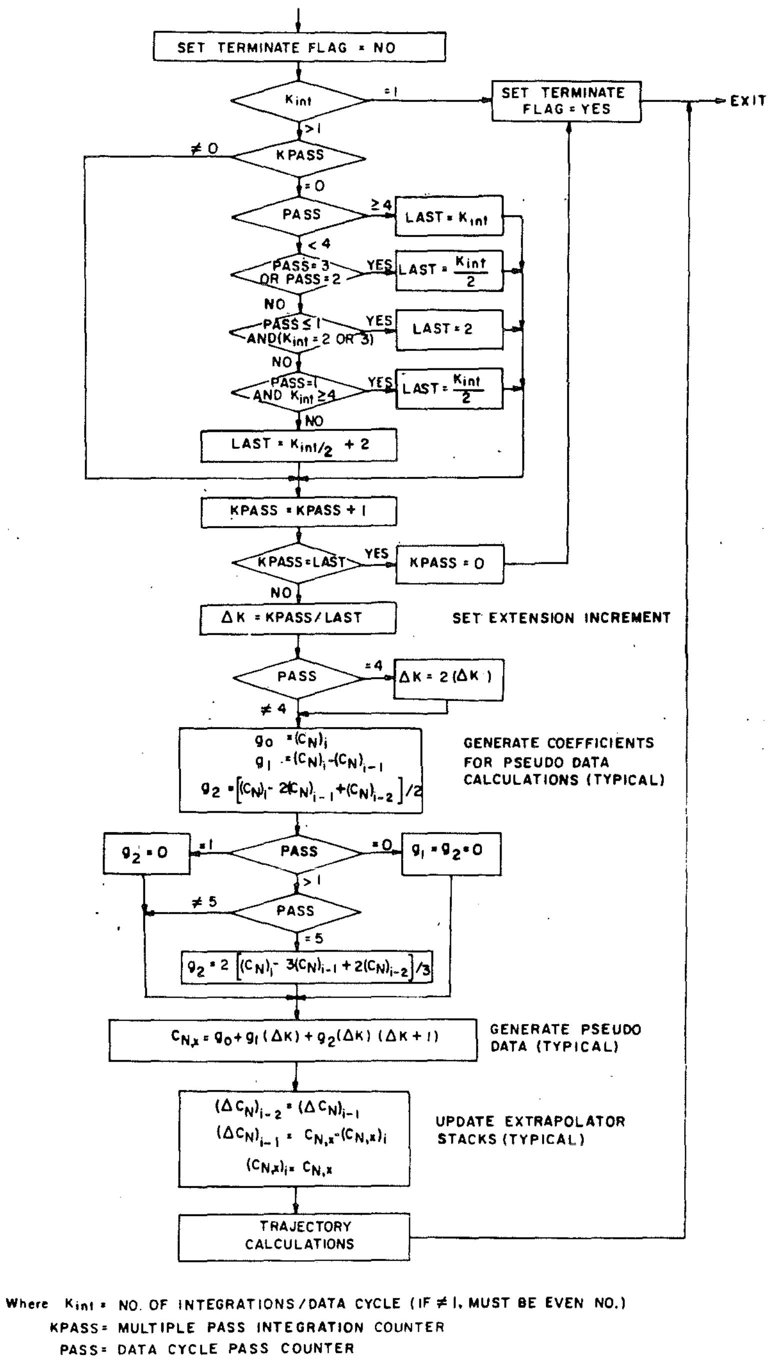

Figure 13. Flow diagram for the pseudo data generation module.

STEP	OPTIONS
0	NO INCREASE
1	DOUBLE DATA CYCLE AND INTEGRATION TIME INCREMENT FOR $z_{L,C} \geq z_{STEP}$
2	DOUBLE DATA CYCLE TIME INCREMENT FOR $z_{L,C} \geq z_{STEP}$

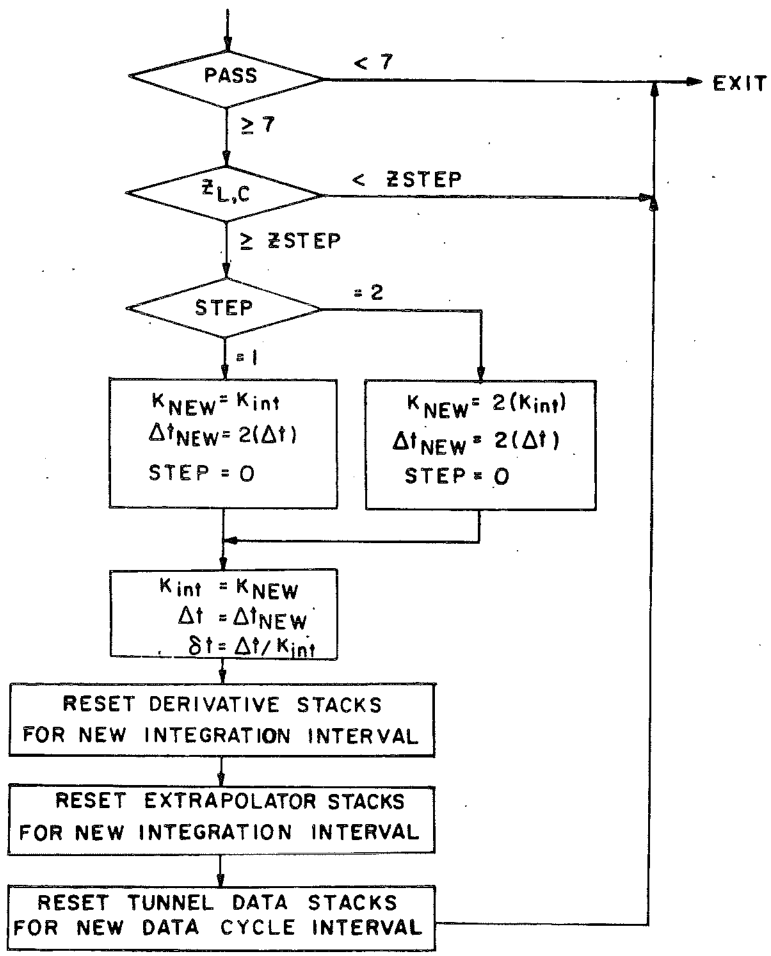

NOTE: NO INCREASE ALLOWED UNTIL THE DERIVATIVE, EXTRAPOLATOR, AND TUNNEL DATA STACKS HAVE BEEN FULLY ESTABLISHED AT EVEN TIME INCREMENTS

Figure 14. Flow diagram for the data cycle/integration interval increase module.

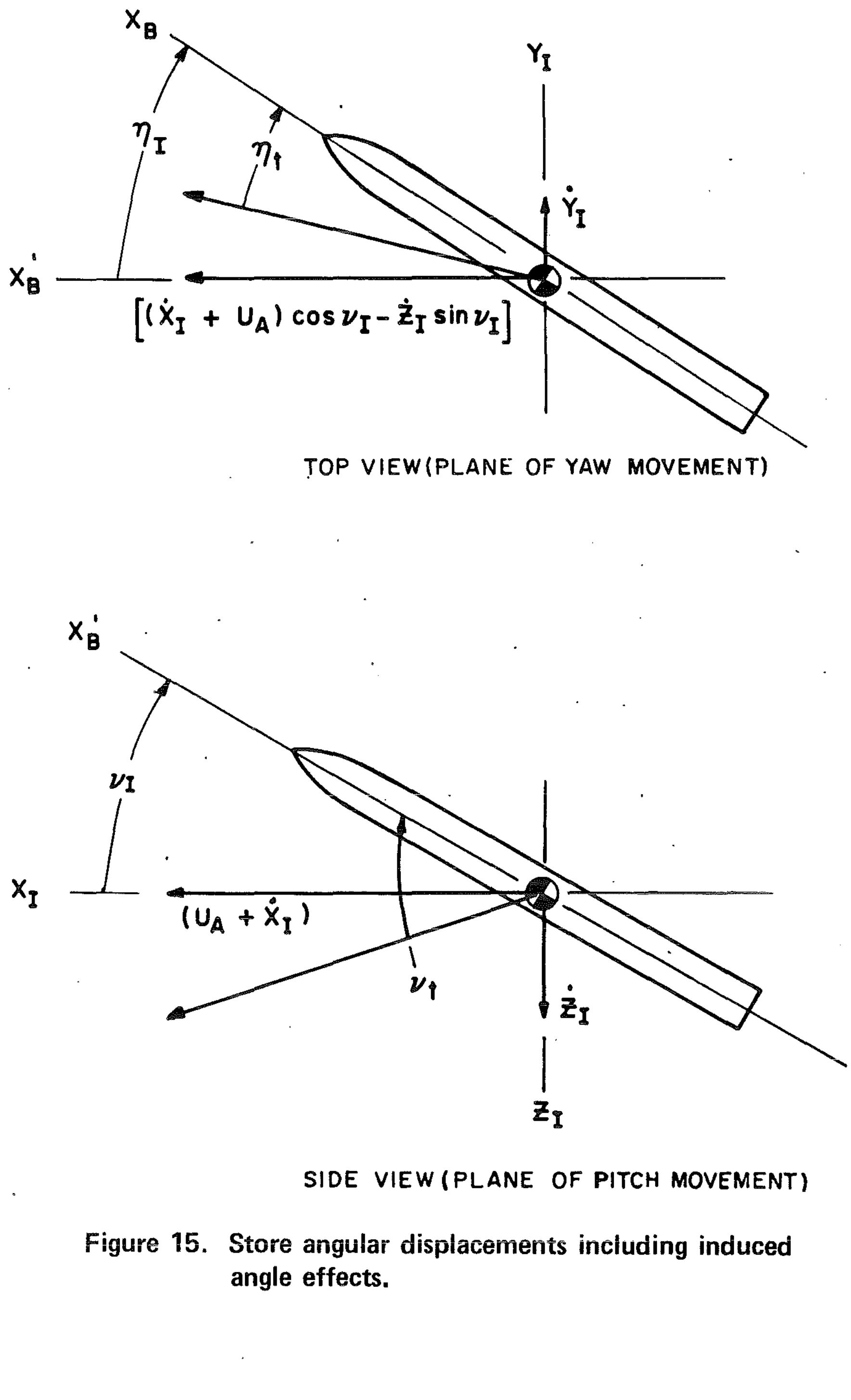

Figure 15. Store angular displacements including induced angle effects.

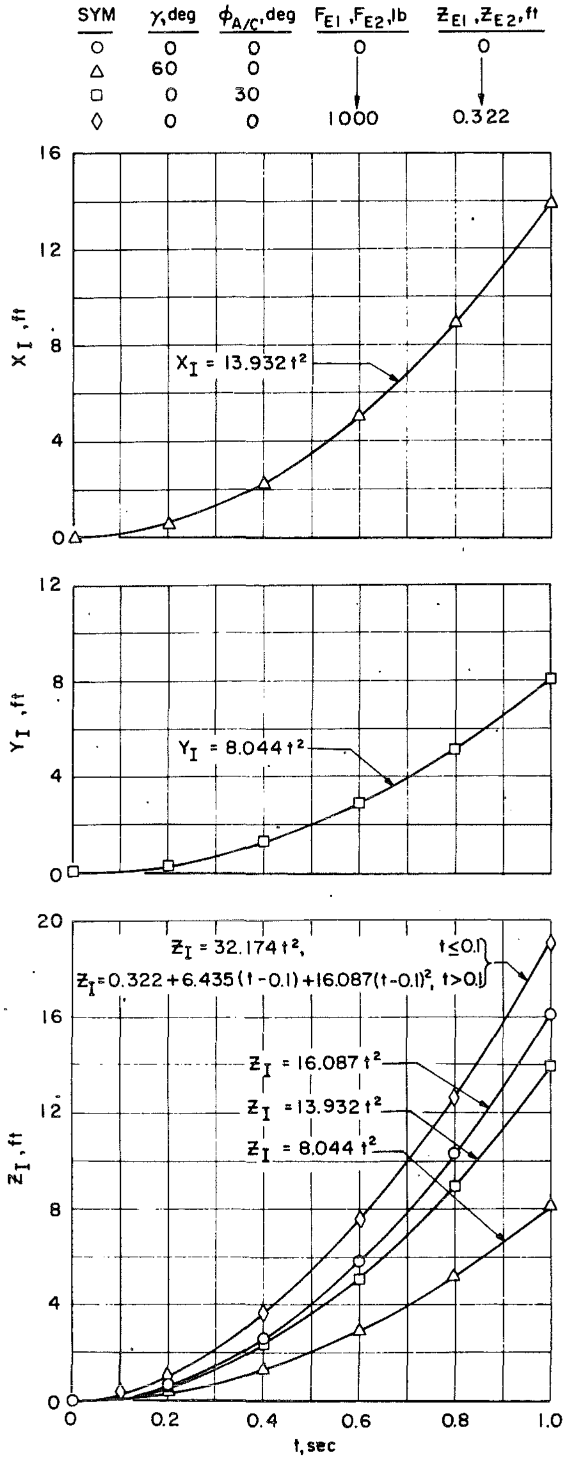

a. Linear displacements

Figure 16. Comparison of trajectory results for a free-falling store with exact solutions, Wt = 2,000 lb.

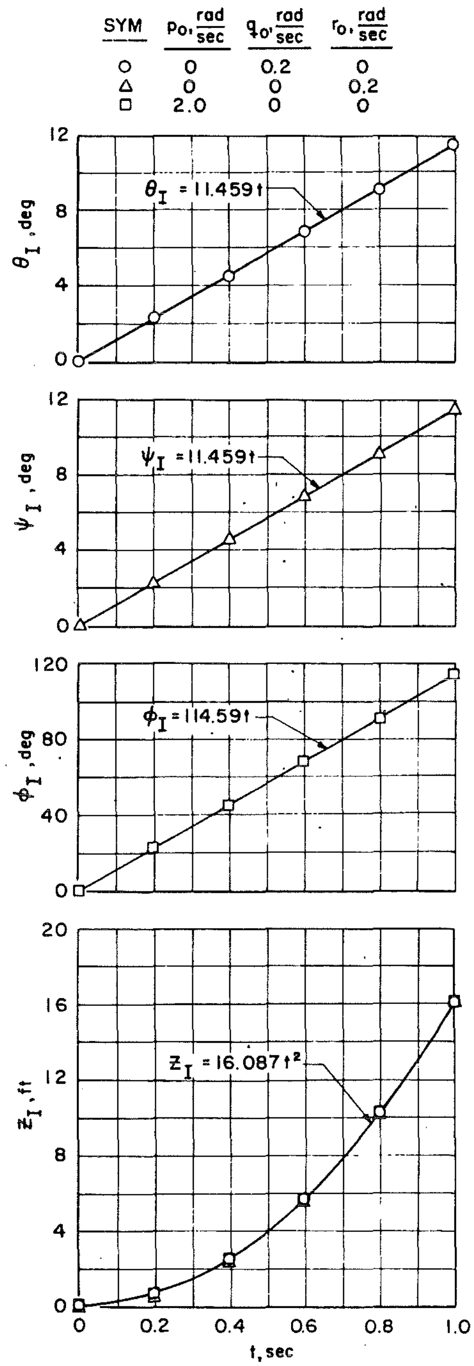

b. Angular displacements
Figure 16. Concluded.

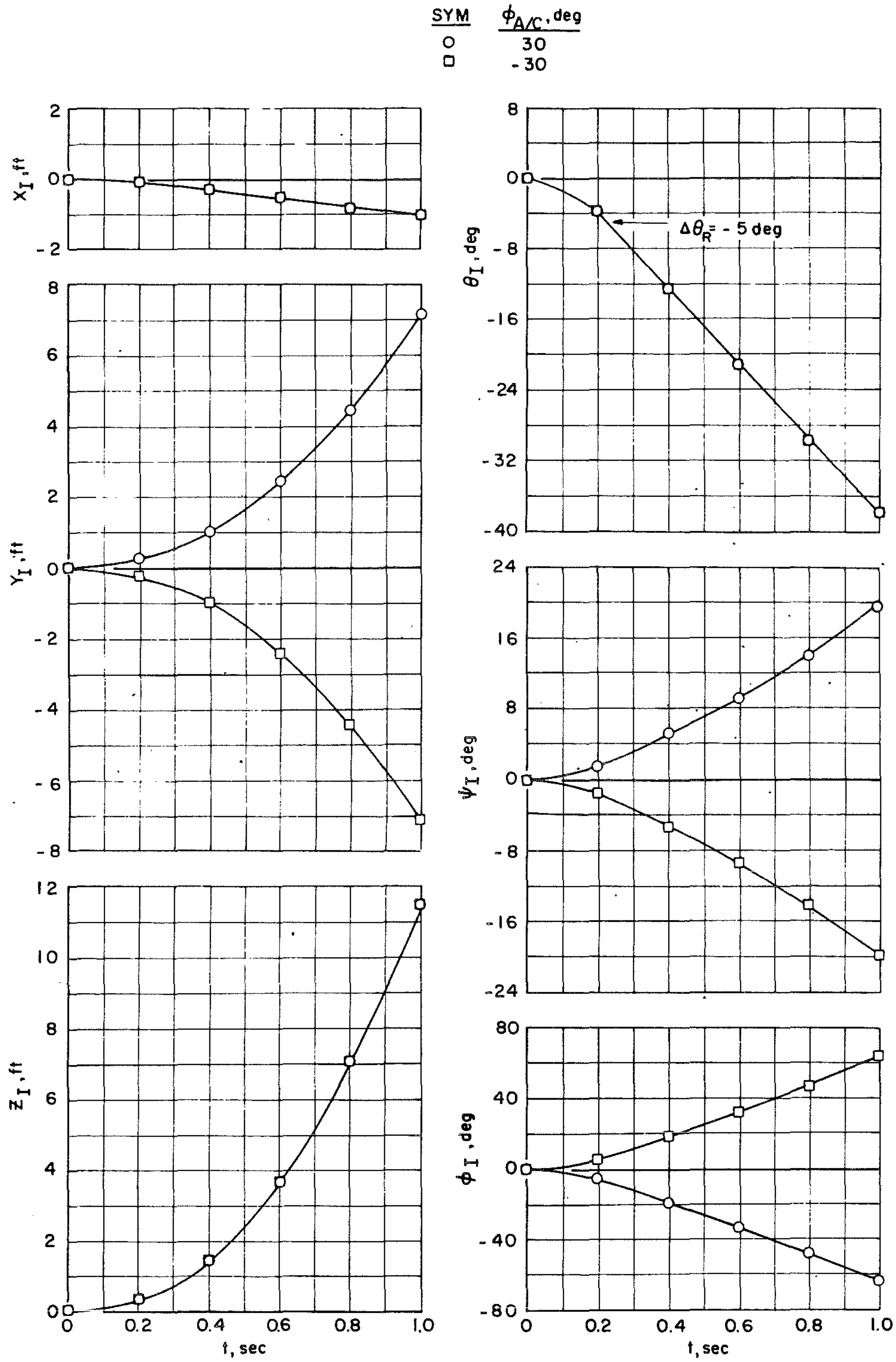

Figure 17. Trajectory results for pivot staged separation, MOTION = 3, Wt = 2,000 lb, γ = 60 deg, X_o = 5 ft, Z_o = 1 ft, Y_o = 0.

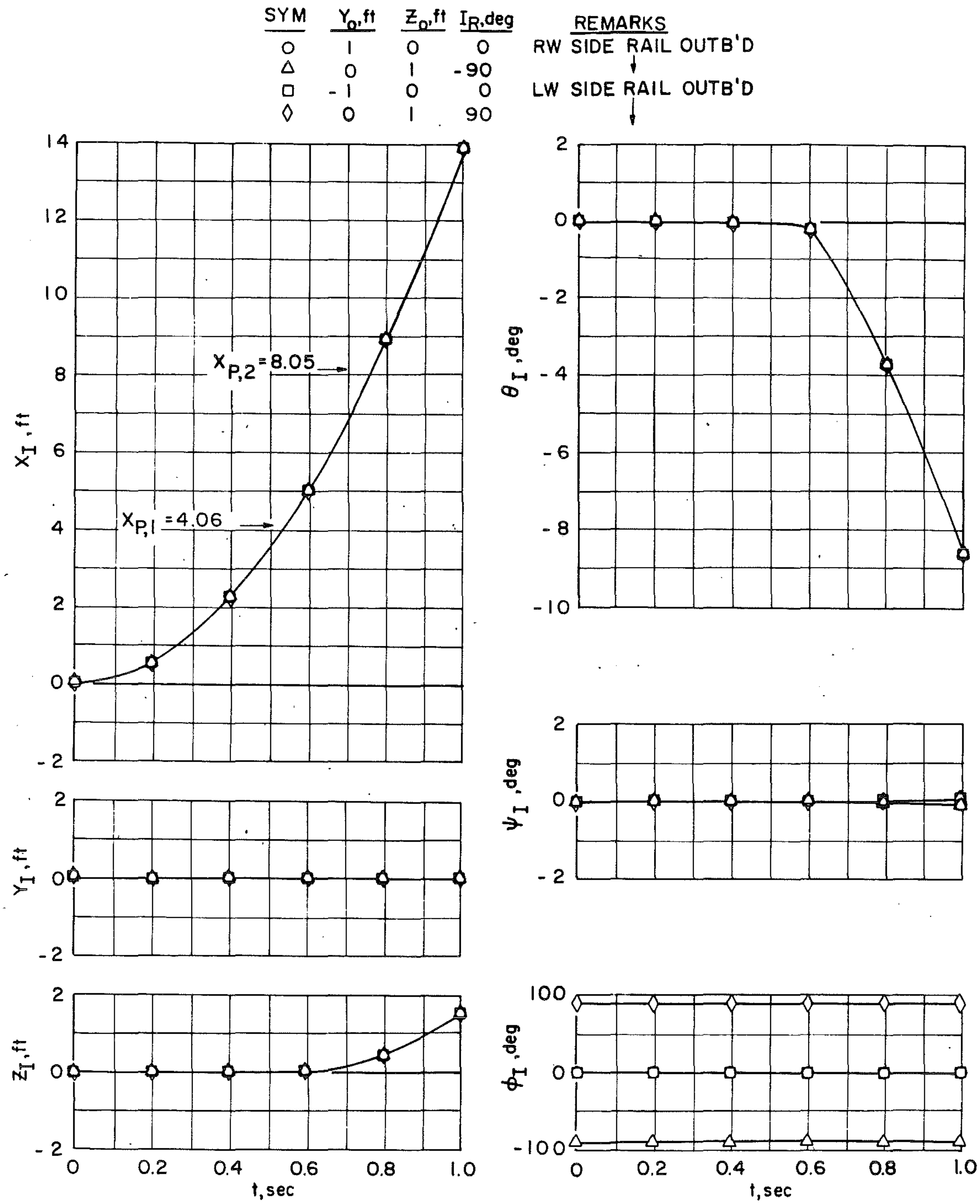

Figure 18. Trajectory results for rail-released staged separation, MOTION = 7, Wt = 2,000 lb, γ = 60 deg, X_o = 5 ft.

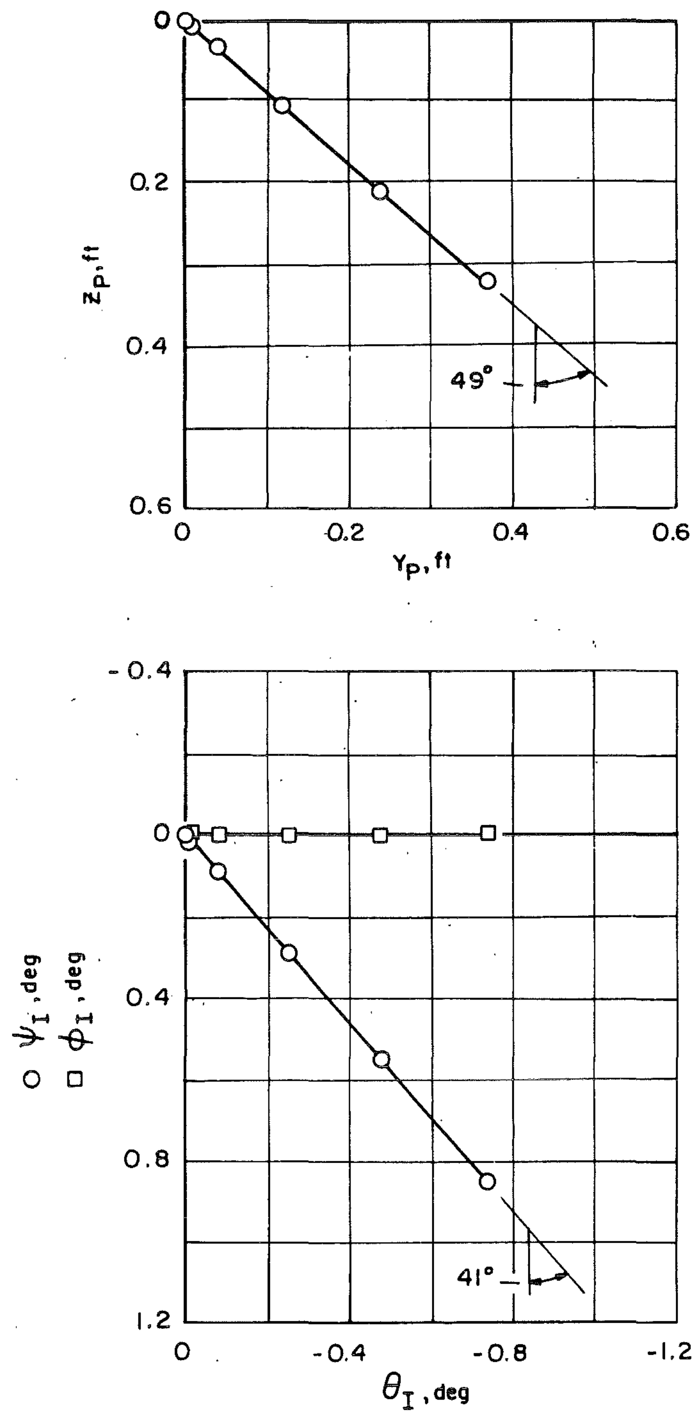

Figure 19. Trajectory results for ejector-plane staged separation, ω_m = 49 deg.

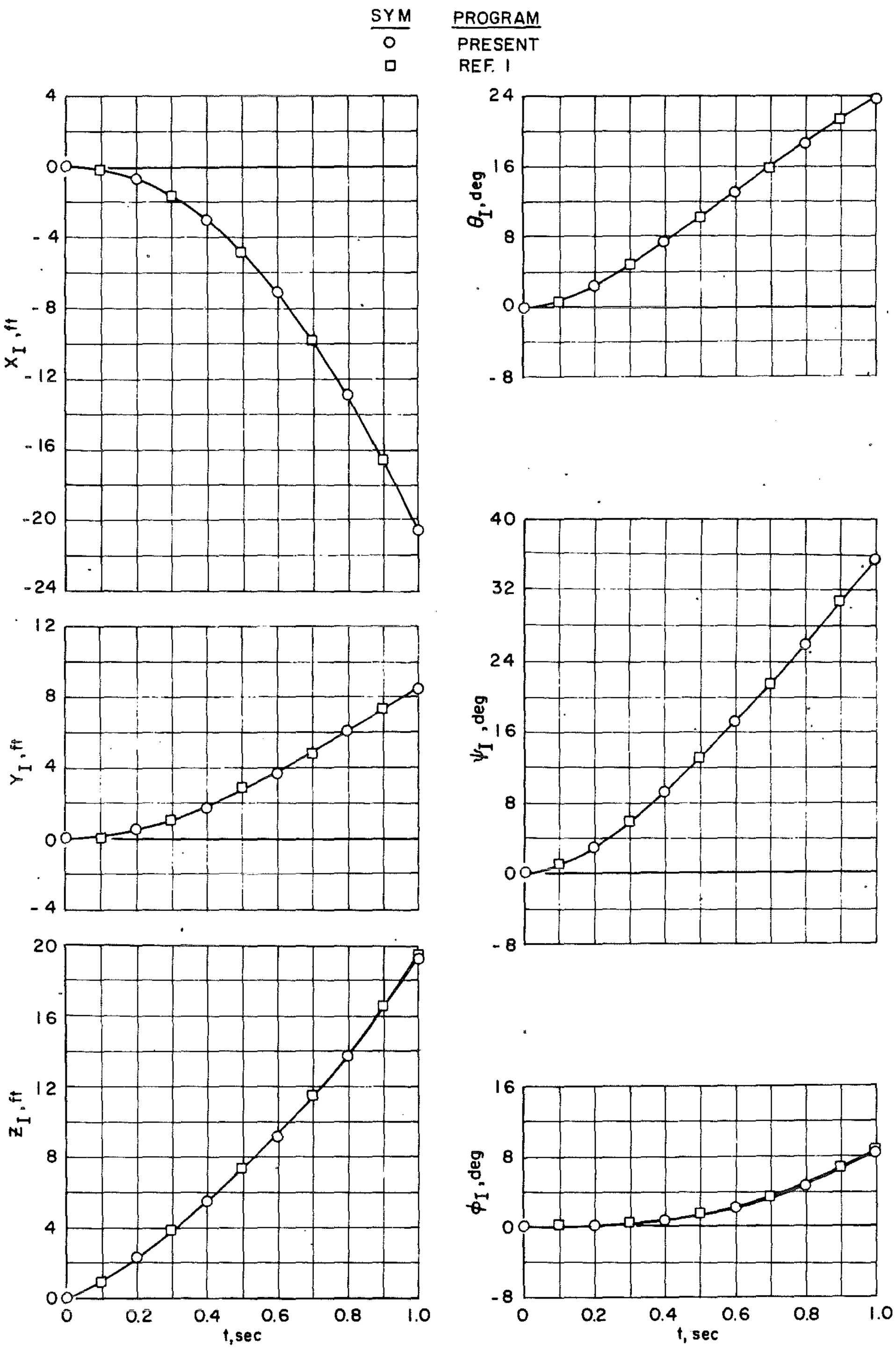

Figure 20. Comparison of typical trajectory results for the present and Ref. 1 programs.

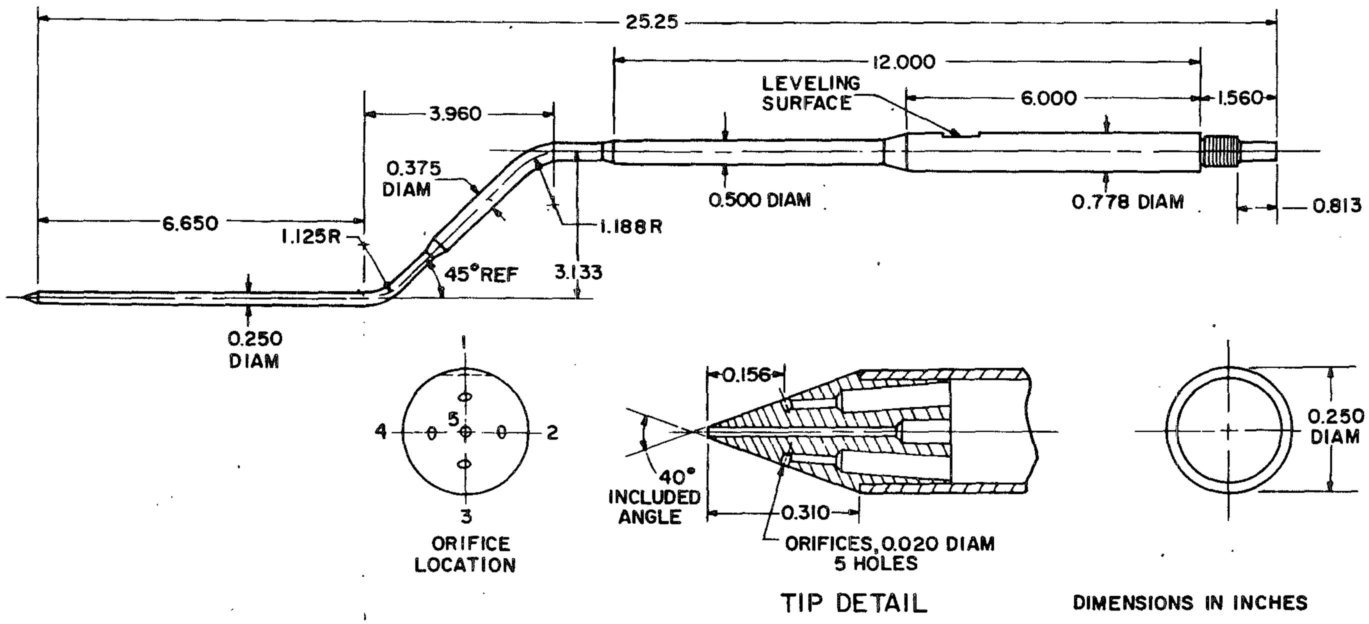

Figure 21. 40-deg conical probe.

Table 1. Standard Trajectory Tabulated Summary Data Format

RUN	TRAJ	M_∞	p_t	T_t	q_∞	p_∞	T_∞	Re_∞	T_{DP}	SH	λ	h	δt	DATE	TIME	CON	SET	ZERO	SET	TRANSONIC	4T
151	1312	0.849	1200.3	541.4	377.9	749.3	473.2	2.4	457.3	0.0012	0.050	5.0K	0.0010	11/27/79	19:55:46	151/	2	146/	2	TEST	TC-635

STORE	Wt	A	ℓ_1	ℓ_2, ℓ_3	X_{cg}	$\Delta X_{m,cg}$	$\Delta X_{n,cg}$	Y_{cg}	Z_{cg}	I_{XX}	I_{XY}	I_{XZ}	I_{YY}	I_{YZ}	I_{ZZ}	C_{ℓ_p}	C_{m_q}	C_{n_r}
MK-83	985.1	1.069	1.167	1.167	4.042	0.000	0.000	0.000	0.000	4.8	0.0	0.0	106.6	0.0	106.6	-2.9	-85.9	-85.9

A/C	α	β	N_Z	γ	$\phi_{A/C}$	I_P	I_Y	I_R	CONFIG	WING	MOTION	NOROLL	POST	COEF	THRUST	EJECT	X_{FE}	ΔX_{AE}	ω_m	Z_{E1}	Z_{E2}
F-4E	1.98	0.00	1.0	0.0	0.0	-1.00	0.00	0.0	3	FUSCL	0	1	0	0	0	2	3.46	1.50	0.0	0.38	0.38

		FLIGHT AXIS POSITIONS AND ORIENTATIONS								BODY AXIS FORCE AND MOMENT COEFFICIENTS								
PN	t	X	Y	Z	ψ	θ	φ	α_S	β_S	C_N	C_m	C_Y	C_n	C_ℓ	$C_{A,t}$	q_A	F_{E1}	F_{E2}
5	0.000	0.00	0.00	0.00	0.00	0.98	0.0	0.98	0.00	0.365	-0.819	-0.090	-0.029	0.039	0.212	890.6	3467.	5251.
7	0.010	-0.00	-0.00	0.02	-0.00	1.03	0.0	1.22	-0.00	0.373	-0.810	-0.090	-0.020	0.038	0.210	890.5	3467.	5251.
9	0.020	-0.00	-0.00	0.06	-0.00	1.18	0.1	1.56	0.00	0.386	-0.802	-0.085	-0.012	0.036	0.208	890.5	3467.	5251.
10	0.030	-0.00	-0.00	0.14	-0.00	1.44	0.2	2.00	0.01	0.395	-0.788	-0.077	-0.005	0.035	0.210	890.6	3467.	5251.
11	0.040	-0.00	-0.00	0.24	-0.01	1.79	0.0	2.54	0.00	0.397	-0.761	-0.070	0.012	0.032	0.212	890.7	3467.	5251.
12	0.050	-0.00	-0.00	0.38	-0.01	2.24	0.2	3.16	0.02	0.416	-0.764	-0.065	0.017	0.031	0.212	890.8	3467.	0.
13	0.060	-0.00	-0.00	0.53	-0.02	2.68	0.0	3.62	0.02	0.426	-0.762	-0.056	0.018	0.030	0.211	890.7	0.	0.
14	0.070	-0.00	-0.00	0.69	-0.02	3.07	0.0	4.02	0.03	0.439	-0.767	-0.054	0.022	0.029	0.212	890.5	0.	0.
15	0.080	-0.00	-0.00	0.84	-0.03	3.41	0.0	4.37	0.04	0.453	-0.775	-0.048	0.021	0.031	0.210	890.4	0.	0.
16	0.090	-0.01	-0.00	1.00	-0.04	3.71	0.0	4.68	0.05	0.459	-0.778	-0.045	0.024	0.031	0.208	890.3	0.	0.
17	0.100	-0.01	0.00	1.16	-0.04	3.95	-0.0	4.94	0.06	0.470	-0.786	-0.042	0.025	0.030	0.209	890.1	0.	0.
18	0.110	-0.01	0.00	1.32	-0.05	4.15	-0.0	5.15	0.08	0.475	-0.783	-0.039	0.026	0.029	0.206	890.0	0.	0.
19	0.120	-0.02	0.01	1.48	-0.06	4.30	-0.0	5.31	0.09	0.474	-0.778	-0.034	0.027	0.032	0.207	889.9	0.	0.
20	0.130	-0.02	0.02	1.65	-0.07	4.41	-0.0	5.42	0.11	0.478	-0.778	-0.031	0.027	0.031	0.208	889.7	0.	0.
21	0.140	-0.03	0.02	1.81	-0.07	4.46	-0.0	5.49	0.13	0.475	-0.766	-0.031	0.030	0.032	0.208	889.6	0.	0.

Table 1. Continued

RUN	TRAJ	M_∞	p_t	T_t	q_∞	p_∞	T_∞	Re_∞	T_{DP}	SH	λ	h	δt	DATE	TIME	CON SET	ZERO SET	TRANSONIC	4T
151	1312	0.849	1200.3	541.4	377.9	749.3	473.2	2.4	457.3	0.0012	0.050	5.0K	0.0010	11/27/79	19:55:46	151/ 2	146/ 2	TEST	TC-635

STORE	Wt	A	ℓ_1	ℓ_2,ℓ_3	X_{cg}	$\Delta X_{m,cg}$	$\Delta X_{n,cg}$	Y_{cg}	Z_{cg}	I_{XX}	I_{XY}	I_{XZ}	I_{YY}	I_{YZ}	I_{ZZ}	C_{ℓ_p}	C_{m_q}	C_{n_r}
MK-83	985.0	1.069	1.167	1.167	4.042	0.000	0.000	0.000	0.000	4.8	0.0	0.0	106.6	0.8	106.6	-2.9	-85.9	-85.9

A/C	α	β	N_Z	γ	$\phi_{A/C}$	I_P	I_Y	I_R	CONFIG	WING	MOTION	NOROLL	POST	COEF	THRUST	EJECT	X_{FE}	ΔX_{AE}	ω_m	Z_{E1}	Z_{E2}
F-4E	1.98	0.00	1.0	0.0	0.0	-1.00	0.00	0.0	3	FUSCL	0	1	0	0	0	2	3.46	1.50	0.0	0.38	0.38

FULL SCALE VELOCITIES AND ACCELERATIONS

PN	t	V_X	V_Y	V_Z	V_R	u	v	w	p	q	r	$\dot{u}$	$\dot{v}$	$\dot{w}$	$\dot{p}$	$\dot{q}$	$\dot{r}$
5	0.000	932.4	0.0	15.9	932.5	0.0	0.0	0.0	0.00	0.00	0.00	-7.1	-2.8	305.6	9.08	17.64	-0.30
7	0.010	932.3	-0.0	19.8	932.5	-0.1	-0.0	3.1	0.09	0.18	-0.00	-7.6	-2.5	305.3	8.74	17.64	-0.22
9	0.020	932.2	0.0	25.4	932.5	-0.2	-0.0	6.1	0.17	0.35	-0.00	-9.3	-1.5	304.9	8.37	17.62	-0.19
10	0.030	932.0	0.1	32.5	932.5	-0.3	-0.1	9.2	0.26	0.53	-0.01	-12.2	0.1	304.5	8.01	17.67	-0.17
11	0.040	931.6	0.1	41.3	932.6	-0.4	-0.0	12.2	0.34	0.71	-0.01	-16.2	1.9	304.3	7.34	17.85	-0.10
12	0.050	931.2	0.3	51.4	932.6	-0.6	-0.0	15.0	0.41	0.81	-0.01	-20.0	4.2	132.0	6.99	-27.40	-0.14
13	0.060	930.7	0.3	58.8	932.6	-0.8	0.0	15.2	0.48	0.72	-0.01	-19.1	5.5	18.3	6.65	-8.35	-0.13
14	0.070	930.2	0.4	65.3	932.5	-1.0	0.1	15.4	0.54	0.64	-0.01	-18.2	6.7	17.8	6.59	-8.36	-0.09
15	0.080	929.7	0.6	71.1	932.4	-1.1	0.2	15.6	0.61	0.56	-0.01	-17.1	8.0	17.3	6.88	-8.40	-0.10
16	0.090	929.2	0.8	76.0	932.4	-1.3	0.3	15.8	0.68	0.47	-0.01	-16.0	9.3	17.8	6.86	-8.37	-0.04
17	0.100	928.8	1.1	80.2	932.3	-1.5	0.4	15.9	0.75	0.39	-0.01	-14.9	10.6	16.6	6.51	-8.41	-0.01
18	0.110	928.4	1.3	83.6	932.2	-1.6	0.5	16.1	0.81	0.30	-0.01	-13.6	11.9	16.4	6.47	-8.33	0.04
19	0.120	928.1	1.5	86.2	932.1	-1.7	0.6	16.3	0.88	0.22	-0.01	-12.4	13.2	16.4	7.09	-8.24	0.10
20	0.130	927.9	1.8	88.1	932.1	-1.9	0.7	16.4	0.95	0.14	-0.01	-11.2	14.6	16.3	6.74	-8.19	0.17
21	0.140	927.7	2.1	89.1	932.0	-2.0	0.9	16.6	1.02	0.06	-0.01	-9.9	15.9	16.3	7.04	-8.01	0.27

Table 1. Concluded

RUN	TRAJ	M_∞	p_t	T_t	q_∞	p_∞	T_∞	Re_∞	T_{DP}	SH	λ	h	δt	DATE	TIME	CON SET	ZERO SET	TRANSONIC 4T
151	1312	0.849	1200.3	541.4	377.9	749.3	473.2	2.4	457.3	0.0012	0.050	5.0K	0.0010	11/27/79	19:55:46	151/ 2	146/ 2	TEST TC-635

STORE	Wt	A	ℓ_1	ℓ_2,ℓ_3	X_{cg}	$\Delta X_{m,cg}$	$\Delta X_{n,cg}$	Y_{cg}	Z_{cg}	I_{XX}	I_{XY}	I_{XZ}	I_{YY}	I_{YZ}	I_{ZZ}	C_{ℓ_p}	C_{m_q}	C_{n_r}
MK-83	985.[illegible]	1.069	1.167	1.167	4.042	0.000	0.000	0.000	0.000	4.8	0.0	0.0	106.6	0.8	106.6	-2.9	-85.9	-85.9

A/C	α	β	N_Z	γ	$\phi_{A/C}$	I_P	I_Y	I_R	CONFIG	WING	MOTION	NOROLL	POST	COEF	THRUST	EJECT	X_{FE}	ΔX_{AE}	ω_m	Z_{E1}	Z_{E2}
F-4E	1.98	0.00	1.0	0.0	0.0	-1.00	0.00	0.0	3	FUSCL	0	1	0	0	0	2	3.46	1.50	0.0	0.38	0.38

PYLON AXIS POSITIONS AND ORIENTATIONS

PN	t	X_P	Y_P	Z_P	$\Delta\psi$	$\Delta\theta$	$\Delta\phi$
5	0.000	0.0	0.0	0.0	0.0	-0.0	0.0
7	0.010	-0.0	-0.0	0.0	-0.0	0.1	0.0
9	0.020	-0.0	-0.0	0.1	-0.0	0.2	0.1
10	0.030	-0.0	-0.0	0.1	-0.0	0.5	0.2
11	0.040	-0.0	-0.0	0.2	-0.0	0.8	0.0
12	0.050	-0.0	-0.0	0.4	-0.0	1.3	0.2
13	0.060	-0.0	-0.0	0.5	-0.0	1.7	0.0
14	0.070	-0.0	-0.0	0.7	-0.0	2.1	0.0
15	0.080	-0.0	-0.0	0.8	-0.0	2.4	0.0
16	0.090	-0.0	-0.0	1.0	-0.0	2.7	0.0
17	0.100	-0.0	0.0	1.2	-0.0	3.0	-0.0
18	0.110	-0.0	0.0	1.3	-0.1	3.2	-0.0
19	0.120	-0.0	0.0	1.5	-0.1	3.3	-0.0
20	0.130	-0.1	0.0	1.6	-0.1	3.4	-0.0
21	0.140	-0.1	0.0	1.8	-0.1	3.5	-0.0

Table 2. Standard Aerodynamic Grid Tabulated Summary Data Format

RUN	SURVEY	M_∞	p_t	T_t	q_∞	p_∞	T_∞	V_∞	Re_∞	T_{DP}	SH	λ	DATE	TIME	CON SET	ZERO SET	TRANSONIC	4T
166	101	0.601	1203.3	535.8	238.2	942.9	499.7	658.2	2.0	473.9	0.0028	0.050	11/27/79	22:38:54	166/ 6	165/ 1	TEST	TC-635

A/C	α	β	I_P	I_Y	I_R	CONFIG	WING	STORE	A	ℓ_1	ℓ_2, ℓ_3	X_{cg}	Y_{cg}	Z_{cg}	ϕ_S
F/S	0.00	0.00	0.00	0.00	0.0	1	FUSEL	MK-83	1.069	1.167	1.167	4.042	0.000	0.000	45.0

REFERENCE AXIS — BODY AXIS COEFFICIENTS

PN	X_{REF}	Y_{REF}	Z_{REF}	$\Delta\psi$	$\Delta\theta$	$\Delta\phi$	α_S	β_S	C_N	C_m	C_Y	C_n	C_ℓ	$C_{A,t}$	q_∞	NDX	RUN
12	-0.02	-0.00	0.00	3.92	-0.01	0.5	0.03	-3.92	0.047	-0.053	0.230	-0.216	0.030	0.135	238.2	3	166
13	-0.02	-0.00	0.01	3.91	0.98	0.6	1.02	-3.90	0.114	-0.130	0.230	-0.226	0.032	0.132	237.2	4	166
14	-0.02	-0.01	0.00	3.90	1.98	0.7	2.03	-3.88	0.183	-0.216	0.232	-0.240	0.032	0.129	237.3	5	166
15	-0.02	-0.01	-0.00	3.88	4.00	0.8	4.05	-3.82	0.318	-0.385	0.246	-0.291	0.029	0.128	237.1	6	166
16	-0.02	-0.01	0.01	3.85	5.99	0.9	6.05	-3.76	0.447	-0.506	0.257	-0.353	0.034	0.133	236.8	7	166
17	-0.02	-0.02	0.01	3.83	7.98	1.0	8.05	-3.68	0.577	-0.620	0.284	-0.471	0.038	0.132	237.5	8	166
18	-0.01	0.01	-0.01	7.95	-2.06	0.8	-1.95	-7.98	-0.107	0.201	0.504	-0.499	0.038	0.121	238.0	9	166
19	-0.02	-0.00	-0.00	7.88	-1.01	0.9	-0.88	-7.89	-0.018	0.056	0.490	-0.469	0.037	0.129	236.5	10	166
20	-0.02	-0.01	0.01	7.85	-0.02	1.1	0.12	-7.85	0.063	-0.079	0.497	-0.509	0.037	0.125	237.4	11	166
21	-0.02	-0.00	0.01	7.83	0.98	1.2	1.15	-7.81	0.142	-0.208	0.492	-0.510	0.037	0.122	237.1	12	166
22	-0.02	0.00	0.00	7.82	1.99	1.3	2.17	-7.77	0.228	-0.346	0.496	-0.518	0.037	0.130	236.9	13	166
23	-0.02	-0.02	0.01	7.76	3.99	1.6	4.20	-7.64	0.378	-0.571	0.503	-0.578	0.039	0.123	237.5	14	166
24	-0.02	-0.01	0.00	7.72	6.00	1.8	6.24	-7.53	0.524	-0.750	0.538	-0.734	0.038	0.134	237.7	15	166
25	-0.01	-0.01	0.01	7.69	7.99	2.1	8.27	-7.40	0.662	-0.862	0.587	-0.929	0.048	0.140	237.5	16	166
2	-0.02	-0.02	-0.01	-0.04	8.05	-0.0	8.05	0.04	0.565	-0.585	-0.010	0.012	0.029	0.124	237.2	17	167
3	-0.02	0.00	-0.02	0.01	3.98	0.0	3.98	-0.01	0.286	-0.280	-0.013	0.064	0.030	0.120	237.3	18	167
4	-0.03	0.01	-0.02	0.01	1.99	0.0	1.99	-0.01	0.163	-0.155	-0.013	0.057	0.032	0.133	238.2	19	167
5	-0.02	0.00	-0.01	0.01	1.00	0.0	1.00	-0.01	0.108	-0.104	-0.010	0.047	0.030	0.132	236.2	20	167
6	-0.00	0.01	-0.02	0.01	-0.00	0.0	-0.00	-0.01	0.038	-0.027	-0.012	0.046	0.027	0.134	238.2	21	167
7	-0.00	0.00	-0.02	0.01	-1.00	0.0	-1.00	-0.01	-0.023	0.039	-0.007	0.031	0.028	0.138	236.4	22	167
8	-0.00	0.00	-0.02	0.01	-2.00	0.0	-2.00	-0.01	-0.091	0.109	-0.004	0.011	0.030	0.135	237.6	23	167
9	-0.00	0.00	-0.02	0.01	-4.00	0.0	-4.00	-0.01	-0.214	0.233	0.006	-0.024	0.034	0.137	236.9	24	167
10	-0.01	0.00	-0.03	0.00	-7.99	0.0	-7.99	-0.00	-0.461	0.466	0.002	-0.007	0.032	0.128	236.3	25	167
11	0.00	0.01	-0.05	0.02	-11.99	-0.0	-11.99	-0.02	-0.742	0.714	-0.009	0.053	0.042	0.119	235.4	26	167
12	0.00	0.01	-0.03	0.01	-16.01	-0.0	-16.01	-0.01	-1.109	1.079	-0.024	0.125	0.038	0.108	237.9	27	167
13	-0.00	0.01	-0.01	0.01	-20.02	-0.0	-20.02	-0.01	-1.514	1.414	-0.042	0.188	0.034	0.099	237.2	28	167
14	-0.03	0.00	-0.01	0.01	-24.03	-0.0	-24.03	-0.01	-1.975	1.788	-0.130	0.381	0.028	0.091	236.8	29	167
15	-0.02	0.00	0.00	0.00	-28.06	-0.0	-28.06	-0.00	-2.499	2.066	-0.151	0.448	0.023	0.076	237.2	30	167
16	-0.03	-0.01	-0.01	-0.03	-32.05	0.0	-32.05	0.02	-3.138	2.532	-0.378	0.727	0.042	0.068	237.7	31	167
17	-0.03	-0.00	-0.00	-0.07	-36.11	0.0	-36.11	0.05	-4.097	3.115	-0.582	0.559	0.094	0.036	238.1	32	167
18	-0.04	-0.01	0.01	-0.13	-40.09	0.1	-40.09	0.07	-5.220	4.430	-0.889	0.141	0.128	0.010	237.1	33	167

Table 3. Standard Flow-Field Grid Tabulated Summary Data Format

RUN	SURVEY	M_∞	p_t	T_t	q_∞	p_∞	T_∞	V_∞	Re_∞	T_{DP}	SH	λ	DATE	TIME	CON SET	ZERO SET	TRANSONIC	4T
879	131	0.952	1740.5	96.6	616.4	971.6	470.9	1012.7	3.5	10.5	0.0017	0.050	11/21/79	16/31/27	877/ 3	819/ 2	TEST	TC-623

A/C	α	β	I_P	I_Y	I_R	CONFIG	WING
F-4C	17.00	0.00	-1.00	0.00	0.0	35	LEFT

SUMMARY 1

	REFERENCE AXIS								PROBE PRESSURES							FLOW ANGLES				
RUN/PN	X_{REF}	Y_{REF}	Z_{REF}	$\Delta\psi$	$\Delta\theta$	$\Delta\phi$	$p_{s,1}$	$p_{s,2}$	$p_{s,3}$	$p_{s,4}$	$p_{p,5}$	$\bar{p}_5$	$\bar{p}_{5,p}$	M_L	$C_{p,\epsilon}$	ϵ	$C_{p,\sigma}$	σ	NDX
879003	-14.75	-0.02	1.17	-0.02	-0.02	-0.1	1280.1	1309.5	1178.7	1169.0	1724.0	0.716	0.7231	0.82	0.194	5.4	-0.268	-6.5	51
879004	-14.24	-0.03	1.18	-0.02	-0.02	-0.1	1283.2	1311.1	1182.2	1172.0	1723.8	0.718	0.7247	0.82	0.194	5.4	-0.267	-6.5	52
879005	-13.75	-0.03	1.17	-0.03	-0.02	0.0	1288.8	1318.6	1188.1	1177.4	1724.1	0.721	0.7283	0.81	0.196	5.5	-0.275	-6.7	53
879006	-13.25	-0.03	1.17	-0.02	-0.02	-0.1	1290.9	1322.1	1190.4	1178.9	1724.0	0.722	0.7298	0.81	0.196	5.5	-0.280	-6.8	54
879007	-12.74	-0.03	1.18	-0.03	-0.02	-0.1	1292.7	1327.0	1192.4	1180.5	1724.3	0.724	0.7314	0.80	0.197	5.5	-0.288	-7.0	55
879008	-12.24	-0.03	1.18	-0.03	-0.02	0.0	1297.0	1336.8	1196.8	1184.4	1724.0	0.727	0.7352	0.79	0.200	5.5	-0.304	-7.4	56
879009	-11.75	-0.03	1.17	-0.02	-0.02	-0.1	1302.7	1342.6	1202.1	1189.0	1724.0	0.730	0.7384	0.79	0.203	5.6	-0.310	-7.6	57
879011	-11.24	-0.03	1.18	-0.03	-0.02	-0.0	1305.7	1349.3	1204.5	1191.1	1724.4	0.732	0.7407	0.78	0.206	5.7	-0.322	-7.9	58
879012	-10.74	-0.03	1.18	-0.03	-0.03	0.0	1308.6	1355.0	1205.7	1192.0	1724.3	0.734	0.7427	0.77	0.211	5.8	-0.335	-8.2	59
879013	-10.25	-0.02	1.17	-0.01	-0.02	-0.0	1311.4	1358.0	1205.9	1192.3	1724.3	0.735	0.7440	0.77	0.218	6.0	-0.342	-8.4	60
879014	-9.74	-0.03	1.18	-0.02	-0.03	0.0	1315.9	1362.5	1206.4	1193.5	1724.4	0.736	0.7460	0.77	0.228	6.3	-0.351	-8.7	61
879015	-9.25	-0.03	1.17	-0.02	-0.02	-0.1	1320.5	1366.4	1206.4	1194.0	1724.4	0.738	0.7478	0.76	0.239	6.5	-0.361	-8.9	62
879016	-8.74	-0.03	1.19	-0.02	-0.03	0.0	1324.6	1368.1	1203.0	1191.7	1724.6	0.737	0.7486	0.76	0.256	7.0	-0.371	-9.2	63
879017	-8.25	-0.03	1.17	-0.02	-0.02	-0.1	1329.4	1369.8	1201.0	1190.5	1724.3	0.738	0.7499	0.76	0.271	7.4	-0.379	-9.4	64
879018	-7.75	-0.02	1.17	-0.02	-0.02	-0.1	1334.1	1370.7	1197.7	1187.9	1724.4	0.738	0.7506	0.76	0.289	7.8	-0.387	-9.6	65
879019	-7.25	-0.02	1.17	-0.01	-0.02	-0.0	1338.3	1370.8	1193.1	1184.4	1724.5	0.737	0.7510	0.75	0.308	8.3	-0.396	-9.9	66
879020	-6.75	-0.03	1.17	-0.02	-0.02	-0.1	1338.9	1367.5	1184.6	1176.7	1724.7	0.735	0.7492	0.76	0.325	8.7	-0.402	-10.0	67
879022	-6.24	-0.03	1.18	-0.02	-0.02	-0.1	1341.1	1363.0	1178.8	1171.8	1724.7	0.733	0.7480	0.76	0.340	9.1	-0.401	-10.0	68
879023	-5.75	-0.03	1.17	-0.03	-0.02	-0.1	1340.8	1359.3	1172.2	1165.4	1724.4	0.730	0.7464	0.77	0.351	9.4	-0.404	-10.1	69
879024	-5.25	-0.02	1.17	-0.02	-0.02	-0.1	1343.2	1354.8	1169.2	1162.3	1724.6	0.729	0.7455	0.77	0.361	9.7	-0.399	-10.0	70
879025	-4.74	-0.02	1.18	-0.02	-0.03	0.0	1347.5	1353.1	1169.8	1162.6	1724.8	0.730	0.7461	0.77	0.370	9.9	-0.396	-9.9	71
879026	-4.24	-0.02	1.18	-0.01	-0.03	0.0	1353.3	1349.7	1170.9	1163.4	1724.8	0.730	0.7468	0.76	0.380	10.2	-0.389	-9.7	72
879027	-3.74	-0.03	1.18	-0.02	-0.02	-0.1	1356.0	1344.0	1167.2	1159.7	1724.7	0.729	0.7458	0.77	0.392	10.5	-0.383	-9.6	73
879028	-3.25	-0.03	1.18	-0.02	-0.03	0.0	1363.8	1339.9	1170.1	1162.3	1724.7	0.730	0.7471	0.76	0.404	10.8	-0.371	-9.3	74
879029	-2.75	-0.02	1.18	-0.01	-0.03	0.0	1372.4	1335.5	1173.3	1164.6	1724.7	0.731	0.7485	0.76	0.418	11.2	-0.359	-9.0	75
879030	-2.25	-0.02	1.17	-0.02	-0.02	-0.1	1382.2	1328.6	1172.5	1163.1	1724.5	0.732	0.7494	0.76	0.442	11.8	-0.349	-8.8	76
879031	-1.75	-0.03	1.18	-0.02	-0.02	-0.1	1387.2	1316.6	1164.5	1155.5	1724.6	0.728	0.7472	0.76	0.465	12.4	-0.337	-8.5	77
879032	-1.25	-0.03	1.18	-0.03	-0.02	-0.1	1390.3	1300.4	1152.2	1143.8	1724.4	0.723	0.7434	0.77	0.490	13.0	-0.322	-8.1	78
879033	-0.74	-0.03	1.18	-0.02	-0.03	-0.0	1394.4	1287.5	1142.7	1135.1	1724.5	0.719	0.7408	0.78	0.513	13.6	-0.310	-7.8	79
879034	-0.25	-0.02	1.18	-0.02	-0.02	-0.0	1394.9	1273.3	1130.4	1124.7	1724.6	0.714	0.7369	0.79	0.531	14.1	-0.298	-7.5	80

Table 3. Concluded

RUN	SURVEY	M_∞	p_t	T_t	q_∞	p_∞	T_∞	V_∞	Re_∞	T_{DP}	SH	λ	DATE	TIME	CON SET	ZERO SET	TRANSONIC	4T
925	136	0.603	2219.1	96.5	441.5	1736.1	518.5	672.7	3.5	30.4	0.0034	0.050	11/21/79	19/21/49	921/ 12	912/ 1	TEST	TC-623

A/C	α	β	I_P	I_Y	I_R	CONFIG	WING
F-4C	5.00	0.00	-1.00	0.00	0.0	55	LEFT

SUMMARY 2

	PYLON AXIS			BODY AXIS FLOW ANGLES AND VELOCITIES																
PN	X_P	Y_P	Z_P	α_{XY}	α_{XZ}	α_{YZ}	V_X	V_{XY}	V_{XZ}	V_Y	V_{YZ}	V_Z	$p_{t,p}$	q_L	V_L	θ_T	M_L	NDX	RUN
1	-5.84	0.33	0.36	-3.4	1.0	286.5	650.1	651.2	650.2	-38.7	40.4	11.5	2216.6	418.0	651.3	3.5	0.58	101	925
2	-5.55	0.33	0.36	-3.5	1.3	290.4	647.9	649.1	648.0	-40.1	42.8	14.9	2216.7	415.8	649.3	3.8	0.58	102	925
3	-5.25	0.33	0.35	-3.7	1.7	295.1	651.7	653.1	652.0	-41.7	46.0	19.5	2220.0	420.8	653.3	4.0	0.58	103	925
4	-4.95	0.33	0.36	-3.8	2.1	298.6	655.8	657.3	656.3	-43.5	49.5	23.7	2215.9	424.7	657.7	4.3	0.59	104	925
5	-4.65	0.33	0.36	-3.9	2.3	301.1	660.8	662.3	661.3	-44.7	52.2	27.0	2215.7	430.2	662.8	4.5	0.59	105	925
6	-4.35	0.33	0.35	-3.9	2.5	302.9	663.3	664.9	664.0	-45.3	54.0	29.4	2214.9	432.8	665.5	4.6	0.60	106	925
7	-4.05	0.33	0.35	-3.9	2.5	303.1	671.2	672.8	671.9	-45.6	54.4	29.7	2214.8	441.3	673.4	4.6	0.60	107	925
8	-3.75	0.33	0.36	-3.8	2.3	301.4	675.8	677.3	676.4	-44.6	52.2	27.2	2213.9	445.8	677.8	4.4	0.61	108	925
9	-3.45	0.33	0.35	-3.6	1.9	297.2	677.3	678.7	677.7	-42.7	48.0	21.9	2215.0	447.4	679.0	4.0	0.61	109	925
10	-3.15	0.33	0.35	-3.4	1.2	289.9	679.6	680.8	679.7	-40.8	43.4	14.8	2216.0	449.5	680.9	3.6	0.61	110	925
11	-2.85	0.33	0.36	-3.2	0.6	280.3	680.4	681.5	680.5	-38.3	38.9	6.9	2217.3	450.4	681.5	3.3	0.61	111	925
12	-2.55	0.33	0.36	-3.0	0.0	270.6	677.9	678.8	677.9	-35.5	35.5	0.4	2214.6	447.0	678.8	3.0	0.61	112	925
13	-2.25	0.34	0.35	-2.8	-0.4	261.1	676.4	677.2	676.4	-33.0	33.4	-5.2	2215.3	445.5	677.2	2.8	0.61	113	925
14	-1.95	0.33	0.35	-2.6	-1.1	246.9	674.8	675.5	674.9	-30.2	32.9	-12.9	2217.0	444.1	675.6	2.8	0.61	114	925
15	-1.65	0.34	0.35	-2.3	-1.7	233.2	658.6	659.1	658.9	-26.3	32.9	-19.7	2218.7	427.0	659.4	2.9	0.59	115	925
16	-1.35	0.33	0.35	-2.2	-1.9	229.0	654.2	654.6	654.5	-24.6	32.7	-21.4	2212.4	421.2	655.0	2.8	0.59	116	925
17	-1.05	0.34	0.35	-2.2	-1.7	232.7	647.4	647.9	647.7	-24.7	31.0	-18.8	2213.2	414.1	648.2	2.7	0.58	117	925
18	-0.75	0.33	0.36	-2.2	-1.2	241.4	642.8	643.3	642.9	-24.7	28.1	-13.5	2215.4	409.4	643.4	2.5	0.57	118	925
19	-0.45	0.34	0.35	-2.2	-0.6	254.9	633.5	634.0	633.5	-24.5	25.4	-6.6	2213.3	399.0	634.0	2.3	0.57	119	925
20	-0.15	0.33	0.35	-2.3	0.2	274.3	634.7	635.2	634.7	-25.2	25.2	1.9	2210.5	399.7	635.2	2.3	0.57	120	925

APPENDIX A
CONSTANTS ASSEMBLY PROCEDURE, WITH STAGING AND INITIALIZATION EQUATIONS

A-1. CONSTANTS ASSEMBLY PROCEDURE

To store a unique set of the 360 constants required for every proposed trajectory in a typical wind tunnel test program is not practical for many reasons. Therefore, a "constants merge" program was developed to assemble the necessary 360 constant inputs into a temporary array, using a categorized permanent storage file. The merge routine is activated each time a constant point is requested and updates the temporary file which is to be used in trajectory calculations.

The structure and operation of the merge program are outlined as follows. A disk file is partitioned into eight different groups — A, B, C, D, E, F, G, and H. The "A" file is designated the main deck group which allows from 1 to 5 arrays of 360 constants each. The constants which are essentially invariant for the test are stored in the "A" file. Normally, only one main deck is necessary unless more than one balance is to be used. The "B," "C," and "D" files each allow from 1 to 9 arrays of 60 constants while the "E," "F," "G," and "H" files each allow from 1 to 99 arrays of 60 constants. These files are used to store constant values which change during testing (e.g., altitude, ejector forces). These "variable" constants are divided into compatible groups as determined by test requirements, and each group is assigned a numerical location in one of the "B" through "H" files. Using the merge program, one can now recall and assemble the constants groups through their alphabetical and numerical designations to provide the unique set of inputs for specific trajectory applications.

Prior to starting a trajectory, the numerical values of each group required are dialed into the respective "A" through "H" constants boxes on the data acquisition panel (DAP). When a constant point is requested, the program scans these constant boxes to define which arrays are to be assembled and then loads the appropriate groups into the temporary file in alphabetical sequence. After the staging calculations are performed, the calculated parameters are appended to the file, which is then ready for access by the trajectory generation job.

A-2. STAGING EQUATIONS

Calculations done during the staging process are listed below:

Model Reference Area and Lengths

$$A_m = A(\lambda^2)(k_\lambda)^2$$

$$\ell_{1,m} = \ell_1(12)(\lambda)(k_\lambda)$$

$$\ell_{2,m} = \ell_2(12)(\lambda)(k_\lambda)$$

$$\ell_{3,m} = \ell_{2,m}$$

Model Moment Transfer Distances (See Fig. A-1)

$$X_m = X_{cg}(12)(\lambda)(k_\lambda)$$

$$Y_m = Y_{cg}(12)(\lambda)(k_\lambda)$$

$$Z_m = Z_{cg}(12)(\lambda)(k_\lambda)$$

$$X_{m,t} = X_{BF} + X_{m,ec} - X_m + \Delta X_{m,cg}(12)(\lambda)(k_\lambda)$$

$$X_{n,t} = X_{BF} + X_{n,ec} - X_m + \Delta X_{n,cg}(12)(\lambda)(k_\lambda)$$

CTS Rig Physical Parameters (See Fig. A-2)

$$\ell_{1,R} = \left\{\left[\left(X_{PITC} + X_{BF} - X_m\right)/\cos\theta_S\right] - 3\right\}/\cos\psi_S$$

$$\ell_{2,R} = -\left(\ell_{1,R}\sin\psi_S + Y_{PITC}\right)$$

$$d_R = (\ell_{1,R}\cos\psi_S + 3)\sin\theta_S + Z_{PITC}$$

$$\ell_{3,R} = \ell_{1,R} + (X_m\cos\theta_S - d_R\sin\theta_S)\cos\psi_S + \ell_{2,R}\sin\psi_S$$

Aircraft Angle of Attack

$$\alpha = -\alpha_{TP}$$

Wing Flag

$$\text{If } (Y_{TP} > RW),\ \text{Wing} = \text{Right } (1)$$

$$\text{If } (LW \leq Y_{TP} \leq RW),\ \text{Wing} = \text{Fuscl } (2)$$

$$\text{If } (Y_{TP} < LW),\ \text{Wing} = \text{Left } (3)$$

Store Initial Attitude - Launch Trajectory

$$\nu_{R,I} = \alpha + I_P - \theta_S$$

$$\eta_{R,I} = I_Y - \beta - \psi_S$$

$$\omega_{R,I} = I_R$$

$$\left[AA\right] = \text{TME } (\nu_{R,I}, \eta_{R,I}, \omega_{R,I}, 1)^*$$

$$\left[BB\right] = \text{TME } (\psi_S, \theta_S, 0, 2)$$

$$\left[CC\right] = \left[BB\right]\left[AA\right]$$

$$\eta_t = \sin^{-1}\left[CC\ (1,2)\right]$$

$$\nu_t = \sin^{-1}\left[-CC\ (1,3)/\cos\eta_t\right]$$

$$\omega_t = \tan^{-1}\left[-CC\ (3,2)/CC\ (2,2)\right]$$

Store Initial Attitude - With Induced Angle Corrections

When $u_o, v_o, w_o \neq 0$:

$$h' = 6.356766(10^3)\ h \Big/ \left[2.0855532\,(10^7) + h\right]$$

$$T_A = 389.97$$

$$\text{If } (h' < 11),\ T_A = 518.67 - 11.7(h')$$

*See Appendix M for matrix definitions.

$$U_A = 49.021\,(M_B)\,\sqrt{T_A}$$

$$\nu_I = \nu_t$$

$$\eta_I = \eta_t$$

$$\omega_I = \omega_t$$

$$\text{If (POST} \neq 0\text{)},\ \nu_I = \nu_{I,o},\ \eta_I = \eta_{I,o},\ \omega_I = \omega_{I,o}$$

$$\left[BB\right] = \text{TME}\,(\nu_I, \eta_I, \omega_I, 1)$$

$$\begin{vmatrix} \dot{X}_{I,o} \\ \dot{Y}_{I,o} \\ \dot{Z}_{I,o} \end{vmatrix} = \left[BB\right]' \begin{vmatrix} u_o \\ v_o \\ w_o \end{vmatrix}$$

$$\nu_t = \nu_I + \tan^{-1}\left[\dot{Z}_{I,o} \Big/ (\dot{X}_{I,o} + U_A)\right]$$

$$\eta_t = \eta_I - \tan^{-1}\left\{\dot{Y}_{I,o} \Big/ \left[(\dot{X}_{I,o} + U_A)\cos\nu_I - \dot{Z}_{I,o}\sin\nu_I\right]\right\}$$

$$\omega_t' = \dot{\omega}_I$$

Store Initial Position - Unaccelerated Flight ($N_z = 1$)

$$X_t = X_{I,o}$$

$$Y_t = Y_{I,o}$$

$$Z_t = Z_{I,o}$$

Store Initial Position - Accelerated Flight ($N_z \neq 1$)

$$a_{Z,p} = (1 - N_Z)\,32.174$$

$$q_p = -a_{Z,p}/U_A$$

$$R_p = a_{Z,p}/q_p^2$$

$$\theta_p = q_p(t_o)\,(57.2958)$$

$$X_C = X_{I,o} + R_p \sin\theta_p + U_A t_o$$

$$Y_C = Y_{I,o}$$

$$Z_C = Z_{I,o} - R_p(1 - \cos\theta_p)$$

$$\left[AA\right] = \text{TME}\,(0, -\theta_p, 0, 2)$$

$$\begin{vmatrix} X_t \\ Y_t \\ Z_t \end{vmatrix} = \left[AA\right]' \begin{vmatrix} X_C \\ Y_C \\ Z_C \end{vmatrix}$$

A-3. INITIALIZATION PROCEDURE

Integrators are assigned and initialized as part of the initialization routine. Integrator outputs (designated P1 through P50) are assigned initial values as indicated below.

Initial Inertial-to-Body-Axis Matrix

$$\nu_{R,I} = \alpha + I_P - \theta_S$$

$$\eta_{R,I} = I_Y - \beta - \psi_S$$

$$\omega_{R,I} = I_R$$

$$\left[AA\right] = \text{TME}\,(\nu_{R,I}, \eta_{R,I}, \omega_{R,I}, 1)$$

$$\left[BB\right] = \text{TME}\,(\psi_S, \theta_S, 0, 2)$$

$$\left[TOBODY_o\right] = \left[BB\right]\left[AA\right]$$

If (POST $\neq$ 0), $\left[TOBODY_o\right] = \text{TME}\,(\nu_{I,o}, \eta_{I,o}, \omega_{I,o}, 1)$

Initial Values	Parameters
$P1 = u_o$, $P2 = v_o$, $P3 = w_o$	Body–axis linear velocities
$P4 = X_{I,o}$, $P5 = Y_{I,o}$, $P6 = Z_{I,o}$	Inertial–axis positions
$P7 = p_o$, $P8 = q_o$, $P9 = r_o$	Body–axis angular velocities
$\begin{bmatrix} P10 & P13 & P16 \\ P11 & P14 & P17 \\ P12 & P15 & P18 \end{bmatrix} = [TOBODY_o]$	Inertial–to–body–axis–matrix direction cosines
$P19 = 0$, $P20 = 0$, $P21 = 0$	Rotation center (hook) velocities (special staged release applications)

Program parameters, flags, and counters which are set on the first-pass loop include data cycle time (Δt), number of integrations per data cycle (K_{int}), integration time ($\delta t = \Delta t/K_{int}$), initial trajectory time (t_o), integrator pass counter (NPASS = 0), data cycle pass counter (PASS = 0), extrapolator pass counter (NXP = 0), number of extrapolators (NX), ejector control flag (EJECT), staged separation control flag (MOTION) and data cycle time increase control flag (STEP).

Once-only calculations are listed below.

Conditions at Simulated Altitude*

$$h' = 6.356766(10^3)\, h / \left[2.0855532(10^7) + h\right]$$

$$\text{If } (h' < 11),\ T_A = 518.67 - 11.7(h')$$

$$p_A = 2116.216\left[1 - 0.0225577(h')\right]^{5.2559}$$

* The pressure and temperature at altitude equations are valid from sea level to 65,800 ft. Reference: 1975 U.S. Standard Atmosphere from NASA-TR-R-459 (May 1976).

$$\text{If } (h' \geq 11),\ T_A = 389.97$$

$$p_A = 472.677 \left[e^{-0.157688\,(h'-11)} \right]$$

$$U_A = 49.021\, M_B \sqrt{T_A}$$

$$\rho_A = 1.4\, p_A\, M_B^2 / U_A^2$$

Weight Components, Mass

$$W_X' = Wt \sin\gamma$$

$$W_Y' = Wt \cos\gamma \sin\phi_{A/C}$$

$$W_Z' = Wt \cos\gamma \cos\phi_{A/C}$$

$$m = Wt/32.174$$

Initial Store Attitude (Pitch, Yaw, Roll Sequence)

$$\eta_o = \sin^{-1} \left[TOBODY_o\,(1,2) \right]$$

$$\nu_o = \sin^{-1} \left[-TOBODY_o\,(1,3)/\cos\eta_o \right]$$

$$\omega_o = \tan^{-1} \left[-TOBODY_o\,(3,2)/TOBODY_o\,(2,2) \right]$$

Initial Store Angular Rates for Accelerated Flight: Launch Trajectory Only

$$\begin{vmatrix} p_{o,p} \\ q_{o,p} \\ r_{o,p} \end{vmatrix} = \left[TOBODY_o \right] \begin{vmatrix} o \\ q_p \\ o \end{vmatrix}$$

$$P7 = P7 + p_{o,p}$$

$$P8 = P8 + q_{o,p}$$

$$P9 = P9 + r_{o,p}$$

Inertia Matrix

$$[I] = \begin{bmatrix} I_{XX} & -I_{XY} & -I_{XZ} \\ -I_{XY} & I_{YY} & -I_{YZ} \\ -I_{XZ} & -I_{YZ} & I_{ZZ} \end{bmatrix}$$

Inverse Inertia Matrix

$$[I]^{-1} = \text{inverse of } [I]$$

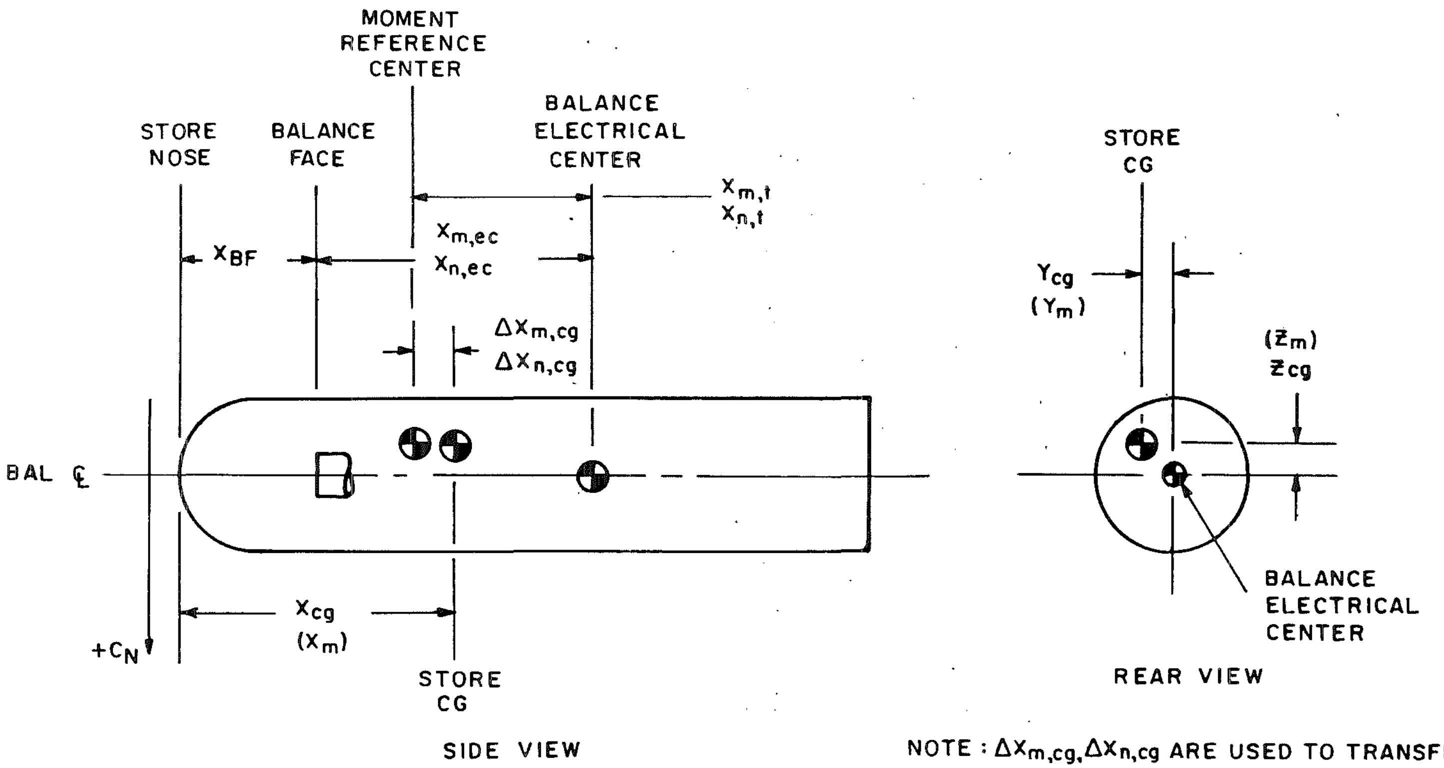

NOTE : $\Delta X_{m,cg}$, $\Delta X_{n,cg}$ ARE USED TO TRANSFER THE C_m AND C_n MOMENT REFERENCES FROM THE CG POSITION. HOWEVER, MOTION IS STILL CALCULATED ABOUT THE TRUE CG POSITION AND THE OFFSET COEFFICIENT DATA ARE USED AS THOUGH OBTAINED ABOUT THE TRUE CG POSITION.

Figure A-1. Store/balance physical definition.

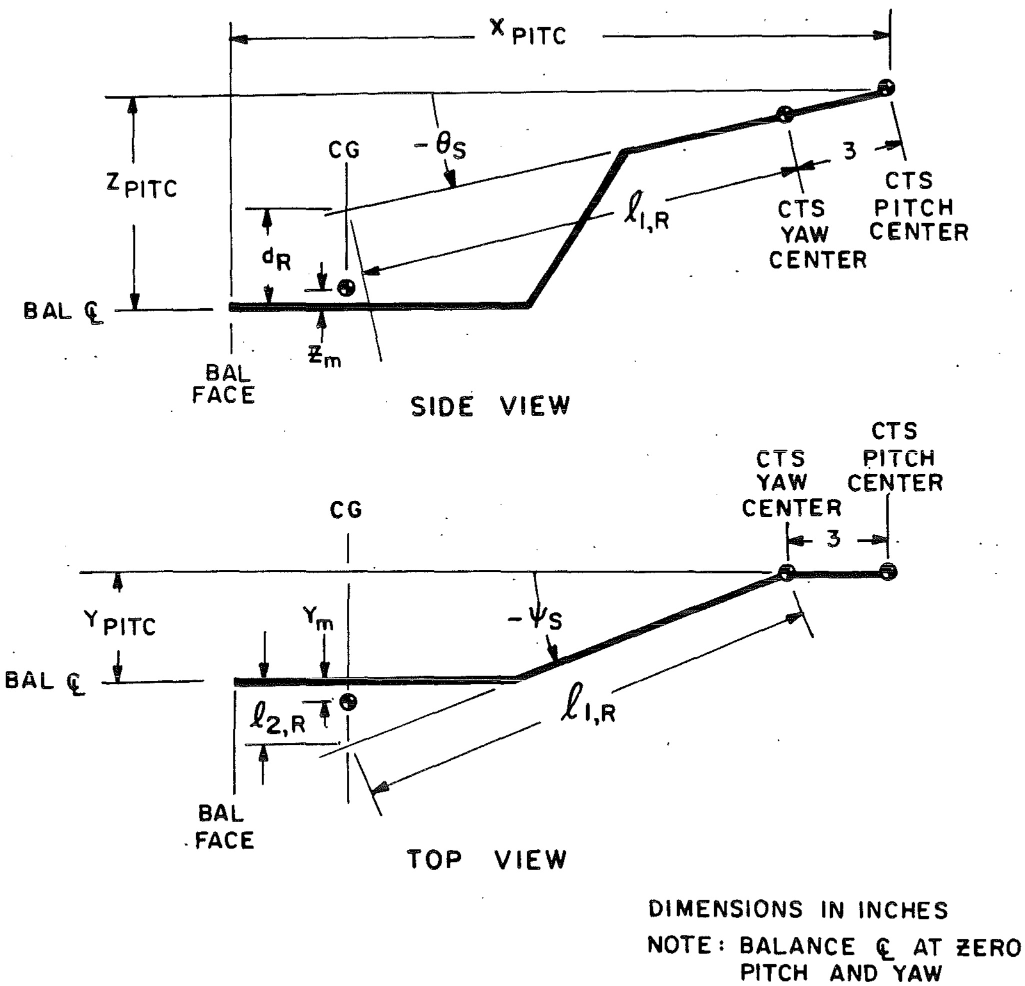

Figure A-2. Captive trajectory support (CTS) mechanism physical definition.

APPENDIX B
INPUT PROCESSING EQUATIONS

Angular Sting Deflections

$$\Delta\nu = \left[K_{\alpha,N}F_{N,g} + K_{\alpha,m}M_{m,g}\right]\cos\omega_R - \left[K_{\psi,Y}F_{Y,g} + K_{\psi,n}M_{n,g}\right]\sin\omega_R$$

$$\Delta\eta = \left[K_{\psi,Y}F_{Y,g} + K_{\psi,n}M_{n,g}\right]\cos\omega_R + \left[K_{\alpha,N}F_{N,g} + K_{\alpha,m}M_{m,g}\right]\sin\omega_R$$

$$\Delta\omega = K_{\phi,\ell}M_{\ell,g}$$

Linear Sting Deflections

$$\Delta X_B = 0$$

$$\Delta Y_B = K_{Y,Y}\left[F_{Y,g}\cos\omega_R + F_{N,g}\sin\omega_R\right] + K_{Y,n}\left[M_{n,g}\cos\omega_R + M_{m,g}\sin\omega_R\right]$$

$$\Delta Z_B = K_{Z,N}\left[F_{N,g}\cos\omega_R - F_{Y,g}\sin\omega_R\right] + K_{Z,m}\left[M_{m,g}\cos\omega_R - M_{n,g}\sin\omega_R\right]$$

$$[AA] = \text{TME}(\nu_t, \eta_t, 0, 1)$$

$$\begin{vmatrix} \Delta X_L \\ \Delta Y_L \\ \Delta Z_L \end{vmatrix} = [AA]' \begin{vmatrix} \Delta X_B \\ \Delta Y_B \\ \Delta Z_B \end{vmatrix}$$

Note: Typical examples showing how angular and linear sting deflection constants are obtained from static loadings are presented in Fig. B-1.

Static Tare Corrections

$$[AA] = \text{TME}(\nu_t, \eta_t, \omega_t, 1)$$

$$\begin{vmatrix} AAA \\ BBB \\ CCC \end{vmatrix} = [AA] \begin{vmatrix} 0 \\ 0 \\ 1 \end{vmatrix}$$

If (δR_1 = 0 and δR_5 = 0) CCC = CCC − 1

$$F_{N,st} = -CCC\,(W_N)$$

$$F_{Y,st} = BBB\,(W_Y)$$

$$F_{A,st} = -AAA\,(W_A)$$

$$M_{\ell,st} = CCC\,(\bar{Y})\,W_N - BBB\,(\bar{Z})\,W_Y$$

$$M_{m,st} = AAA\,(\bar{Z})\,W_A - CCC\,(\bar{X}_m)\,W_N$$

$$M_{n,st} = BBB\,(\bar{X}_n)\,W_Y - AAA\,(\bar{Y})\,W_A$$

Net Loads

$$F_N = F_{N,g} - F_{N,st}$$

$$F_Y = F_{Y,g} - F_{Y,st}$$

$$F_{A,t} = F_{A,g} - F_{A,st}$$

$$M_\ell = M_{\ell,g} - M_{\ell,st} + Y_m(F_N) + Z_m(F_Y)$$

$$M_m = M_{m,g} - M_{m,st} - X_{m,t}(F_N) + Z_m(F_{A,t})$$

$$M_n = M_{n,g} - M_{n,st} - X_{n,t}(F_Y) - Y_m(F_{A,t})$$

Aerodynamic Coefficients

$$C_N = F_N/q_\infty A_m$$

$$C_Y = F_Y/q_\infty A_m$$

$$C_{A,t} = F_{A,t}/q_\infty A_m$$

$$C_\ell = M_\ell/q_\infty A_m \;\; \ell_{3,m}$$

$$C_m = M_m/q_\infty A_m \;\; \ell_{1,m}$$

$$C_n = M_n/q_\infty A_m \;\; \ell_{2,m}$$

Identify Extrapolation Parameters

$$C_{N,x} = C_N \ , \ C_{Y,x} = C_Y \ , \ C_{A,t,x} = C_{A,t}$$

$$C_{\ell,x} = C_\ell \ , \ C_{m,x} = C_m \ , \ C_{n,x} = C_n$$

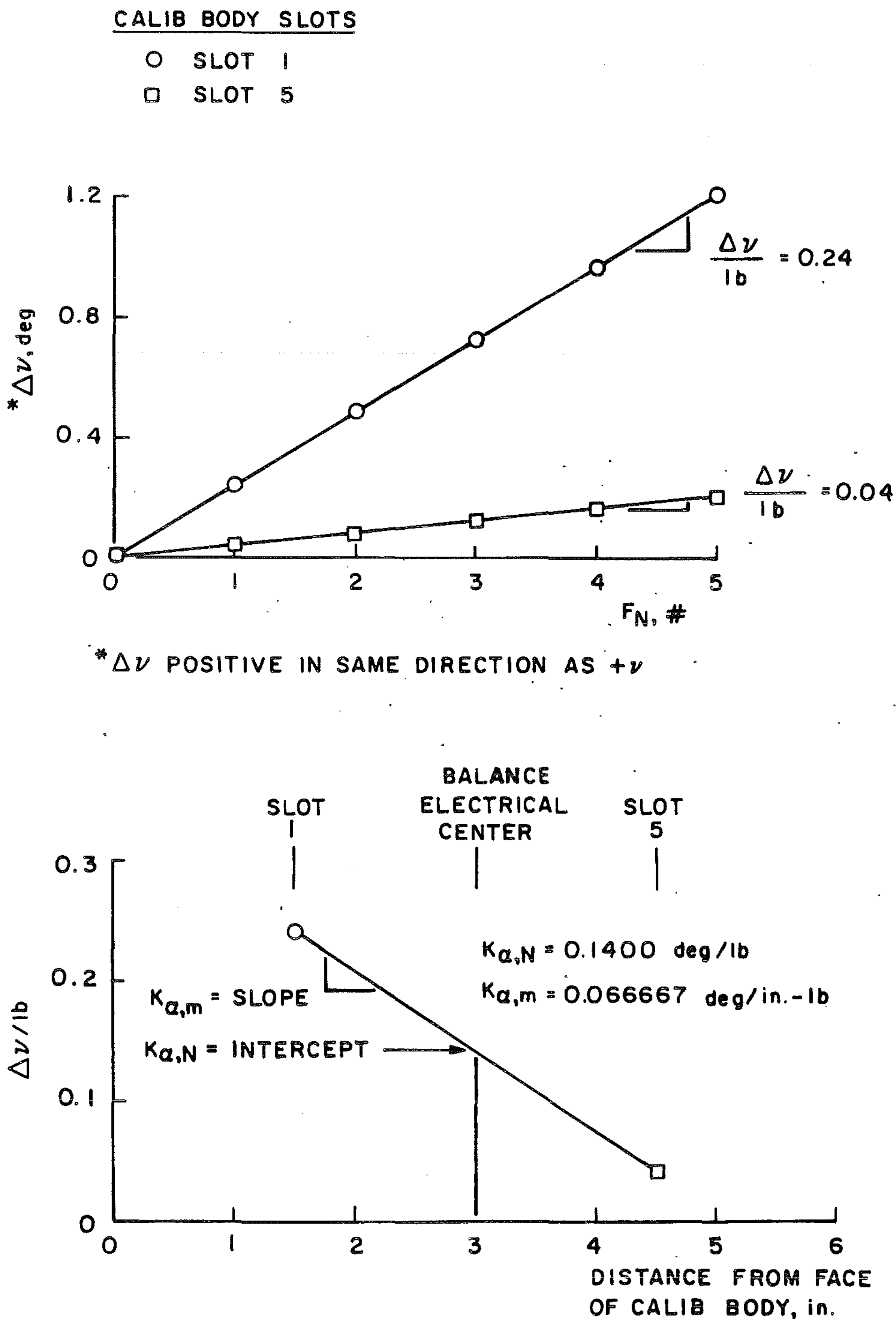

a. Angular (pitch plane)

Figure B-1. Typical sting deflections constants definition.

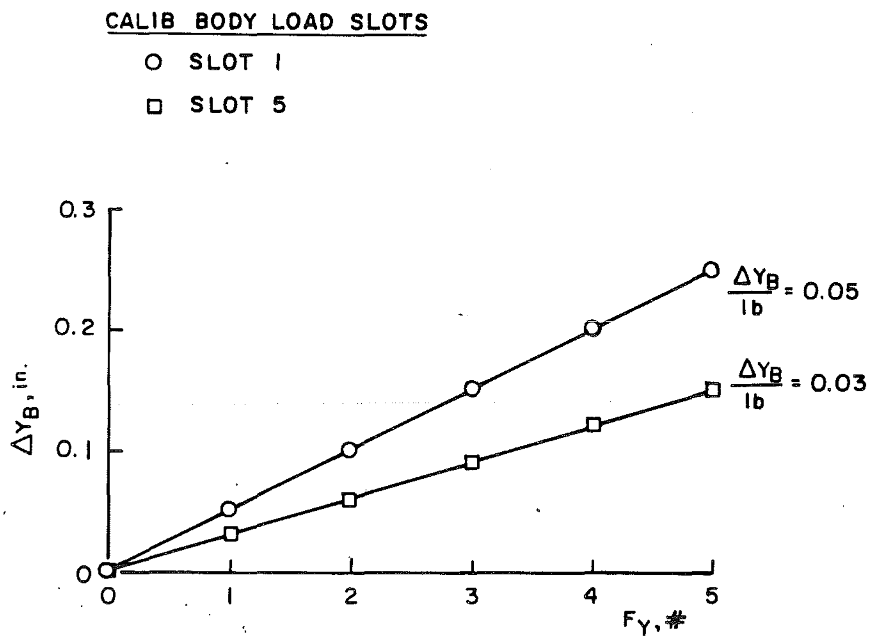

*ΔY_B MEASURED AT BALANCE ELECTRICAL CENTER
ΔY_B POSITIVE IN SAME DIRECTION AS $+F_Y$

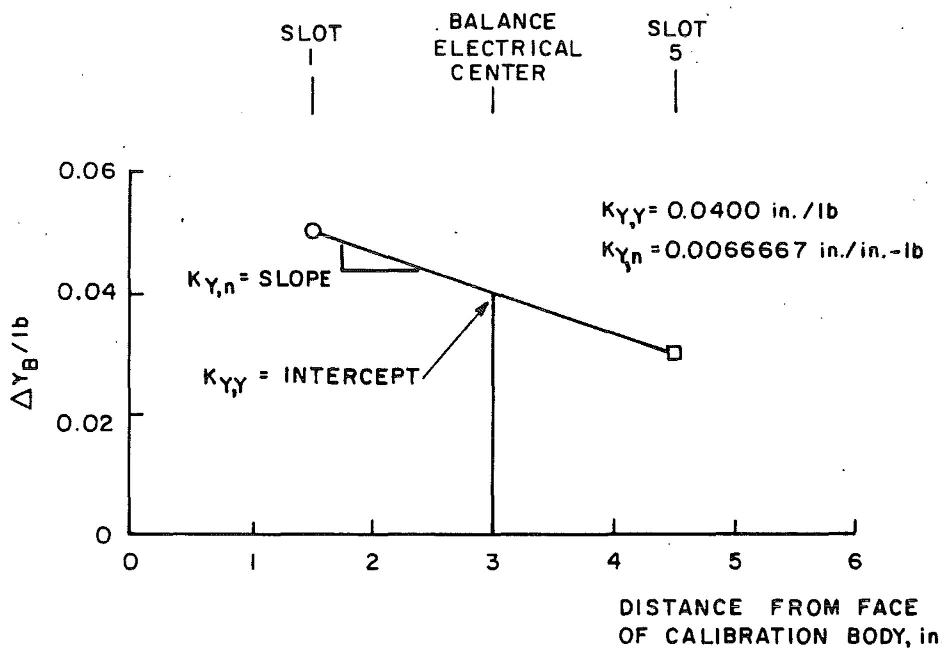

b. Linear (side plane)
Figure B-1. Concluded.

APPENDIX C
CONVERSION MODULE EQUATIONS

Pickup Integration Results

$$\left.\begin{aligned} u &= P1 \\ v &= P2 \\ w &= P3 \end{aligned}\right\} \quad \text{Body-axis linear velocities}$$

$$\left.\begin{aligned} X_I &= P4 \\ Y_I &= P5 \\ Z_I &= P6 \end{aligned}\right\} \quad \text{Inertial-axis positions}$$

$$\left.\begin{aligned} p &= P7 \\ q &= P8 \\ r &= P9 \end{aligned}\right\} \quad \text{Body-axis angular velocities}$$

$$\left[\text{TOBODY}\right] = \begin{bmatrix} P10 & P13 & P16 \\ P11 & P14 & P17 \\ P12 & P15 & P18 \end{bmatrix} \quad \begin{array}{l}\text{Inertial-to-body-axis} \\ \text{direction cosine matrix}\end{array}$$

$$\left.\begin{aligned} u_B &= P19 \\ v_B &= P20 \\ w_B &= P21 \end{aligned}\right\} \quad \begin{array}{l}\text{Rotation center (hook) velocities} \\ \text{(staged release applications)}\end{array}$$

Euler Orientation (see Fig. C-1)

$$\theta_I = \sin^{-1}\left[-\text{TOBODY}\ (1,3)\right]$$

$$\psi_I = \sin^{-1}\left[\text{TOBODY}\ (1,2)/\cos\theta_I\right]$$

$$\phi_I = \tan^{-1}\left[\text{TOBODY}\ (2,3)/\text{TOBODY}\ (3,3)\right]$$

Pitch, Yaw, Roll Orientation (see Fig. C-2)

$$\eta_I = \sin^{-1}\left[\text{TOBODY}\ (1,2)\right]$$

$$\nu_I = \sin^{-1}\left[-\text{TOBODY}\ (1,3)/\cos\eta_I\right]$$

$$\omega_I = \tan^{-1}\left[-\text{TOBODY}\ (3,2)/\text{TOBODY}\ (2,2)\right]$$

If (NOROLL ≠ 0), call nonrolling capacity routine (see Appendix L.)

Inertial-Axis Velocities

$$\begin{vmatrix} \dot{X}_I \\ \dot{Y}_I \\ \dot{Z}_I \end{vmatrix} = \left[\text{TOBODY} \right]' \begin{vmatrix} u \\ v \\ w \end{vmatrix}$$

Weight Components, Total Store Velocity, and Dynamic Pressure at Altitude

$$\begin{vmatrix} \overline{W}_X \\ \overline{W}_Y \\ \overline{W}_Z \end{vmatrix} = \left[\text{TOBODY} \right] \begin{vmatrix} W'_X \\ W'_Y \\ W'_Z \end{vmatrix}$$

$$U_R = \left[(U_A + \dot{X}_I)^2 + (\dot{Y}_I)^2 + (\dot{Z}_I)^2 \right]^{1/2}$$

$$q_A = 0.5\, \rho_A U_R^2$$

Total Velocity Components (Body Axis)

$$\begin{vmatrix} U_{A,X} \\ U_{A,Y} \\ U_{A,Z} \end{vmatrix} = \left[\text{TOBODY} \right] \begin{vmatrix} U_A \\ 0 \\ 0 \end{vmatrix}$$

$$V_X = U_{A,X} + u$$

$$V_Y = U_{A,Y} + v$$

$$V_Z = U_{A,Z} + w$$

Store Angle of Attack and Sideslip Angle

$$\alpha_S = \tan^{-1} (V_Z / V_X)$$

$$\beta_S = \sin^{-1} (V_Y / U_R)$$

Lanyard Length

$$\begin{vmatrix} X_{L,o} \\ Y_{L,o} \\ Z_{L,o} \end{vmatrix} = \left[\text{TOBODY}\right]' \begin{vmatrix} -X_1 \\ -Y_1 \\ -Z_1 \end{vmatrix}$$ Define reference point on aircraft (initial pass only).

$$\theta_p = q_p(t)\, 57.2958$$

$$\begin{vmatrix} X_{L,S} \\ Y_{L,S} \\ Z_{L,S} \end{vmatrix} = \left[\text{TOBODY}\right]' \begin{vmatrix} -X_o \\ -Y_o \\ -Z_o \end{vmatrix}$$ Define reference point on store.

$$\left.\begin{aligned} \Delta X_{L,S} &= X_{L,S} + X_I - X_{L,o} \\ \Delta Y_{L,S} &= Y_{L,S} + Y_I - Y_{L,o} \\ \Delta Z_{L,S} &= Z_{L,S} + Z_I - Z_{L,o} \end{aligned}\right\} \text{ For } \theta p = 0.$$

$$\left.\begin{aligned} \Delta X_{L,S} &= X_{L,S} + X_I - X_{L,o} + R_p \sin\theta_p + U_A t \\ \Delta Y_{L,S} &= Y_{L,S} + Y_I - Y_{L,o} \\ \Delta Z_{L,S} &= Z_{L,S} + Z_I - Z_{L,o} - R_p (1 - \cos\theta_p) \end{aligned}\right\} \text{ For } \theta p \neq 0.$$

$$Z_{L,C} = \left[(\Delta X_{L,S})^2 + (\Delta Y_{L,S})^2 + (\Delta Z_{L,S})^2\right]^{1/2}$$ Lanyard length.

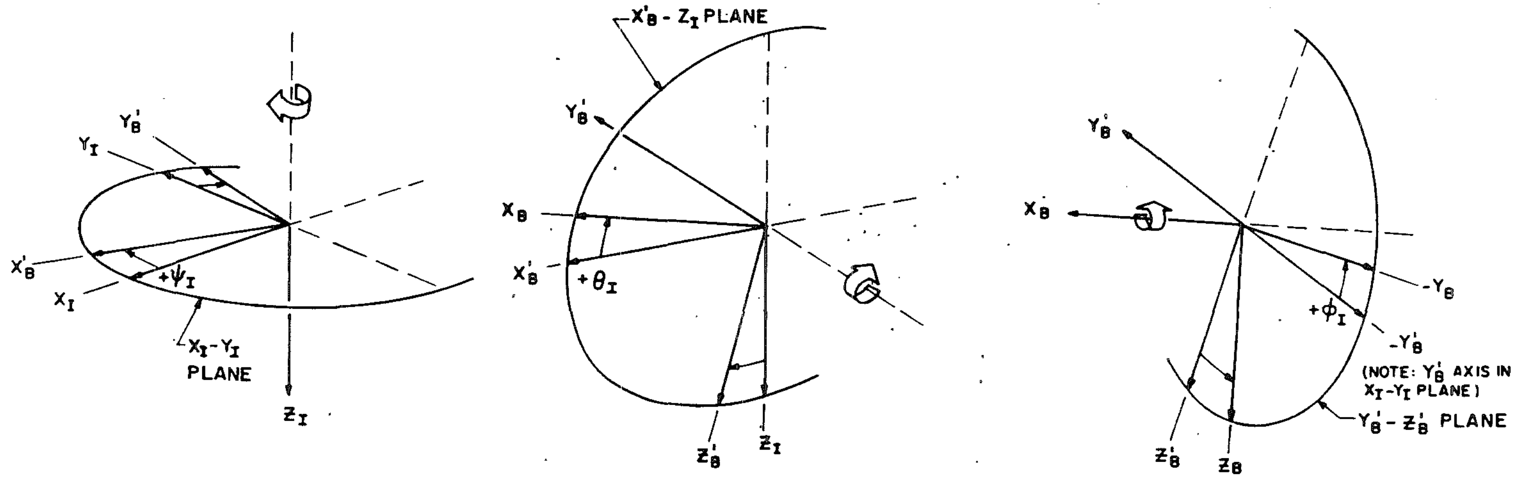

a). FIRST ROTATION, YAW ANGLE (ψ_I)
(ROTATE ABOUT Z_I AXIS)

b) SECOND ROTATION, PITCH ANGLE (θ_I)
(ROTATE ABOUT Y'_B AXIS)

c) THIRD ROTATION, ROLL ANGLE (ϕ_I)
(ROTATE ABOUT X_B AXIS)

Figure C-1. Graphic illustration of a yaw, pitch, roll (Euler) orientation sequence.

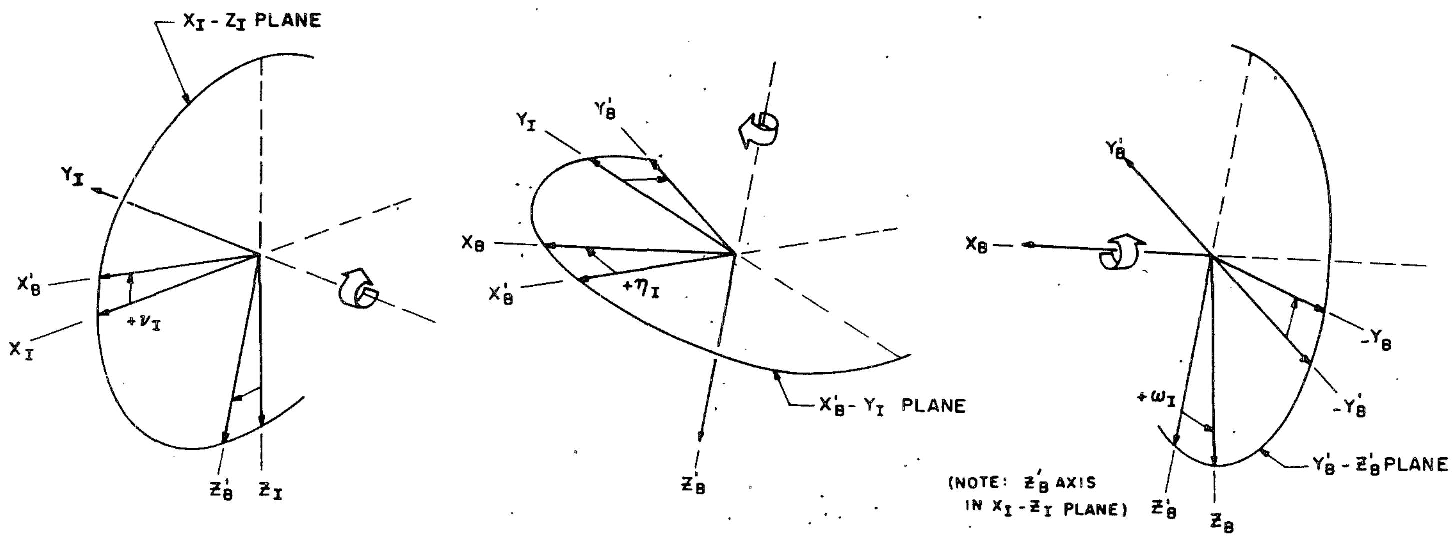

a) FIRST ROTATION, PITCH ANGLE (ν_I)
(ROTATE ABOUT Y_I AXIS)

b) SECOND ROTATION, YAW ANGLE (η_I)
(ROTATE ABOUT Z'_B AXIS)

c) THIRD ROTATION, ROLL ANGLE (ω_I)
(ROTATE ABOUT X_B AXIS)

Figure C-2. Graphic illustration of a pitch, yaw, roll orientation sequence.

APPENDIX D
OFFSET COEFFICIENT MODULE EQUATIONS

The flow diagram for the standard offset coefficient module is shown in Fig. D-1. The equations are listed below.

Initial Values, Control Flag (Section A)

$$t_{DEL} = 0 \qquad C_{A,o} = \left(C_{A,o}\right)_o \qquad C_{\ell,o} = \left(C_{\ell,o}\right)_o$$

$$COEF = COEFI \qquad C_{Y,o} = \left(C_{Y,o}\right)_o \qquad C_{m,o} = \left(C_{m,o}\right)_o$$

$$C_{N,o} = \left(C_{N,o}\right)_o \qquad C_{n,o} = \left(C_{n,o}\right)_o$$

Ramp Axial-Force Equation (Section B)

$$C_{A,o} = \frac{dC_{A,o}}{dt}\left(t - t_{DEL}\right) + \left(C_{A,o}\right)_o$$

COEF	OPTIONS
0	CONSTANT COEFFICIENTS
1	RAMP AXIAL FORCE
2	DELAYED RAMP AXIAL FORCE

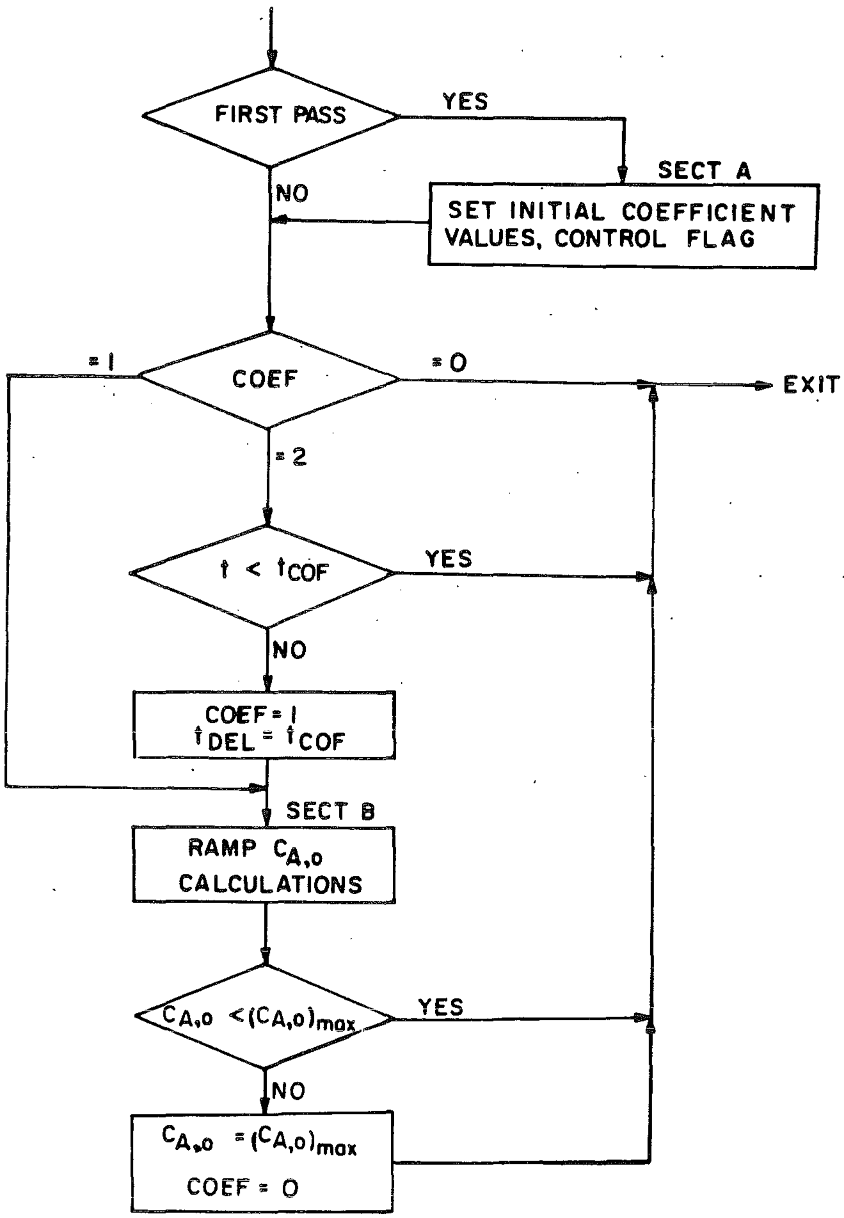

Figure D-1. Flow diagram of the standard offset coefficient module.

APPENDIX E
TOTAL COEFFICIENT MODULE EQUATIONS

Total Coefficient Calculations

$$C_{A,t,T} = C_{A,t,x} + C_{A,o}$$

$$C_{Y,T} = C_{Y,x} + C_{Y,o}$$

$$C_{N,T} = C_{N,x} + C_{N,o}$$

$$C_{\ell,T} = C_{\ell,x} + C_{\ell,o} + C_{\ell_p} \left[p\ell_3/2U_R \right]$$

$$C_{m,T} = C_{m,x} + C_{m,o} + C_{m_q} \left[q\ell_1/2U_R \right]$$

$$C_{n,T} = C_{n,x} + C_{n,o} + C_{n_r} \left[r\ell_2/2U_R \right]$$

If (NOROLL $= 3$) $C_{\ell,T} = 0$

APPENDIX F
THRUST MODULE EQUATIONS

The flow diagram for the standard thrust module is shown in Fig. F-1, and a graphic description is presented in Fig. F-2. The equations for calculating thrust force and moment contributions are as follows:

Initialization, Control Flags (Section A)

$$THRUST = THRSTI \qquad F_{T,X} = 0 \qquad M_{T,X} = 0$$

$$t_{DEL} = 0 \qquad F_{T,Y} = 0 \qquad M_{T,Y} = 0$$

$$t_{t,C1} = 0 \qquad F_{T,Z} = 0 \qquad M_{T,Z} = 0$$

$$t_{t,C2} = 0$$

$$Z_{T,C} = 0$$

First Polynomial for $F_{T,X}$ (Section B)

$$F_{T,X} = \sum_{o}^{5} a_n (t_t)^n$$

Second Polynomial for $F_{T,X}$ (Section C)

$$F_{T,X} = \sum_{o}^{5} b_n (t_t)^n$$

Thrust Moment Contributions (from Jet Damping) (Section D)

$$M_{T,X} = C_{jd_\ell} (p) F_{T,X}$$

$$M_{T,Y} = C_{jd_m} (q) F_{T,X}$$

$$M_{T,Z} = C_{jd_n} (r) F_{T,X}$$

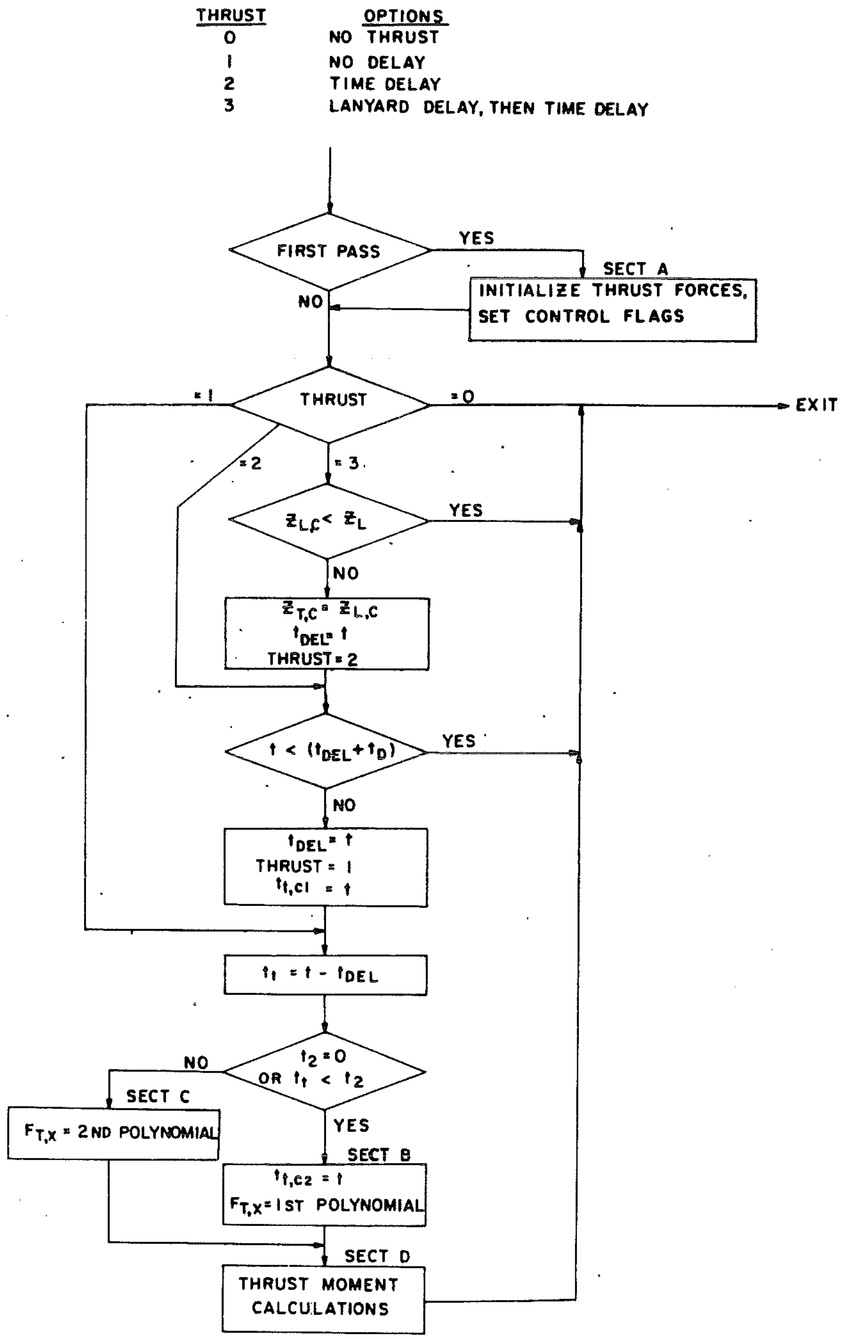

Figure F-1. Flow diagram of the thrust module.

THRUST	CONTROL PARAMETER
0	NO THRUST FORCES
1	NO DELAY (TIME OR LANYARD LENGTH)
2	TIME DELAY ONLY
3	LANYARD DELAY, THEN TIME DELAY

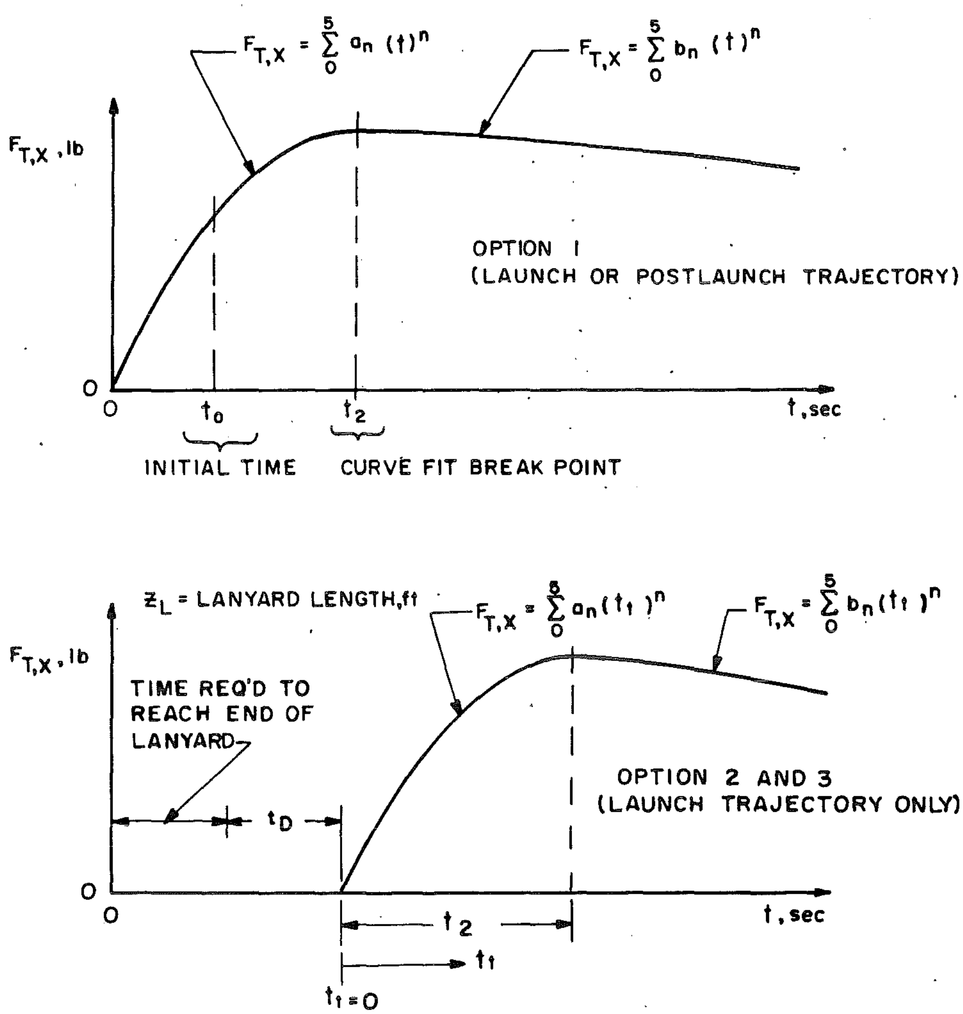

Figure F-2. Graphic description of thrust force.

APPENDIX G
EJECTOR MODULE EQUATIONS

The flow diagram for the standard ejector module is shown in Fig. G-1, and a graphic description is presented in Fig. G-2. The equations for calculating forward and aft ejector force and moment contributions are as follows:

Initialization Equations, Control Flags (Section A)

$$\text{E1 FLAG} = 0 \qquad X_{E1} = X_{cg} - X_{FE}$$

$$\text{E2 FLAG} = 0 \qquad X_{E2} = X_{E1} - \Delta X_{AE}$$

$$Z_{1C} = 0$$

$$Z_{2C} = 0$$

Set Ejector Forces, Moments to Zero (Section B)

$$F_{E1} = 0 \qquad F_{E,X} = 0 \qquad M_{E,X} = 0$$

$$F_{E2} = 0 \qquad F_{E,Y} = 0 \qquad M_{E,Y} = 0$$

$$F_{E,Z} = 0 \qquad M_{E,Z} = 0$$

Stroke Length Equations (Section C)

$$\theta_p = q_p\,(t)\,57.2958$$

$$[AA] = \text{TME}\,(\nu_o + \theta_p, \eta_o, 0, 1)$$

$$[BB] = [\text{TOBODY}]\,[AA]'$$

$$\Delta\theta = \sin^{-1}\left[-BB\,(1, 3)\right]$$

$$\Delta\psi = \sin^{-1}\left[BB\,(1, 2)/\cos\Delta\theta\right]$$

$$Z_{1E} = \left[Z_I - R_p\,(1 - \cos\theta_p) - X_{E1}\sin\Delta\theta\right]\cos\,(I_R + \omega_m) - \left[Y_I + X_{E1}\sin\Delta\psi\right]\sin\,(I_R + \omega_m)$$

$$Z_{2E} = \left[Z_I - R_p\,(1 - \cos\theta_p) - X_{E2}\sin\Delta\theta\right]\cos\,(I_R + \omega_m) - \left[Y_I + X_{E2}\sin\Delta\psi\right]\sin\,(I_R + \omega_m)$$

Forward Ejector, First Polynomial

$$F_{E1} = \sum_{o}^{5} c_n (Z_{1E})^n \qquad (\text{Eject} \leq 2)$$

$$F_{E1} = \sum_{o}^{5} c_n (t)^n \qquad (\text{Eject} = 3)$$

Forward Ejector, Second Polynomial

$$F_{E1} = \sum_{o}^{5} d_n (Z_{1E})^n \qquad (\text{Eject} \leq 2)$$

$$F_{E1} = \sum_{o}^{5} d_n (t)^n \qquad (\text{Eject} = 3)$$

Aft Ejector, First Polynomial

$$F_{E2} = \sum_{o}^{5} e_n (Z_{2E})^n \qquad (\text{Eject} \leq 2)$$

$$F_{E2} = \sum_{o}^{5} e_n (t)^n \qquad (\text{Eject} = 3)$$

Aft Ejector, Second Polynomial

$$F_{E2} = \sum_{o}^{5} f_n (Z_{2E})^n \qquad (\text{Eject} \leq 2)$$

$$F_{E2} = \sum_{o}^{5} f_n (t)^n \qquad (\text{Eject} = 3)$$

Component Resolution Equations (Section D)

$$F_{E,X} = 0$$

$$F_{E,Y} = -(F_{E1} + F_{E2}) \sin \omega_m$$

$$F_{E,Z} = (F_{E1} + F_{E2}) \cos \omega_m$$

$$M_{E,X} = 0$$

$$M_{E,Y} = -\left[F_{E1} X_{E1} + F_{E2} X_{E2}\right] \cos \omega_m$$

$$M_{E,Z} = -\left[F_{E1} X_{E1} + F_{E2} X_{E2}\right] \sin \omega_m$$

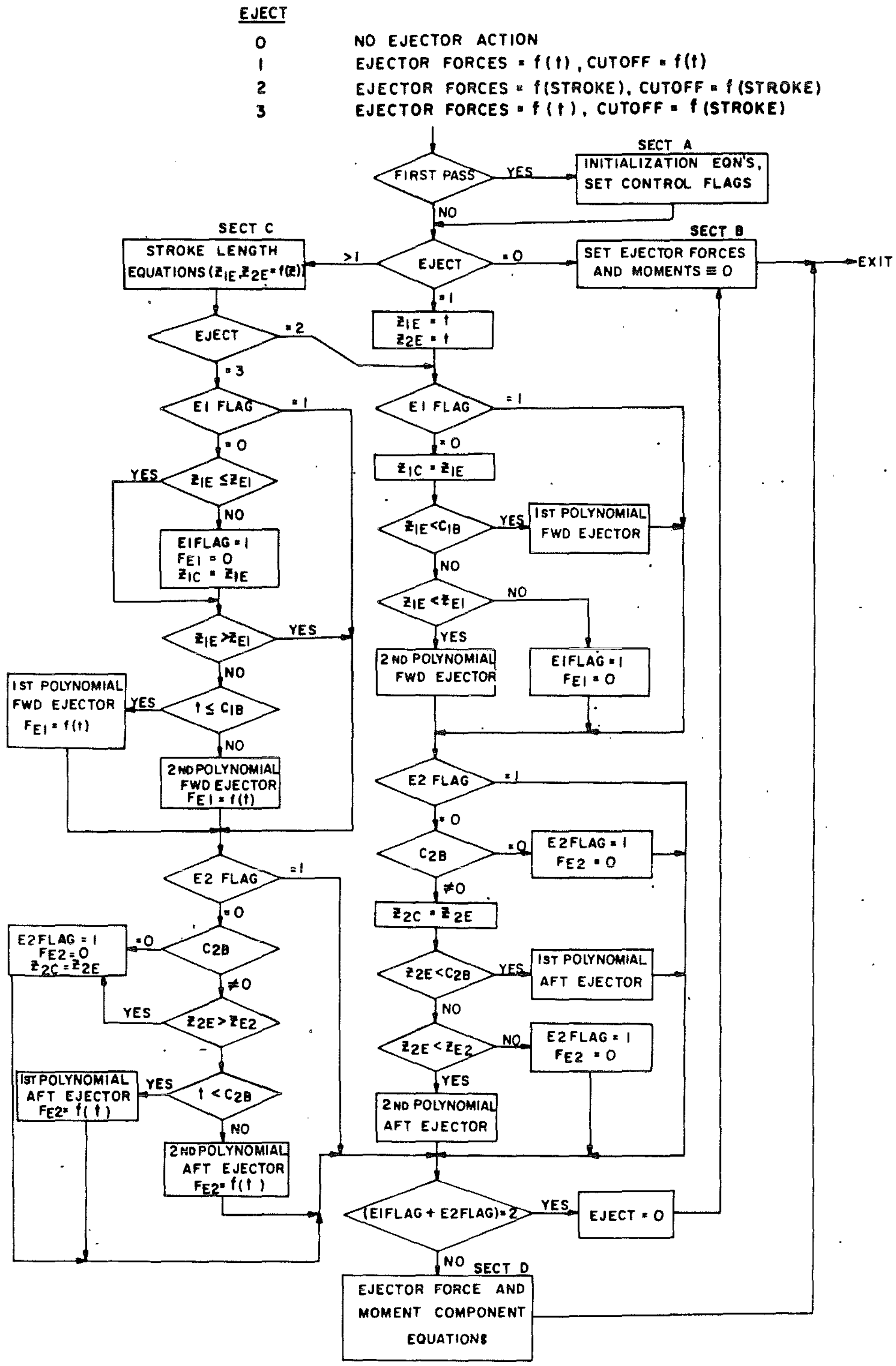

Figure G-1. Flow diagram of the ejector module.

EJECT	CONTROL PARAMETER
0	NO EJECTOR FORCES
1	EJECTOR FORCES & CUTOFF = f(TIME)
2	EJECTOR FORCES & CUTOFF = f(STROKE)
3	EJECTOR FORCES = f(TIME), CUTOFF = f(STROKE)

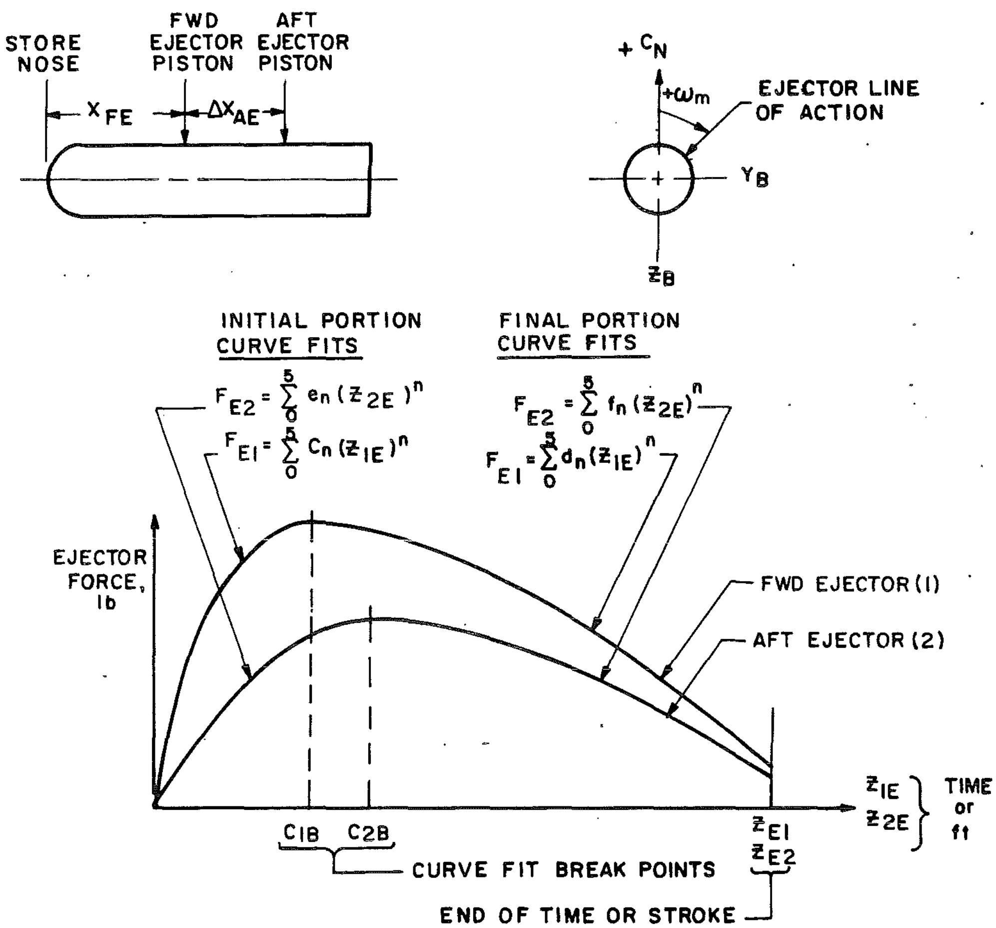

Figure G-2. Graphic description of ejector forces.

APPENDIX H
FULL-SCALE FORCE AND MOMENT MODULE EQUATIONS

For a free-falling store, components of the full-scale forces and moments acting through or about the store cg are described as follows:

Forces

$$F_X = \overline{W}_X - q_A A C_{A,t,T} + F_{T,X} + F_{E,X}$$

$$F_Y = \overline{W}_Y + q_A A C_{Y,T} + F_{T,Y} + F_{E,Y}$$

$$F_Z = \overline{W}_Z - q_A A C_{N,T} + F_{T,Z} + F_{E,Z}$$

Moments

$$M_X = q_A A \ell_3 C_{\ell,T} + M_{T,X} + M_{E,X}$$

$$M_Y = q_A A \ell_1 C_{m,T} + M_{T,Y} + M_{E,Y}$$

$$M_Z = q_A A \ell_2 C_{n,T} + M_{T,Z} + M_{E,Z}$$

When staged release occurs, additional terms required to define the full-scale moments and forces are given in Appendix I.

APPENDIX I
DYNAMIC EQUATIONS OF MOTION MODULE

The flow diagram for the dynamic equations of motion module is shown in Fig. I-1. Positive directions for the full-scale forces and moments are given in Fig. I-2, and graphic descriptions of pivoting, rail-restricted, and ejector-restricted motion are presented in Fig. I-3. The equations for calculating restraining forces and moments, accelerations, and velocities are listed as follows in blocks as noted on the flow diagram.

Unrestricted Motion (Section A)

$$\dot{u} = F_X/m - qw + rv$$
$$\dot{v} = F_Y/m - ru + pw$$
$$\dot{w} = F_Z/m - pv + qu$$

Body–axis linear accelerations

$$\begin{vmatrix} \dot{X}_I \\ \dot{Y}_I \\ \dot{Z}_I \end{vmatrix} = \left[\text{TOBODY} \right]' \begin{vmatrix} u \\ v \\ w \end{vmatrix}$$

Inertial–axis linear velocities

$$\begin{vmatrix} H_X \\ H_Y \\ H_Z \end{vmatrix} = \left[I \right] \begin{vmatrix} p \\ q \\ r \end{vmatrix}$$

Angular momentum

$$\dot{H}_X = M_X + rH_Y - qH_Z$$
$$\dot{H}_Y = M_Y + pH_Z - rH_X$$
$$\dot{H}_Z = M_Z + qH_X - pH_Y$$

Angular momentum derivatives

$$\begin{vmatrix} \dot{p} \\ \dot{q} \\ \dot{r} \end{vmatrix} = \left[I \right]^{-1} \begin{vmatrix} \dot{H}_X \\ \dot{H}_Y \\ \dot{H}_Z \end{vmatrix}$$

Body–axis angular accelerations

From Inertia to body: $\vec{F} = m \left.\frac{d\vec{V}_c}{dt}\right|_{Body} + m(\vec{\omega} \times \vec{V}_c)$

$\vec{M} = \frac{d\vec{H}}{dt} + (\vec{\omega} \times \vec{H})$

were ω = angular velocity

Identity for derivative of an arbitrary vector referred to a rotating body frame of angular velocity ω is;

$\frac{d\vec{A}}{dt} = \left.\frac{d\vec{A}}{dt}\right|_{Body} + \vec{\omega} \times \vec{A}$

$\vec{\omega} = p i + q j + r k$

$\vec{r} = x i + y j + z k$

Allows so that moments of inertia will not vary with time (ref. frame rotates with body)

Matrix to convert from body to inertia axis

$$[I] = \begin{bmatrix} I_x & -I_{xy} & -I_{xz} \\ -I_{xy} & I_y & -I_{yz} \\ -I_{xz} & -I_{yz} & I_z \end{bmatrix}$$

$H_x = pI_x - qI_{xy} - rI_{xz}$

$H_y = -pI_{xy} + qI_y - rI_{yz}$

$H_z = -pI_{xz} - qI_{yz} + rI_z$

L (Rolling Moment), M (Pitching Moment), N (Yawing Moment)

Assumes Body Axis is placed at xz plane of symmetry $I_{yz} = I_{xy} = 0$

Inertia Conversion (Section B1)

X_o, Y_o, Z_o – Distance from pivot point to store cg

$$\bar{I}_{XX} = I_{XX} + m\left(Y_o^2 + Z_o^2\right)$$

$$\bar{I}_{XY} = I_{XY} + m\,X_oY_o$$

$$\bar{I}_{XZ} = I_{XZ} + m\,X_oZ_o$$

$$\bar{I}_{YY} = I_{YY} + m\left(X_o^2 + Z_o^2\right)$$

$$\bar{I}_{YZ} = I_{YZ} + m\,Y_oZ_o$$

$$\bar{I}_{ZZ} = I_{ZZ} + m\left(X_o^2 + Y_o^2\right)$$

$$\left[\bar{I}\right] = \begin{bmatrix} \bar{I}_{XX} & -\bar{I}_{XY} & -\bar{I}_{XZ} \\ -\bar{I}_{XY} & \bar{I}_{YY} & -\bar{I}_{YZ} \\ -\bar{I}_{XZ} & -\bar{I}_{YZ} & \bar{I}_{ZZ} \end{bmatrix}$$ Inertia matrix about rotation center

$$\left[\bar{I}\right]^{-1} = \text{inverse of } \left[\bar{I}\right]$$ Inverse inertia matrix about rotation center

Hook Motion from Accelerating Aircraft (Section B2) in pullup/pushover maneuver (Fig 10)

– from flight axis to aircraft

$$\theta_p = q_p(t)\,57.2958$$ pitch rate at pullup/pushover maneuver

$$[BB] = \text{TME}\,(\nu_o + \theta_p, \eta_o, 0, 1)$$ Inertial–to–pylon matrix (pitch, yaw, roll sequence)

$$[BPYLON] = [TOBODY]\,[BB]'$$ Pylon–to–body matrix

$$[AA] = \text{TME}\,(0, -\theta_p, 0, 2)$$ (Yaw, Pitch, Roll)

$$[EE] = [TOBODY]\,[AA]$$ Flight–to–body matrix

$$\begin{vmatrix} a_{o,X} \\ a_{o,Y} \\ a_{o,Z} \end{vmatrix} = [EE] \begin{vmatrix} 0 \\ 0 \\ a_{Z,p} \end{vmatrix}$$ Resolve A/C (hook) acceleration to body axis

Pivot Motion Equations (Section B3)

For all pivot motion, Y_o must be zero; hence, $\bar{I}_{XY} = \bar{I}_{YZ} \equiv 0$

$R_m = 0$ Pitch reaction moment always "0"

$V_{Z,p} \doteq a_{Z,p} t$ A/C (hook) velocity

$$\begin{vmatrix} v_{o,X} \\ v_{o,Y} \\ v_{o,Z} \end{vmatrix} = [EE] \begin{vmatrix} 0 \\ 0 \\ V_{Z,p} \end{vmatrix}$$ Resolve hook velocity into body axis

$\Delta\dot{\theta}_{CK} = \sin^{-1}\left[-\text{BPYLON}(1,3)\right]$ Store pitch motion travel

Reaction Moments, Pivot Motion, Pitch Only (Section B4A)

Set reaction moments to force $\dot{H}_X = \dot{H}_Z = 0$; hence, $\dot{p} = \dot{r} = p = r = 0$.

$$R_\ell = -\left[M_X - Z_o(F_Y - ma_{o,Y}) - mX_o\, qv_{o,Y}\right]$$

$$R_n = -\left[M_Z + X_o(F_Y - ma_{o,Y}) - mZ_o\, qv_{o,Y}\right]$$

Reaction Moments, Pivot Motion, Pitch and Yaw (Section B4B)

Set reaction moment to force $\dot{p} = 0$; hence $p = 0$.

$$R_n = 0$$

$$R_\ell = -(\bar{I}_{XZ}/\bar{I}_{ZZ})\left[M_Z + X_o(F_Y - ma_{o,Y}) - mZ_o\, qv_{o,Y} - qr\bar{I}_{XZ}\right] - M_X + Z_o\left[F_Y - m(a_{o,Y} + rv_{o,X})\right] + mX_o(qv_{o,Y} + rv_{o,Z}) - qr(\bar{I}_{YY} - \bar{I}_{ZZ})$$

Reaction Moments, Pivot Motion, Pitch, Yaw, and Roll (Section B4C)

$$R_\ell = 0$$

$$R_n = 0$$

Rail Motion (Section B5)

$$\begin{vmatrix} X_{L,S} \\ Y_{L,S} \\ Z_{L,S} \end{vmatrix} = \left[\text{TOBODY}\right]' \begin{vmatrix} -X_o \\ -Y_o \\ -Z_o \end{vmatrix}$$ Define hook reference in inertial axis

$$X_{C,H} = X_{L,S} + X_I + R_p \sin\theta_p$$

$$Y_{C,H} = Y_{L,S} + Y_I$$

$$Z_{C,H} = Z_{L,S} + Z_I - R_p (1 - \cos\theta_p)$$

$$\text{If } (\theta_p \neq 0),\ X_{C,H} = X_{C,H} + U_A(t)$$

$$\begin{vmatrix} X_{P,H} \\ Y_{P,H} \\ Z_{P,H} \end{vmatrix} = \left[\text{BB}\right] \begin{vmatrix} X_{C,H} \\ Y_{C,H} \\ Z_{C,H} \end{vmatrix}$$ Define hook travel along pylon

$$X_{P,CK} = X_{P,H} + X_o$$

$$\begin{vmatrix} F_{P,X} \\ F_{P,Y} \\ F_{P,Z} \end{vmatrix} = \left[\text{BPYLON}\right]' \begin{vmatrix} F_X \\ F_Y \\ F_Z \end{vmatrix}$$ Resolve full-scale forces into pylon axis

$$\begin{vmatrix} a_{P,X} \\ a_{P,Y} \\ a_{P,Z} \end{vmatrix} = \left[\text{BPYLON}\right]' \begin{vmatrix} a_{o,X} \\ a_{o,Y} \\ a_{o,Z} \end{vmatrix}$$ Resolve hook accelerations into pylon axis

$$a_{P,X} = F_{P,X}/m$$ Define hook accelerations along pylon X-axis

$$\begin{vmatrix} \dot{u}_B \\ \dot{v}_B \\ \dot{w}_B \end{vmatrix} = \begin{bmatrix} BPYLON \end{bmatrix} \begin{vmatrix} a_{P,X} \\ a_{P,Y} \\ a_{P,Z} \end{vmatrix}$$ Resolve hook accelerations into body axis

$$\left.\begin{aligned} a_{o,X} &= \dot{u}_B \\ a_{o,Y} &= \dot{v}_B \\ a_{o,Z} &= \dot{w}_B \end{aligned}\right\}$$ Hook accelerations

$$\left.\begin{aligned} v_{o,X} &= u_B \\ v_{o,Y} &= v_B \\ v_{o,Z} &= w_B \end{aligned}\right\}$$ Hook velocities

Reaction Moments, Rail Motion, Translate and Pitch, Side Rail Only (Section B6A)

Z_o must be zero; hence $\bar{I}_{XZ} = \bar{I}_{YZ} \equiv 0$. Reaction moments force, $\dot{p}$, $\dot{r}$ = 0; hence p = r = 0.

$$R_m = 0$$

$$R_\ell = -M_X - F_Z Y_o + mY_o (a_{o,Z} - qv_{o,X}) + mX_o\, qv_{o,Y}$$
$$-(\bar{I}_{XY}/\bar{I}_{YY}) \left[M_Y - F_Z X_o + mX_o\, a_{o,Z} \right]$$

$$R_n = -M_Z - F_Y X_o + F_X Y_o + mX_o\, a_{o,Y} - mY_o (a_{o,X} + qv_{o,Z}) + q^2 \bar{I}_{XY}$$

Reaction Moments, Rail Motion, Translate and Yaw, Bottom Rail Only (Section B6B)

Y_o must be zero; hence $\bar{I}_{XY} = \bar{I}_{YZ} = 0$. Reaction moments force $\dot{p}, \dot{q} = 0$; hence p = 0 and q = 0 or constant.

$$R_n = 0$$

$$R_\ell = -M_X + F_Y Z_o - mZ_o (a_{o,Y} + rv_{o,X}) + mX_o (rv_{o,Z} + qv_{o,Y}) + qr (\bar{I}_{ZZ} - \bar{I}_{YY})$$
$$-(\bar{I}_{XZ}/\bar{I}_{ZZ}) \left[M_Z + F_Y X_o - mX_o\, a_{o,Y} - mZ_o\, qv_{o,Y} - qr \bar{I}_{XZ} \right]$$

$$R_m = -M_Y + F_Z X_o - F_X Z_o + mZ_o (a_{o,X} - rv_{o,Y}) - mX_o\, a_{o,Z} - r^2 \bar{I}_{XZ}$$

Reaction Moments, Rail Motion, Translate, Pitch and Yaw (Section B6C)

Either Y_o or Z_o must be zero; hence $\bar{I}_{YZ} \equiv 0$. Reaction moments force $\dot{p} = 0$; hence $p = 0$.

$$R_m = R_n = 0$$

$$\begin{aligned} R_\ell = & -M_X + F_Y Z_o - F_Z Y_o + mY_o (a_{o,Z} - qv_{o,X}) - mZ_o (a_{o,Y} + rv_{o,X}) \\ & + mX_o (qv_{o,Y} + rv_{o,Z}) + qr (\bar{I}_{ZZ} - \bar{I}_{YY}) \\ & - (\bar{I}_{XY}/\bar{I}_{YY}) \left[M_Y - F_Z X_o + F_X Z_o - mZ_o (a_{o,X} - rv_{o,Y}) \right. \\ & \left. + mX_o a_{o,Z} - mY_o rv_{o,Z} + qr \bar{I}_{XY} + r^2 \bar{I}_{XZ} \right] \\ & - (\bar{I}_{XZ}/\bar{I}_{ZZ}) \left[M_Z + F_Y X_o - F_X Y_o - mX_o a_{o,Y} + mY_o (a_{o,X} + qv_{o,Z}) \right. \\ & \left. - mZ_o qv_{o,Y} - q^2 \bar{I}_{XY} - qr \bar{I}_{XZ} \right] \end{aligned}$$

Pylon Axis Reaction Moments (Section B7)

$$\begin{vmatrix} R_{P,\ell} \\ R_{P,m} \\ R_{P,n} \end{vmatrix} = \left[\text{BPYLON} \right]' \begin{vmatrix} R_\ell \\ R_m \\ R_n \end{vmatrix}$$

Rail Translation Only Motion (Section C1)

For this case, a rotation center is undefined; consequently, cg velocities and accelerations are equal to hook velocities and accelerations.

$$R_\ell = -M_X + F_Y Z_o - F_Z Y_o + mY_o (a_{o,Z} - qv_{o,X}) - mZ_o (a_{o,Y} + rv_{o,X})$$

$$R_m = -M_Y$$

$$R_n = -M_Z$$

$$\begin{vmatrix} R_{P,\ell} \\ R_{P,m} \\ R_{P,n} \end{vmatrix} = \left[\text{BPYLON} \right]' \begin{vmatrix} R_\ell \\ R_m \\ R_n \end{vmatrix} \quad \text{Pylon-axis reaction moments}$$

$$\left.\begin{aligned} \dot{p} &= 0 \\ \dot{q} &= 0 \\ \dot{r} &= 0 \end{aligned}\right\}$$ Body-axis angular accelerations

$$\left.\begin{aligned} \dot{u} &= \dot{u}_B \\ \dot{v} &= \dot{v}_B \\ \dot{w} &= \dot{w}_B \end{aligned}\right\}$$ Body-axis linear accelerations

$$\begin{vmatrix} \dot{X}_I \\ \dot{Y}_I \\ \dot{Z}_I \end{vmatrix} = \left[\mathrm{TOBODY}\right]' \begin{vmatrix} u \\ v \\ w \end{vmatrix}$$ Inertial-axis linear velocities

$$\begin{aligned} R_{P,X} &= 0 \\ R_{P,Y} &= m\,a_{o,Y} - F_{P,Y} \\ R_{P,Z} &= m\,a_{o,Z} - F_{P,Z} \end{aligned}$$ Pylon-axis reaction forces

$$\begin{vmatrix} R_X \\ R_Y \\ R_Z \end{vmatrix} = \left[\mathrm{BPYLON}\right] \begin{vmatrix} R_{P,X} \\ R_{P,Y} \\ R_{P,Z} \end{vmatrix}$$ Body-axis reaction forces

Restrained Motion Rotational Dynamics (Section C2)

$$\begin{vmatrix} H_X \\ H_Y \\ H_Z \end{vmatrix} = \left[\bar{I}\right] \begin{vmatrix} p \\ q \\ r \end{vmatrix}$$ Angular momentum

$$\dot{H}_X = M_X + F_Z Y_o - F_Y Z_o + R_\ell + rH_Y - qH_Z - mX_o (qv_{o,Y} + rv_{o,Z})$$
$$- mY_o (a_{o,Z} - qv_{o,X}) + mZ_o (a_{o,Y} + rv_{o,X})$$
$$\dot{H}_Y = M_Y - F_Z X_o + F_X Z_o + R_m + pH_Z - rH_X + mX_o (a_{o,Z} + pv_{o,Y})$$
$$- mY_o (rv_{o,Z} + pv_{o,X}) - mZ_o (a_{o,X} - rv_{o,Y})$$
$$\dot{H}_Z = M_Z + F_Y X_o - F_X Y_o + R_n + qH_X - pH_Y - mX_o (a_{o,Y} - pv_{o,Z})$$
$$+ mY_o (a_{o,X} + qv_{o,Z}) - mZ_o (pv_{o,X} + qv_{o,Y})$$

$$\begin{vmatrix} \dot{p} \\ \dot{q} \\ \dot{r} \end{vmatrix} = \left[\bar{I}\right]^{-1} \begin{vmatrix} \dot{H}_X \\ \dot{H}_Y \\ \dot{H}_Z \end{vmatrix}$$ Body-axis angular accelerations

Restrained Motion Translational Dynamics (Section C3)

If (MOTION $\neq$ 3), $\dot{p} = 0$

$$\left.\begin{aligned} \dot{u} &= a_{o,X} + \dot{q}Z_o - \dot{r}Y_o \\ \dot{v} &= a_{o,Y} + \dot{r}X_o - \dot{p}Z_o \\ \dot{w} &= a_{o,Z} - \dot{q}X_o \end{aligned}\right\}$$ Body-axis linear accelerations

$$\begin{vmatrix} \dot{X}_I \\ \dot{Y}_I \\ \dot{Z}_I \end{vmatrix} = \left[\text{TOBODY}\right]' \begin{vmatrix} u \\ v \\ w \end{vmatrix}$$ Inertial-axis linear velocities

Reaction Forces (Section C4)

$$a_X = a_{o,X} - X_o (q^2 + r^2) + Y_o (pq - \dot{r}) + Z_o (\dot{q} + pr) + qv_{o,Z} - rv_{o,Y}$$
$$a_Y = a_{o,Y} + X_o (\dot{r} + pq) - Y_o (r^2 + p^2) + Z_o (qr - \dot{p}) + rv_{o,X} - pv_{o,Z}$$
$$a_Z = a_{o,Z} + X_o (pr - \dot{q}) + Y_o (\dot{p} + qr) - Z_o (p^2 + q^2) + pv_{o,Y} - qv_{o,X}$$

$$\left.\begin{aligned} R_X &= ma_X - F_X \\ R_Y &= ma_Y - F_Y \\ R_Z &= ma_Z - F_Z \end{aligned}\right\}$$ Body-axis reactions forces

$$\begin{vmatrix} R_{P,X} \\ R_{P,Y} \\ R_{P,Z} \end{vmatrix} = \left[\text{BPYLON}\right]' \begin{vmatrix} R_X \\ R_Y \\ R_Z \end{vmatrix}$$ Pylon-axis reaction forces

Rail Reaction Forces (Section C5B)

$$R_{P,X} = 0$$

$$\begin{vmatrix} R_X \\ R_Y \\ R_Z \end{vmatrix} = \left[\text{BPYLON}\right] \begin{vmatrix} R_{P,X} \\ R_{P,Y} \\ R_{P,Z} \end{vmatrix}$$ Body-axis reaction forces

Ejector Plane Restraint Equations (Section C5C)

$$\theta_p = q_p(t)\,57.2958$$

$$\left[\text{EJ}\right] = \text{TME}\,(\nu_o + \theta_p,\ \eta_o,\ \omega_m + I_R,\ 1)$$ Inertial-to-ejector matrix

$$\left[\text{EBODY}\right] = \left[\text{TOBODY}\right]\left[\text{EJ}\right]'$$ Ejector-to-body matrix

$$\left[\text{AA}\right] = \text{TME}\,(0,\ -\theta_p,\ 0,\ 2)$$

$$\left[\text{EE}\right] = \left[\text{TOBODY}\right]\left[\text{AA}\right]$$ Flight-to-body matrix

$$\left[\text{BB}\right] = \text{TME}\,(\nu_o + \theta_p,\ \eta_o,\ 0,\ 1)$$ Inertial-to-pylon matrix

$$\left[\text{BPYLON}\right] = \left[\text{TOBODY}\right]\left[\text{BB}\right]'$$ Pylon-to-body matrix

$$\left.\begin{aligned} M_{X,B} &= M_X + qr\,(I_{YY} - I_{ZZ}) \\ M_{Y,B} &= M_Y + pr\,(I_{ZZ} - I_{XX}) \\ M_{Z,B} &= M_Z + pq\,(I_{XX} - I_{YY}) \end{aligned}\right\} \quad \text{Unrestrained body-axis moments}$$

$$\begin{vmatrix} M_{X,E} \\ M_{Y,E} \\ M_{Z,E} \end{vmatrix} = \left[\text{EBODY}\right]' \begin{vmatrix} M_{X,B} \\ M_{Y,B} \\ M_{Z,B} \end{vmatrix} \quad \text{Unrestrained ejector-axis moments}$$

$$\left.\begin{aligned} R_{\ell,E} &= -M_{X,E} \\ R_{m,E} &= 0 \\ R_{n,E} &= -M_{Z,E} \end{aligned}\right\} \quad \text{Reaction moments, ejector axis}$$

$$\begin{vmatrix} R_\ell \\ R_m \\ R_n \end{vmatrix} = \left[\text{EBODY}\right] \begin{vmatrix} R_{\ell,E} \\ R_{m,E} \\ R_{n,E} \end{vmatrix} \quad \text{Reaction moments, body axis}$$

$$\begin{vmatrix} R_{P,\ell} \\ R_{P,m} \\ R_{P,n} \end{vmatrix} = \left[\text{BPYLON}\right]' \begin{vmatrix} R_\ell \\ R_m \\ R_n \end{vmatrix} \quad \text{Reaction moments, pylon axis}$$

$$\left.\begin{aligned} \dot{H}_X &= M_X + qr\,(I_{YY} - I_{ZZ}) + R_\ell \\ \dot{H}_Y &= M_Y + pr\,(I_{ZZ} - I_{XX}) + R_m \\ \dot{H}_Z &= M_Z + pq\,(I_{XX} - I_{YY}) + R_n \end{aligned}\right\} \quad \text{Angular momentum derivatives}$$

$$\begin{vmatrix} \dot{p} \\ \dot{q} \\ \dot{r} \end{vmatrix} = \left[I \right]^{-1} \begin{vmatrix} \dot{H}_X \\ \dot{H}_Y \\ \dot{H}_Z \end{vmatrix}$$

Body-axis angular accelerations

$$\begin{vmatrix} a_{o,X} \\ a_{o,Y} \\ a_{o,Z} \end{vmatrix} = \left[EE \right] \begin{vmatrix} 0 \\ 0 \\ a_{Z,p} \end{vmatrix}$$

Resolve A/C acceleration to body axis

$$\begin{vmatrix} a_{X,E} \\ a_{Y,E} \\ a_{Z,E} \end{vmatrix} = \left[EBODY \right]' \begin{vmatrix} a_{o,X} \\ a_{o,Y} \\ a_{o,Z} \end{vmatrix}$$

Resolve A/C acceleration to ejector axis

$$\begin{vmatrix} F_{X,E} \\ F_{Y,E} \\ F_{Z,E} \end{vmatrix} = \left[EBODY \right]' \begin{vmatrix} F_X \\ F_Y \\ F_Z \end{vmatrix}$$

Resolve unrestrained body-axis forces into ejector axis

$$\left.\begin{aligned} R_{X,E} &= m\, a_{X,E} - F_{X,E} \\ R_{Y,E} &= m\, a_{Y,E} - F_{Y,E} \\ R_{Z,E} &= 0 \end{aligned}\right\}$$

Reaction forces, ejector axis

$$\begin{vmatrix} R_X \\ R_Y \\ R_Z \end{vmatrix} = \left[EBODY \right] \begin{vmatrix} R_{X,E} \\ R_{Y,E} \\ R_{Z,E} \end{vmatrix}$$

Reaction forces, body axis

$$\begin{vmatrix} R_{P,X} \\ R_{P,Y} \\ R_{P,Z} \end{vmatrix} = \left[\text{BLYLON} \right]' \begin{vmatrix} R_X \\ R_Y \\ R_Z \end{vmatrix}$$

Reaction forces, pylon axis

$$\left.\begin{aligned} \dot{u} &= (F_X + R_X)/m - qw + rv \\ \dot{v} &= (F_Y + R_Y)/m - ru + pw \\ \dot{w} &= (F_Z + R_Z)/m - pv + qu \end{aligned}\right\}$$

Body–axis linear accelerations

$$\begin{vmatrix} \dot{X}_I \\ \dot{Y}_I \\ \dot{Z}_I \end{vmatrix} = \left[\text{TOBODY} \right]' \begin{vmatrix} u \\ v \\ w \end{vmatrix}$$

Inertial–axis linear velocities

Termination Equations (Section C6)

$R_X = 0$	$R_{P,X} = 0$
$R_Y = 0$	$R_{P,Y} = 0$
$R_Z = 0$	$R_{P,Z} = 0$
$R_\ell = 0$	$R_{P,\ell} = 0$
$R_m = 0$	$R_{P,m} = 0$
$R_n = 0$	$R_{P,n} = 0$
	$\text{MOTION} = 0$

Assign Integrator Inputs (Section D)

$$\dot{P}1 = \dot{u}$$
$$\dot{P}2 = \dot{v}$$
$$\dot{P}3 = \dot{w}$$
$$\dot{P}4 = \dot{X}_I$$

$$\dot{P}5 = \dot{Y}_I$$

$$\dot{P}6 = \dot{Z}_I$$

$$\dot{P}7 = \dot{p}$$

$$\dot{P}8 = \dot{q}$$

$$\dot{P}9 = \dot{r}$$

$$\dot{P}10 = \left[\text{TOBODY }(2,1)\right]r - \left[\text{TOBODY }(3,1)\right]q$$

$$\dot{P}11 = \left[\text{TOBODY }(3,1)\right]p - \left[\text{TOBODY }(1,1)\right]r$$

$$\dot{P}12 = \left[\text{TOBODY }(1,1)\right]q - \left[\text{TOBODY }(2,1)\right]p$$

$$\dot{P}13 = \left[\text{TOBODY }(2,2)\right]r - \left[\text{TOBODY }(3,2)\right]q$$

$$\dot{P}14 = \left[\text{TOBODY }(3,2)\right]p - \left[\text{TOBODY }(1,2)\right]r$$

$$\dot{P}15 = \left[\text{TOBODY }(1,2)\right]q - \left[\text{TOBODY }(2,2)\right]p$$

$$\dot{P}16 = \left[\text{TOBODY }(2,3)\right]r - \left[\text{TOBODY }(3,3)\right]q$$

$$\dot{P}17 = \left[\text{TOBODY }(3,3)\right]p - \left[\text{TOBODY }(1,3)\right]r$$

$$\dot{P}18 = \left[\text{TOBODY }(1,3)\right]q - \left[\text{TOBODY }(2,3)\right]p$$

$$\dot{P}19 = \dot{u}_B$$

$$\dot{P}20 = \dot{v}_B$$

$$\dot{P}21 = \dot{w}_B$$

MOTION	OPTIONS
0	UNRESTRAINED
1	PIVOT; PITCH ONLY
2	PIVOT; PITCH AND YAW
3	PIVOT; PITCH, YAW AND ROLL
4	RAIL; TRANSLATE ONLY
5	RAIL; TRANSLATE AND PITCH
6	RAIL; TRANSLATE AND YAW
7	RAIL; TRANSLATE, PITCH AND YAW
8	TRANSLATE, ROTATE IN EJECTOR PLANE

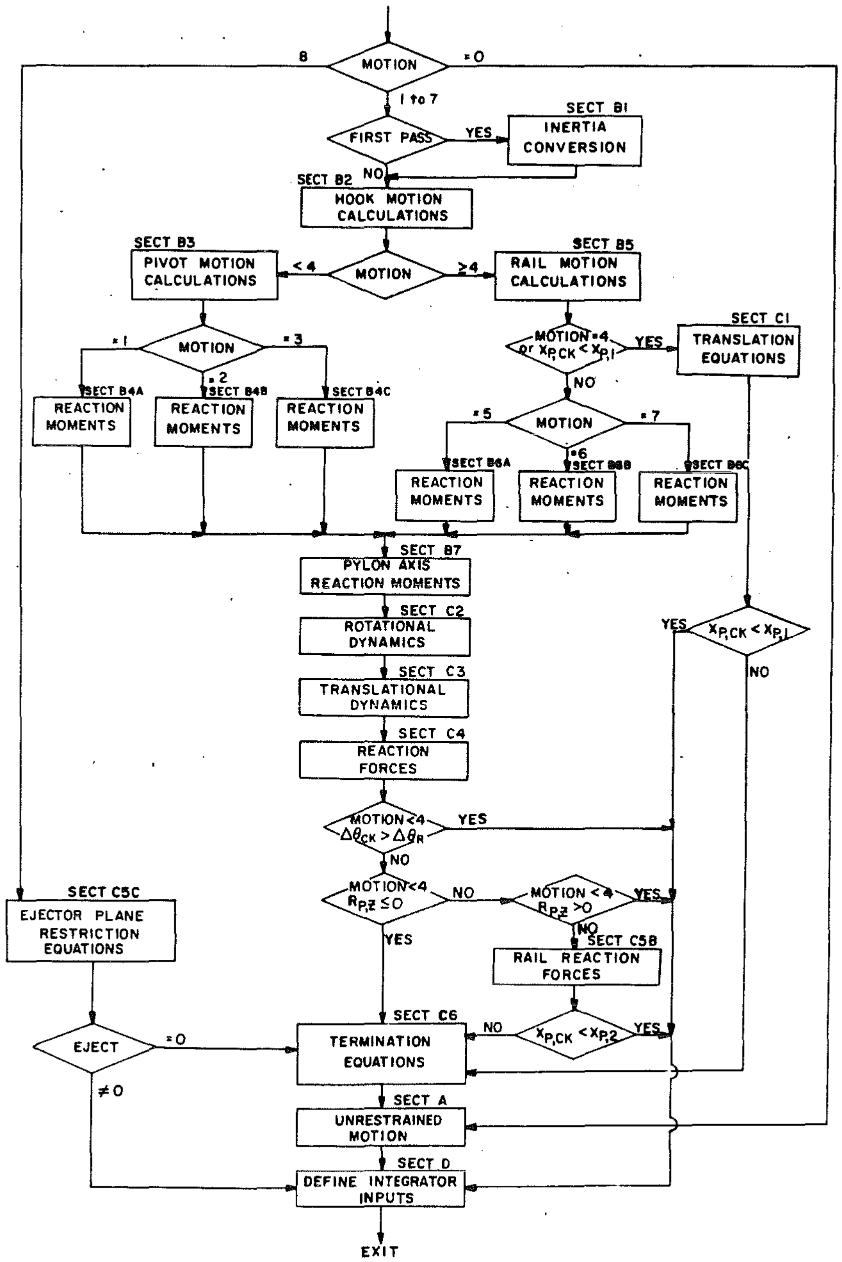

Figure I-1. Flow diagram of the dynamics module.

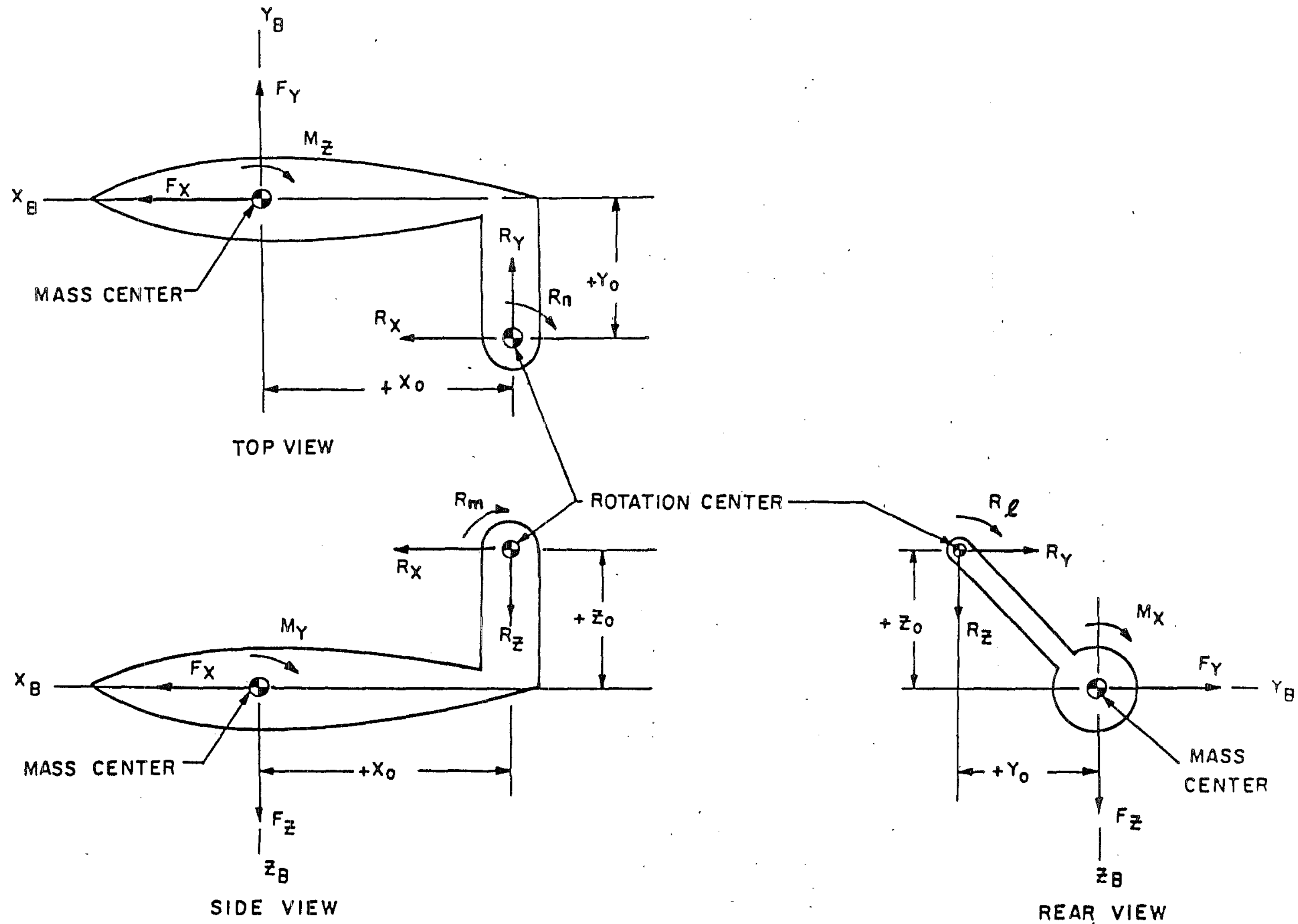

Figure I-2. Positive directions of full-scale forces and moments.

CONTROL PARAMETER IS MOTION

MOTION	TYPE MOTION	INITIAL RELEASE CRITERION	FINAL RELEASE CRITERION
0	UNRESTRICTED	—	—
1	PIVOT; PITCH ONLY	$\Delta\theta_R$	$R_{P,z}$
2	PIVOT; PITCH AND YAW	$\Delta\theta_R$	$R_{P,z}$
3	PIVOT; PITCH, YAW, ROLL	$\Delta\theta_R$	$R_{P,z}$
4	RAIL; TRANSLATE ONLY	$x_{P,1}$	$x_{P,1}$
5	RAIL; TRANSLATE AND PITCH	$x_{P,1}$	$x_{P,2}$
6	RAIL; TRANSLATE AND YAW	$x_{P,1}$	$x_{P,2}$
7	RAIL; TRANSLATE, PITCH AND YAW	$x_{P,1}$	$x_{P,2}$
8	TRANSLATE, ROTATE IN EJECTOR PLANE	EJECT	EJECT

PIVOT MOTION (OPTIONS 1,2,3)

RESTRICTION: $Y_0 \equiv 0$

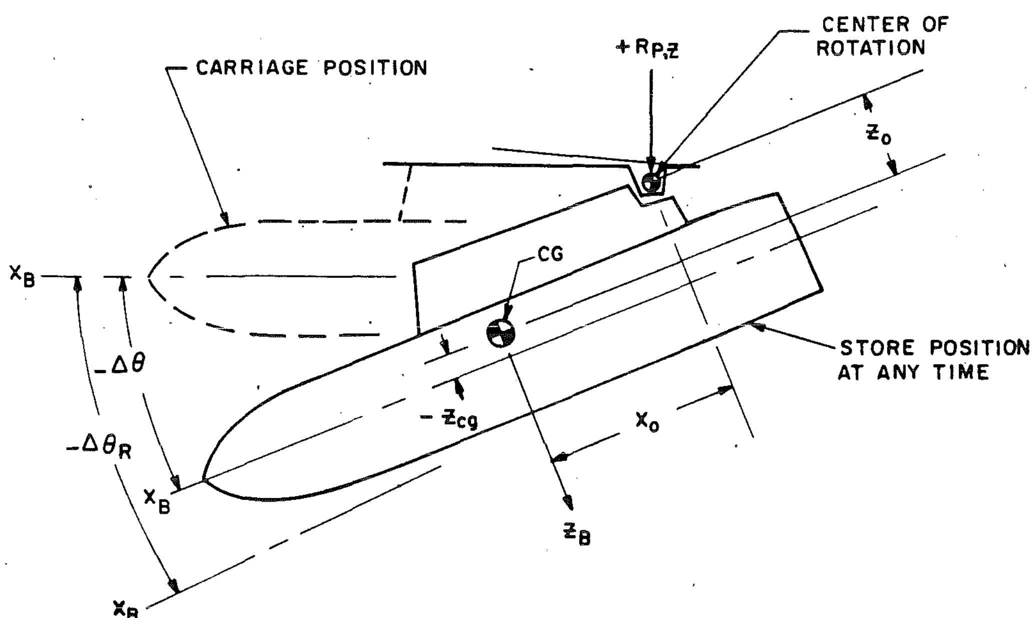

RELEASE CRITERIA

INITIAL IF $(\Delta\theta - \Delta\theta_R) < 0$, CHECK $R_{P,z}$

FINAL IF $R_{P,z} \leq 0$, GO TO UNRESTRICTED MOTION

a. Pivot motion (options 1 through 3)

Figure I-3. Graphic descriptions of staged release options.

RESTRICTIONS: 4 NONE
5 SIDE RAIL ONLY ($Z_o \equiv 0$)
6 BOTTOM RAIL ONLY ($Y_o \equiv 0$)
7 SIDE OR BOTTOM RAIL (Z_o OR Y_o MUST $\equiv 0$)

NOTES: a) OPTIONS 4→7, TRANSLATE ONLY FOR AFT HOOK TRAVEL LESS THAN $X_{P,1}$
b) OPTIONS 5→7, ANGULAR MOTION (AS DESCRIBED) IN ADDITION TO TRANSLATION FOR AFT HOOK TRAVEL GREATER THAN $X_{P,1}$ BUT LESS THAN $X_{P,2}$
c) UNRESTRICTED MOTION FOR AFT HOOK TRAVEL GREATER THAN $X_{P,1}$ (OPTION 4), GREATER THAN $X_{P,2}$ (OPTIONS 5→7)

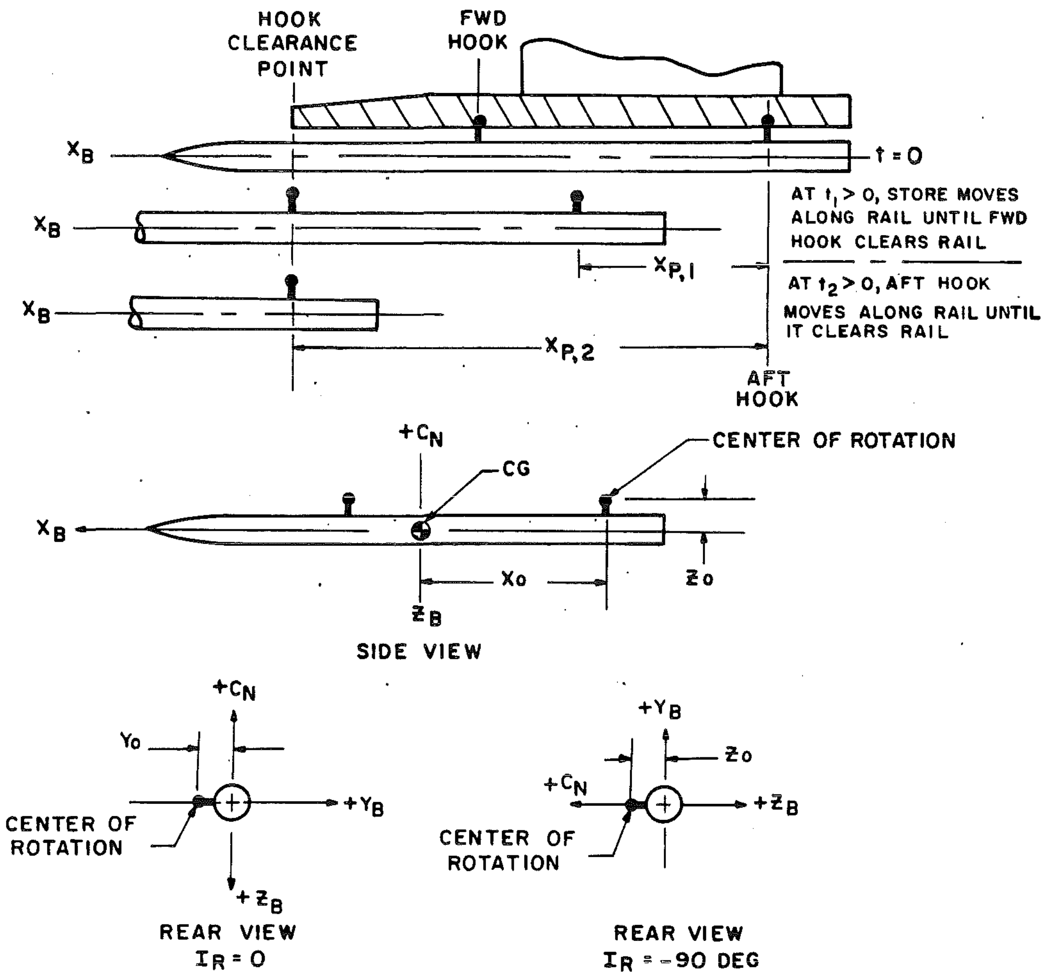

b. Rail motion (options 4 through 7)
Figure I-3. Continued.

TRANSLATE, ROTATE ONLY IN PLANE OF EJECTORS (OPTION 8)

ASSUMPTION: MOTION ABOUT cg, NO INERTIA TRANSFER REQ'D
RESTRICTION: $I_{XY} = I_{XZ} = I_{YZ} \equiv 0$

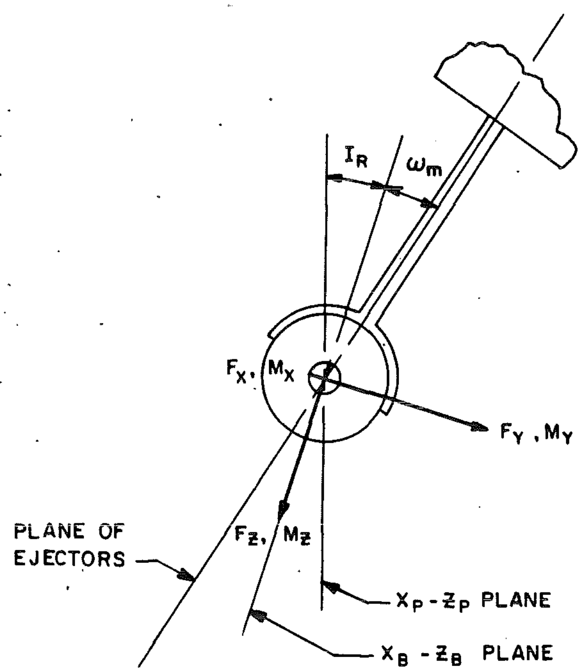

STORE IS RESTRAINED TO TRANSLATION AND ROTATION IN THE PLANE OF THE EJECTORS DURING EJECTOR ACTION

RELEASE CRITERIA: IF EJECT = 0, GO TO UNRESTRAINED MOTION

c. Ejector plane motion
Figure I-3. Concluded.

APPENDIX J
OUTPUT PROCESSING EQUATIONS

Calculate Store Coordinates With Respect to the Flight-Axis System Origin (See Fig. 10).

$$\theta_p = q_p\,(t)\,57.2958$$

For unaccelerated flight ($\theta_p = 0$)

$$X_t = X_I$$

$$Y_t = Y_I$$

$$Z_t = Z_I$$

For accelerated flight ($\theta_p \neq 0$)

$$\left[AA\right] = \text{TME}\,(0, -\theta_p, 0, 2)$$

$$X_C = X_I + R_p \sin\theta_p + U_A\, t$$

$$Y_C = Y_I$$

$$Z_C = Z_I - R_p\,(1 - \cos\theta_p)$$

$$\begin{vmatrix} X_t \\ Y_t \\ Z_t \end{vmatrix} = \left[AA\right]' \begin{vmatrix} X_C \\ Y_C \\ Z_C \end{vmatrix}$$

Calculate Store Attitude With Respect to the Free-stream Wind Vector (See Fig. 15).

$$\nu_t = \nu_I + \tan^{-1}\left[\dot{Z}_I / (\dot{X}_I + U_A)\right]$$

$$\eta_t = \eta_I - \tan^{-1}\left\{\dot{Y}_I \Big/ \left[(\dot{X}_I + U_A)\cos\nu_I - \dot{Z}_I \sin\nu_I\right]\right\}$$

$$\omega_t = \omega_I$$

APPENDIX K
CTS CLOSED-LOOP POSITIONING MODULE EQUATIONS

The flow diagram for the CTS closed-loop positioning module is shown in Fig. K-1, and the equations used for calculating CTS rig coordinates and attitudes follow.

CTS Rig Angles* (Section A)

$$[AA] = \text{TME}\ (\nu_t, \eta_t, 0, 1)$$

Store attitude with respect to free-stream wind vector

$$[BB] = \text{TME}\ (\Delta\nu, \Delta\eta, 0, 1)$$

$$[DD] = [BB]'[AA]$$

Account for deflections

$$[BB] = \text{TME}\ (\psi_S, \theta_S, 0, 2)$$

$$[CC] = [BB]'[DD]$$

Account for sting bend angles

$$\eta_R = \sin^{-1}\left[CC\ (1,2)\right]$$

$$\nu_R = \sin^{-1}\left[-CC\ (1,3)/\cos\eta_R\right]$$

$$\omega_R = \omega_t - \Delta\omega$$

CTS rig angles in pitch, yaw, roll sequence

CTS Rig Linear Coordinates† (Section B)

$$[AA] = \text{TME}\ (\nu_t, \eta_t, \omega_t, 1)$$

$$\begin{vmatrix} \Delta X_{R,1} \\ \Delta Y_{R,1} \\ \Delta Z_{R,1} \end{vmatrix} = [AA]' \begin{vmatrix} 0 \\ Y_m \\ Z_m \end{vmatrix}$$

*See Fig. 15.

†See Figs. A-1 and A-2.

$$[AA] = \text{TME}\ (\nu_R,\ \eta_R,\ 0,\ 1)$$

$$[BB] = \text{TME}\ (\psi_S,\ \theta_S,\ 0,\ 2)$$

$$[CC] = [BB]\,[AA]$$

$$\begin{vmatrix} \Delta X_{R,2} \\ \Delta Y_{R,2} \\ \Delta Z_{R,2} \end{vmatrix} = [CC]' \begin{vmatrix} 0 \\ 0 \\ -d_R \end{vmatrix}$$

$$\begin{vmatrix} \Delta X_{R,3} \\ \Delta Y_{R,3} \\ \Delta Z_{R,3} \end{vmatrix} = [AA]' \begin{vmatrix} \ell_{1,R} \\ 0 \\ 0 \end{vmatrix}$$

$$[BB] = \text{TME}\ (\psi_S,\ 0,\ 0,\ 2)$$

$$[CC] = [BB]\,[AA]$$

$$\begin{vmatrix} \Delta X_{R,4} \\ \Delta Y_{R,4} \\ \Delta Z_{R,4} \end{vmatrix} = [CC]' \begin{vmatrix} 0 \\ -\ell_{2,R} \\ 0 \end{vmatrix}$$

$$[AA] = \text{TME}\ (\nu_R,\ 0,\ 0,\ 1)$$

$$\begin{vmatrix} \Delta X_{R,5} \\ \Delta Y_{R,5} \\ \Delta Z_{R,5} \end{vmatrix} = [AA]' \begin{vmatrix} 3 \\ 0 \\ 0 \end{vmatrix}$$

$$\left.\begin{aligned} \Delta X_R &= \sum_{n=1}^{5} \Delta X_{R,n} \\ \Delta Y_R &= \sum_{n=1}^{5} \Delta Y_{R,n} \\ \Delta Z_R &= \sum_{n=1}^{5} \Delta Z_{R,n} \end{aligned}\right\} \quad \text{Distance from CTS pitch center to store cg}$$

$$\left.\begin{aligned} X_{t,R} &= X_t\,(12\lambda) \\ Y_{t,R} &= Y_t\,(12\lambda) \\ Z_{t,R} &= Z_t\,(12\lambda) \end{aligned}\right\} \quad \textbf{Convert from ft, full scale, to in., model scale}$$

$$\left.\begin{aligned} X_R &= X_{TP,o} - \Delta X_R - \Delta X_L + X_{t,R} \\ Y_R &= Y_{TP,o} - \Delta Y_R - \Delta Y_L + Y_{t,R} + \Delta Y_C \\ Z_R &= Z_{TP,o} - \Delta Z_R - \Delta Z_L + Z_{t,R} + \Delta Z_C \end{aligned}\right\} \quad \text{CTS rig coordinates}$$

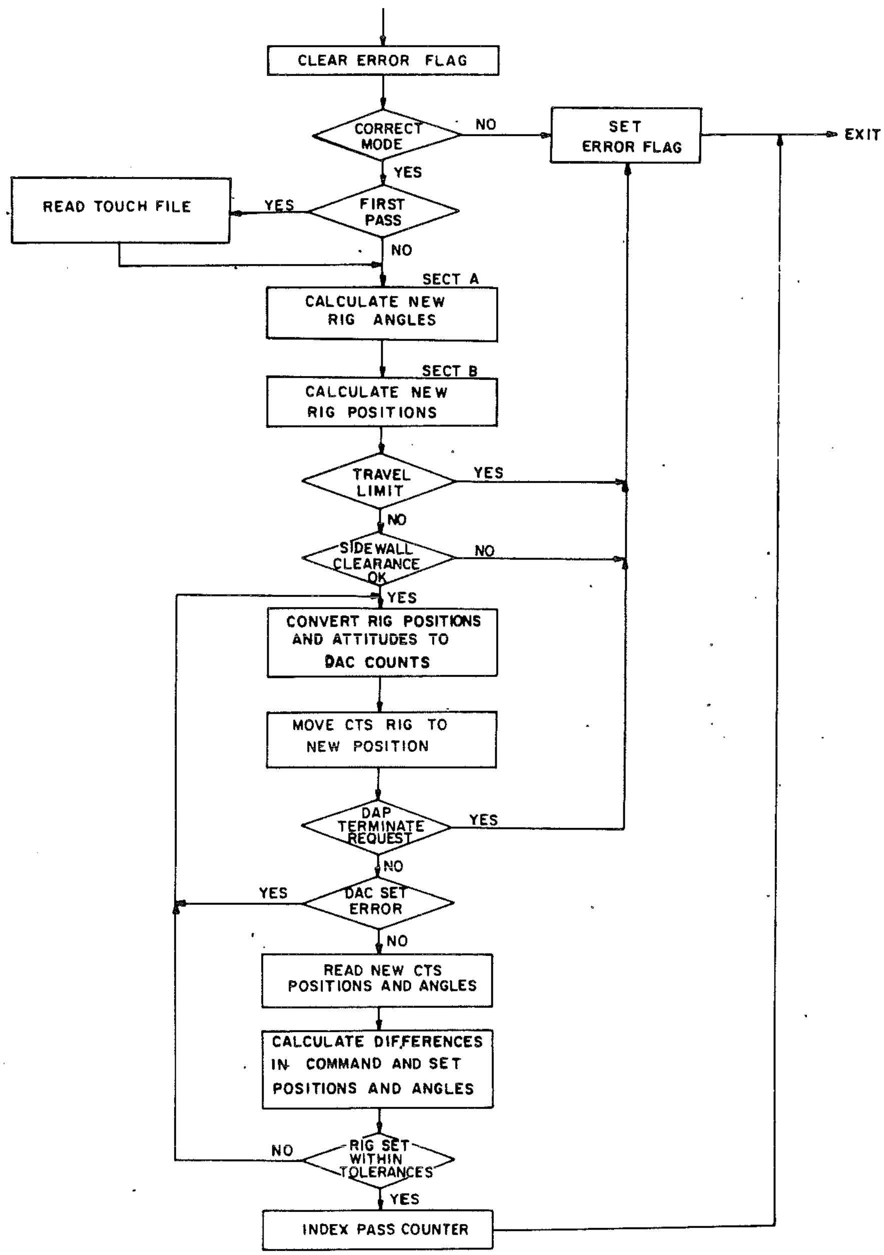

NOTE: ERROR FLAG ≡ TRAVEL LIMIT IN FLOW DIAGRAM OF TRAJECTORY GENERATION CLOSED-LOOP PROGRAM

Figure K-1. Flow diagram of the CTS closed-loop positioning module.

APPENDIX L
NONROLLING STING APPLICATIONS

For trajectory tests which use a nonrolling sting support, roll commands which are generated in the simulation obviously cannot be executed by the CTS rig. Therefore, if not restrained in some manner, the simulated roll position (as determined from trajectory calculations) and actual model roll position could possibly digress to a point where trajectory results are not representative. For the Tunnel 4T trajectory program, the restraint chosen was to set the simulated roll position equal to the actual model roll position for the pass through the conversion module of the trajectory equations made just after input processing. For stores with similar planforms in the X_B-Z_B and X_B-Y_B planes, application of this restriction would probably have only minor effects on the trajectory outcome since the roll attitude would not be expected to significantly affect aerodynamic loading. For stores with dissimilar planforms in the X_B-Z_B and X_B-Y_B planes, effects of this restriction on trajectory results are potentially more significant since aerodynamic loading would be expected to change with roll attitude. Equations used to apply this restraint are listed as follows:

NONROLL	Options
0	Roll capability
1	No roll capability, set simulated roll position equal to actual model roll position each pass through the conversion module after input processing
2	Same as option 1, but use instead for 0– or 6–in. offset roll mechanisms with no roll capacity to impose additional sting moment limitations
3	Same as option 1 except set $C_{\ell,T} = 0$ in trajectory calculations

Calculate Roll Position As Set

$$[AA] = TME(\nu_R, \eta_R, 0, 1)$$

$$[BB] = TME(\psi_S, \theta_S, 0, 2)$$

$$[DD] = [BB][AA]$$

$$[BB] = TME(\Delta\nu, \Delta\eta, 0, 1)$$

$$[AA] = [BB][DD]$$

$$\omega_{TR} = \tan^{-1}\left[-AA(3,2)/AA(2,2)\right]$$

Calculate Difference Between Actual and Simulated Roll (Euler Sequence)

$$[RO] = [TOBODY][AA]'$$

$$\Delta\phi_{TR} = \tan^{-1}\left[RO(2,3)/RO(3,3)\right]$$

Calculate Roll Difference (Pitch, Yaw, Roll Sequence)

$$\Delta\omega_{TR} = |\omega_I - \omega_{TR}|$$

If any of following checks is true, bypass the remainder of the calculations.

If $(\Delta\omega_{TR} < 0.25)$

If $(NPASS \leq 5)$

If $(ROLFLG = 1)$[1]

If not, continue:

Set Simulated Roll Equal to Actual Model Roll

$$\omega_I = \omega_{TR}$$

Update Inertial-to-Body Matrix

$$[TOBODY] = TME\ (\nu_I, \eta_I, \omega_I, 1)$$

$$\phi_I = \tan^{-1}\left[TOBODY\ (2,3)/TOBODY\ (3,3)\right]$$

Update Integrator Outputs

P11 = TOBODY (2,1)

P12 = TOBODY (3,1)

P14 = TOBODY (2,2)

P15 = TOBODY (3,2)

P17 = TOBODY (2,3)

P18 = TOBODY (3,3)

[1]The flag (ROLFLG) is set equal to one after the pass through the trajectory calculations in input processing and is set equal to zero just after the pass counter is updated in output processing. This procedure prevents the integrator outputs from being manipulated when the trajectory modules are called during the integration process.

APPENDIX M
MATRIX DEFINITIONS

Notation of Terms

$$[a] = \begin{bmatrix} a(1,1) & a(1,2) & a(1,3) \\ a(2,1) & a(2,2) & a(2,3) \\ a(3,1) & a(3,2) & a(3,3) \end{bmatrix}$$

For Pitch, Yaw, Roll Sequence

$$\text{TME}\,(\alpha, \alpha_1, \alpha_2, 1) = \begin{bmatrix} \cos\alpha \cos\alpha_1 & \sin\alpha_1 & -\sin\alpha \cos\alpha_1 \\ \begin{matrix}\sin\alpha_2 \sin\alpha \\ -\cos\alpha_2 \cos\alpha \sin\alpha_1\end{matrix} & \cos\alpha_2 \cos\alpha_1 & \begin{matrix}\cos\alpha_2 \sin\alpha \sin\alpha_1 \\ +\cos\alpha \sin\alpha_2\end{matrix} \\ \begin{matrix}\sin\alpha_2 \cos\alpha \sin\alpha_1 \\ +\cos\alpha_2 \sin\alpha\end{matrix} & -\sin\alpha_2 \cos\alpha_1 & \begin{matrix}\cos\alpha_2 \cos\alpha \\ -\sin\alpha_2 \sin\alpha_1 \sin\alpha\end{matrix} \end{bmatrix}$$

For Euler Sequence

$$\text{TME}\,(\alpha, \alpha_1, \alpha_2, 2) = \begin{bmatrix} \cos\alpha \cos\alpha_1 & \cos\alpha_1 \sin\alpha & -\sin\alpha_1 \\ \begin{matrix}\sin\alpha_2 \sin\alpha_1 \cos\alpha \\ -\cos\alpha_2 \sin\alpha\end{matrix} & \begin{matrix}\sin\alpha_2 \sin\alpha_1 \sin\alpha \\ +\cos\alpha_2 \cos\alpha\end{matrix} & \sin\alpha_2 \cos\alpha_1 \\ \begin{matrix}\cos\alpha_2 \sin\alpha_1 \cos\alpha \\ +\sin\alpha_2 \sin\alpha\end{matrix} & \begin{matrix}\cos\alpha_2 \sin\alpha_1 \sin\alpha \\ -\sin\alpha_2 \cos\alpha\end{matrix} & \cos\alpha_2 \cos\alpha_1 \end{bmatrix}$$

NOMENCLATURE

A, A_m	Store full-scale and model-scale reference areas, respectively, ft^2
A/C	Aircraft model designation
a_n, b_n	Fifth-order polynomial curve fit coefficient values which define the thrust force as a function of time (see Appendix F)
$a_{o,X}, a_{o,Y}, a_{o,Z}$	Accelerations of the store rotation center (if not coincident with the mass center), positive in the positive X_B, Y_B, and Z_B directions, respectively, ft/sec^2
a_X, a_Y, a_Z	Accelerations of the store mass center, positive in the positive X_B, Y_B, and Z_B directions, respectively, ft/sec^2
$a_{Z,p}$	Acceleration of the aircraft in the Z_F direction, ft/sec^2 (see Fig. 10)
BPYLON	Notation for the matrix (3x3) which converts pylon-axis quantities to body-axis quantities
$C_{A,o}, C_{N,o}, C_{Y,o}$	Current values of the external input axial-force, normal-force, and side-force coefficients, respectively
$(C_{A,o})_o, (C_{N,o})_o, (C_{Y,o})_o$	Initial values of the external input axial-force, normal-force, and side-force coefficients, respectively
$(C_{A,o})_{max}$	Maximum value of the external input axial-force coefficient for ramp axial-force coefficient calculations (see Appendix D)
$C_{A,t}, C_N, C_Y$	Store measured axial-force, normal-force, and side-force coefficients, positive in the negative X_B, negative Z_B, and positive Y_B directions, respectively
$C_{A,t,T}, C_{N,T}, C_{Y,T}$	Sum of the aerodynamic force coefficient contributions acting on the full-scale store, positive in the negative X_B, negative Z_B, and positive Y_B directions, respectively (see Appendix E)
$C_{A,t,x}, C_{N,x}, C_{Y,x}$	Extrapolated (or measured) values of the axial-force, normal-force, and side-force coefficients, respectively
$C_{jd_\ell}, C_{jd_m}, C_{jd_n}$	Jet roll-damping, pitch-damping, and yaw-damping coefficients, respectively, ft-sec

C_ℓ, C_m, C_n	Store measured rolling-moment, pitching-moment, and yawing-moment coefficients, respectively; the positive vectors are coincident with the positive X_B, Y_B, and Z_B directions
$C_{\ell,o}, C_{m,o}, C_{n,o}$	Current values of the external input rolling-moment, pitching-moment, and yawing-moment coefficients, respectively
$(C_{\ell,o})_o, (C_{m,o})_o, (C_{n,o})_o$	Initial values of the external input rolling-moment, pitching-moment, and yawing-moment coefficients, respectively
$C_{\ell_p}, C_{m_q}, C_{n_r}$	Store roll-damping, pitch-damping, and yaw-damping derivatives, respectively, per radian
$C_{\ell,T}, C_{m,T}, C_{n,T}$	Sum of the aerodynamic moment coefficient contributions acting on the full-scale store; the positive vectors are coincident with the positive X_B, Y_B, and Z_B axes, respectively (see Appendix E)
$C_{\ell,x}, C_{m,x}, C_{n,x}$	Extrapolated (or measured) values of the rolling-moment, pitching-moment, and yawing-moment coefficients, respectively
ΔC_N	Difference in successively measured values of normal-force coefficient
COEF,COEFI	Current and initial values of the offset coefficient module control flag
CONFIG	Aircraft model configuration designation
CON SET	Run/point number of constants set used in data reduction
$C_{p,\epsilon}$	Difference in pressure coefficient between probe orifices 1 and 3, positive for positive ϵ, $(p_{s,1} - p_{s,3})/q_L$
$C_{p,\sigma}$	Difference in pressure coefficient between probe orifices 2 and 4, positive for positive σ, $(p_{s,4} - p_{s,2})/q_L$
C_{1B}, C_{2B}	Break points for forward and aft ejector force polynomial curve fits, respectively, sec or ft (see Appendix G)
c_n, d_n	Fifth-order polynomial curve fit coefficient values which define the forward ejector force as a function of time or stroke, sec or ft (see Appendix G)
DATE	Calendar time at which data were recorded

$dC_{A,o}/dt$	Slope of the external input axial-force coefficient for ramp axial-force coefficient calculations (see Appendix D)
d_R	Vertical offset of the CTS support sting, in. (see Fig. A-2)
EE	Notation for the matrix (3x3) which converts flight-axis quantities to body-axis quantities
EJECT,EJECTI	Current and initial values of the ejector module control flag
E1FLAG,E2FLAG	Forward and aft ejector cutoff control flags, respectively
e_n,f_n	Fifth-order polynomial curve fit coefficient values which define the aft ejector force as a function of time or stroke, sec or ft (see Appendix G)
$F_{A,g},F_{N,g},$ $F_{Y,g}$	Total forces measured by the store balance, positive in the negative X_B, negative Z_B, and positive Y_B directions, respectively, lb
$F_{A,t},F_N,F_Y$	Measured aerodynamic forces acting on the store model, positive in the negative X_B, negative Z_B, and positive Y_B directions, respectively,lb
$F_{E,X},F_{E,Y},$ $F_{E,Z}$	Components of the ejector force acting on the store, positive in the positive X_B, Y_B, and Z_B directions, respectively, lb
F_{E1},F_{E2}	Forward and aft ejector forces, respectively, lb
$F_{T,X},F_{T,Y},$ $F_{T,Z}$	Components of the thrust force acting on the store, positive in the positive X_B, Y_B, and Z_B directions, respectively, lb
F_X,F_Y,F_Z	Components of total force acting on a free-falling store, positive in the positive X_B, Y_B, and Z_B directions, respectively, lb
f	Notation for derivatives stored in the derivative history file (see Fig. 11)
g	Acceleration of gravity, ft/sec^2
H_X,H_Y,H_Z	Components of the angular momentum; the positive vectors are coincident with the positive X_B, Y_B, and Z_B axes, respectively, ft-lb-sec
h	Simulated pressure altitude, ft
I	Notation for the inertia matrix of a store which is calculated about the mass center (see Appendix I)

I^{-1}	Notation for the inverse of the inertia matrix (I)
$\bar{I}$	Notation for the inertia matrix of a store which is calculated about a point (rotation center) other than the mass center (see Appendix I)
$\bar{I}^{-1}$	Notation for the inverse of the inertia matrix($\bar{I}$)
I_P, I_Y	Pitch and yaw incidence angles of the store longitudinal axis at carriage with respect to the aircraft longitudinal axis, positive nose up and nose to the right, respectively, as seen by the pilot, deg
I_R	Roll incidence of the store Z_B axis at carriage with respect to the aircraft plane of symmetry, positive for clockwise roll looking upstream, deg
ITR	Number of iterations in the flow-field calculations required for the difference in successive calculations of θ_T to be less than 0.1 deg
I_{XX}, I_{YY}, I_{ZZ}	Full-scale moments of inertia about the store X_B, Y_B, and Z_B axes, respectively, slug-ft^2, and referenced to the store mass center
$\bar{I}_{XX}, \bar{I}_{YY}, \bar{I}_{ZZ}$	Full-scale moments of inertia about the store X_B, Y_B, and Z_B directions, respectively, slug-ft^2, but referenced to a point (rotation center) other than the mass center
I_{XY}, I_{XZ}, I_{YZ}	Full-scale products of inertia in the store X_B-Y_B, X_B-Z_B, and Y_B-Z_B planes, respectively, slug-ft^2, and referenced to the store mass center
$\bar{I}_{XY}, \bar{I}_{XZ}, \bar{I}_{YZ}$	Full-scale products of inertia in the store X_B-Y_B, X_B-Z_B, and Y_B-Z_B planes, respectively, slug-ft^2, but referenced to a point (rotation center) other than the mass center
K_{int}, X_{int}	Current and initial values of the parameter which determines the number of integrator passes per data cycle
KPASS	Multiple-pass integration counter
$K_{Y,Y}, K_{Y,n}$	Linear deflection constants of the store model support sting in the Y_B direction and measured at the balance center, in./lb and in./in.-lb, respectively

$K_{Z,N}, K_{Z,m}$	Linear deflection constants of the store model support sting in the Z_B direction and measured at the balance center, in./lb and in./in.-lb, respectively
$K_{\alpha,N}, K_{\alpha,m}$	Angular deflection constants of the store model support sting in the X_B-Z_B plane, deg/lb and deg/in.-lb, respectively
$K_{\phi,\ell}$	Angular deflection constant of the store model support sting in the Y_B-Z_B plane, deg/in.-lb
$K_{\psi,Y}, K_{\psi,n}$	Angular deflection constants of the store model support sting in the X_B-Y_B plane, deg/lb and deg/in.-lb, respectively
k_λ	Store model scaling change factor (normally equals 1)
LW,RW	Wing identification print control constants
ℓ_1, ℓ_2, ℓ_3	Store full-scale reference dimensions for pitching-moment, yawing-moment, and rolling-moment coefficients, respectively, ft
$\ell_{1,m}, \ell_{2,m}, \ell_{3,m}$	Store model-scale reference dimensions for pitching-moment, yawing-moment, and rolling-moment coefficients, respectively, in.
$\ell_{1,R}, \ell_{2,R}, \ell_{3,R}$	Physical dimensions of the CTS support sting used in model positioning and clearance calculations, in. (see Fig. A-2)
M_B	Nominal test Mach number
$M_{E,X}, M_{E,Y}, M_{E,Z}$	Components of ejector moment; the positive vectors are coincident with the positive X_B, Y_B, and Z_B axes, respectively, ft-lb
M_L	Local Mach number calculated from probe $\bar{p}_5$ measurements
M_ℓ, M_m, M_n	Measured aerodynamic moments acting on the store model; the positive vectors are coincident with the positive X_B, Y_B, and Z_B directions, respectively, in.-lb
$M_{\ell,g}, M_{m,g}, M_{n,g}$	Total moments measured by the store balance; the positive vectors are coincident with the positive X_B, Y_B, and Z_B axes, respectively, in.-lb
MODE	Parameter which defines type of CTS operation
MOTION, HOLDI	Current and initial values of staged separation control parameter

$M_{T,X}, M_{T,Y}, M_{T,Z}$	Components of the thrust moment acting on the store; the positive vectors are coincident with the positive X_B, Y_B, and Z_B axes, respectively, ft-lb
M_X, M_Y, M_Z	Components of the total moment acting on a free-falling body; the positive vectors are coincident with the positive X_B, Y_B, and Z_B axes, respectively, ft-lb
M_∞	Wind tunnel free-stream Mach number
m	Store mass, slugs
NDX	Sequential indexing number for referencing data obtained during a grid set; indexes for each position in the set
NOROLL	CTS rig roll control parameter
NPASS	Integrator pass counter
NX	Number of extrapolators
NXP	Extrapolator pass counter
N_Z	Aircraft "g"-loading factor
$P, P1 \rightarrow P50$	Integrator output designation
$\dot{P}, \dot{P1} \rightarrow \dot{P50}$	Integrator input designation
PASS	Data cycle pass counter
PN	Data point number
POST	Launch/postlaunch control parameter
p,q,r	Store angular velocity about the X_B, Y_B, and Z_B axes, respectively; the positive vectors are coincident with the positive X_B, Y_B, and Z_B axes, rad/sec
p_A	Static pressure at the simulated altitude, psfa
p_o, q_o, r_o	Initial values of the store angular velocity about the X_B, Y_B, and Z_B axes, respectively, rad/sec
$p_{s,1} \rightarrow p_{s,4}, p_{p,5}$	Measured pressures for probe orifices 1 through 5, respectively, psfa

p_t	Wind tunnel total pressure, psfa
$p_{t,p}$	Probe measured free-stream total pressure corrected for local Mach number, psfa
p_∞	Wind tunnel free-stream static pressure, psfa
$\bar{p}_5$	Ratio of the average of the four static pressures and the probe total pressure, $(p_{s,1} + p_{s,2} + p_{s,3} + p_{s,4})/4(p_{p,5})$
$\bar{p}_{5,p}$	$\bar{p}_5$ ratio corrected for probe attitude, equivalent value for $\theta_T = 0$
q_A	Dynamic pressure at the simulated altitude, psf
q_L	Local dynamic pressure, psf (from probe measurements)
q_p	Pitch rate of the aircraft during a pullup/pushover maneuver, rad/sec (see Fig. 10)
q_∞	Wind tunnel free-stream dynamic pressure, psf
Re_∞	Wind tunnel free-stream unit Reynolds number, millions per ft
R_ℓ, R_m, R_n	Full-scale body-axis restraining moments about the pivot (rotation center); the positive vectors are coincident with the positive X_B, Y_B, and Z_B directions, respectively, ft-lb
ROLFLG	Roll simulation control parameter (see Appendix L)
$R_{P,\ell}, R_{P,m}, R_{P,n}$	Full-scale pylon-axis pivot (rotation center) restraining moments; the positive vectors are coincident with the positive X_P, Y_P, and Z_P directions, respectively, ft-lb
$R_{P,X}, R_{P,Y}, R_{P,Z}$	Full-scale pylon-axis pivot (rotation center) restraining forces, positive in the positive X_P, Y_P, and Z_P directions, lb
R_p	Effective rotation arm of the aircraft during a pullup/pushover maneuver, ft (see Fig. 10)
RUN	Data set identification number
R_X, R_Y, R_Z	Full-scale body-axis pivot (rotation center) restraining forces, positive in the positive X_B, Y_B, and Z_B directions, lb
$\delta R_1, \delta R_5$	Differential balance readings because of model weight at wind-off conditions for balance gages 1 and 5, counts

SH	Wind tunnel specific humidity, lbm H_2O per lbm air
STEP,STEPI	Current and initial values of the data cycle/integration interval increase control parameter
STORE	Store model designation
SURVEY	Configuration indexing number used to correlate data with the test log; survey may be used to identify all or portion of a grid set
T_A	Static temperature at the simulated altitude, °R
T_{DP}	Wind tunnel dewpoint temperature, °R
TEST	Alphanumeric notation for referencing a specific test program in a specific test unit
THRUST,THRSTI	Current and initial values of the thrust module control flag
TIME	Time at which data were recorded (hr/min/sec)
TOBODY,$TOBODY_o$	Notation for current and initial values of the matrix (3x3) which converts inertial-axis quantities to body-axis quantities
TRAJ	Number which identifies a particular set of trajectory constants/test conditions
T_t	Wind tunnel total temperature, °R
T_∞	Wind tunnel free-stream static temperature, °R
t	Trajectory time from the instant of store release from the aircraft, sec
Δt	Data acquisition time increment, sec
δt	Trajectory integration time increment, sec
t_{COF}	Time delay before initiation of the external input ramp axial force, sec (see Appendix D)
t_D	Time delay before initiation of the thrust force, sec (see Appendix F)
t_{DEL}	Internally calculated time delay parameter, sec
t_o	Initial value of trajectory time, sec

t_t	Time from thrust initiation, sec
$t_{t,C1}, t_{t,C2}$	Thrust module event designation parameters, sec (see Appendix F)
t_2	Break point for thrust force polynomial curve fits, sec (see Appendix F)
U_A	Velocity of the aircraft at the simulated altitude, ft/sec
U_R	Total velocity of the full-scale store with respect to a space-fixed point, ft/sec
u,v,w	Velocities of the full-scale store relative to the origin of the flight-axis system, positive in the positive X_B, Y_B, and Z_B directions, respectively, ft/sec
u_B, v_B, w_B	Velocities of the hook (rotation center) relative to the origin of the flight-axis system, positive in the positive X_B, Y_B, and Z_B directions, respectively, ft/sec
u_o, v_o, w_o	Initial values of the velocity of the full-scale store relative to the origin of the flight-axis system, positive in the positive X_B, Y_B, and Z_B directions, respectively, ft/sec
V_L	Local velocity, ft/sec (from probe measurements)
V_X, V_Y, V_Z	Velocity components relative to a space-fixed axis and parallel to the X_B, Y_B, and Z_B axes, positive in the $-X_B$, Y_B, and $-Z_B$ directions, respectively, ft/sec
V_{XY}, V_{XZ}, V_{YZ}	Velocity components relative to a spaced-fixed axis in the body-axis X_B-Y_B, X_B-Z_B, and Y_B-Z_B planes, respectively, ft/sec
$V_{Z,p}$	Velocity of the aircraft in the Z_F direction, ft/sec
V_∞	Wind tunnel free-stream velocity, ft/sec
$v_{o,X}, v_{o,Y}, v_{o,Z}$	Components of rotation center velocity, positive in the positive X_B, Y_B, and Z_B directions, respectively, ft/sec
W_A, W_N, W_Y	Model weight tares along the X_B, Z_B, and Y_B axes, respectively, lb
WING	Location of store launch position
Wt	Store full-scale weight, lb

W'_X, W'_Y, W'_Z	Components of the full-scale store weight, positive in the positive X_I, Y_I, and Z_I directions, respectively, lb
$\overline{W}_X, \overline{W}_Y, \overline{W}_Z$	Components of the full-scale store weight, positive in the positive X_B, Y_B, and Z_B directions, respectively, lb (including effects of simulated dive or bank angles)
X, Y, Z	Separation distance of the store cg from the flight-axis system origin in the positive X_F, Y_F, and Z_F directions, respectively, ft, full scale
ΔX_{AE}	Distance between forward and aft ejector pistons, ft, full scale
X_{BF}	Distance from the store model nose to the balance face, in.
X_C, Y_C, Z_C	Separation distance of the store cg from the flight-axis system origin in the positive X_I, Y_I, and Z_I directions, respectively, ft, full scale
X_{cg}	Axial distance from the store nose to the cg location, ft, full scale
X_{E1}, X_{E2}	Full-scale distances from store center of gravity to line of action of forward and aft ejector forces measured along X_B axis, positive if force is forward of center of gravity, ft, full scale
X_{FE}	Axial distance from the store nose to the forward ejector piston, ft, full scale
X_I, Y_I, Z_I	Separation distance of the store cg from the inertial-axis system origin in the positive X_I, Y_I, and Z_I, directions, respectively, ft, full scale
$X_{I,o}, Y_{I,o}, Z_{I,o}$	Positions of the store cg with respect to the carriage position at trajectory initiation, positive in the positive X_I, Y_I, and Z_I directions, respectively, ft, full scale
$\Delta X_L, \Delta Y_L, \Delta Z_L$	Linear deflections of the CTS model support sting, positive in the positive X_I, Y_I, and Z_I directions, respectively, in.
X_m	Axial distance from the store nose to the cg location, in., model scale
$\Delta X_{m,cg}, \Delta X_{n,cg}$	Axial distances from the store center of gravity to the pitching-moment and yawing-moment reference centers, respectively, positive in the positive X_B direction, ft, full scale

$X_{m,ec}, X_{n,ec}$	Axial distances from the balance face to the balance electrical center in the pitch and yaw planes, respectively, in.
$X_{m,t}, X_{n,t}$	Axial distances from the balance electrical center to the store pitching-moment and yawing-moment reference centers, respectively, positive in the positive X_B direction, in., model scale
X_o, Y_o, Z_o	Distances from the pivot (rotation center) to the store center of gravity along the X_B, Y_B, and Z_B axes, respectively, positive in the positive X_B, Y_B, and Z_B directions, ft, full scale
X_P, Y_P, Z_P	Separation distances of the store cg from the pylon-axis system origin in the positive X_P, Y_P, and Z_P directions, respectively, ft, full scale
$X_{P,CK}$	Translation of the store hook from the carriage position in the X_P direction, ft, full scale
$X_{PITC}, Y_{PITC}, Z_{PITC}$	Physical dimensions of the CTS support sting, in. (see Fig. A-2)
$X_{P,1}$	For restricted motion, distance store must travel along rail in a translate-only mode, ft, full scale
$X_{P,2}$	For restricted motion, distance aft hook must travel along rail before becoming free of rail, ft, full scale
X_R, Y_R, Z_R	Positions of the CTS pitch center with respect to its midpoint of travel, positive in the positive X_t, Y_t, and Z_t directions, respectively, in.
$\Delta X_R, \Delta Y_R, \Delta Z_R$	Distances (excluding deflections) from the CTS pitch center to the store cg, positive in the positive X_t, Y_t, and Z_t directions, respectively, in.
$X_{REF}, Y_{REF}, Z_{REF}$	Positions of the store cg with respect to the reference-axis system origin in the X_{REF}, Y_{REF}, and Z_{REF} directions, respectively, ft, full scale
X_t, Y_t, Z_t	Separation distances of the store cg from the flight-axis system origin, positive in the positive X_t, Y_t, and Z_t directions, respectively, ft, full scale

$X_{TP,o}, Y_{TP,o}$ $Z_{TP,o}$	Distances from the midpoint of CTS pitch center travel to the store cg at carriage, positive in the positive X_t, Y_t, and Z_t directions, respectively
X_l, Y_l, Z_l	Distances from the lanyard attachment point on the aircraft to the store cg at carriage, positive in the positive X_B, Y_B, and Z_B directions, respectively, ft, full scale
$\bar{x}_m, \bar{x}_n$	Axial distances from the balance electrical center to the model mass center in the pitch and yaw planes, respectively, in., positive in the positive X_B direction
Y_{cg}, Z_{cg}	Full-scale lateral and vertical distances from the balance axis to the store cg, respectively, ft, positive in the positive Y_B and Z_B directions
$\Delta Y_c, \Delta Z_c$	Input constants used to modify touch point coordinates in the lateral and vertical directions, respectively, in.
Y_m, Z_m	Lateral and vertical distances from the balance axis to the store cg, respectively, in., model scale, positive in the positive Y_B and Z_B directions
Y_{TP}	Touch point value in the lateral direction, counts
$\bar{y}, \bar{z}$	Lateral and vertical distances from the balance electrical center to the model mass center, respectively, in., positive in the positive Y_B and Z_B directions
ZERO SET	Run/point number of the air-off set of instrument readings used in data reduction
Z_{E1}, Z_{E2}	Input values of stroke length (or time of action) of the forward and aft ejectors, respectively, sec or ft
Z_L	Input value of lanyard length, ft
$Z_{L,C}$	Current value of straight-line distance between lanyard attachment points on store and aircraft, ft
ZSTEP	Input value of lanyard length at which the data cycle/integration time interval increase option is exercised, ft
$Z_{T,C}$	Thrust module event designation parameter, ft (see Appendix F)

Z_{1C}, Z_{2C}	Ejector module event designation parameters, sec or ft (see Appendix G)
Z_{1E}, Z_{2E}	Current values of stroke length (or time of action) of forward and aft ejectors, respectively, sec or ft
α, β	Aircraft model angle of attack and sideslip angle relative to the free-stream velocity vector, respectively, deg
α_s, β_s	Store model angle of attack and sideslip angle relative to the free-stream velocity vector, respectively, deg
α_{TP}	Aircraft angle-of-attack value recorded in the touch point file, deg
$\alpha_{XY}, \alpha_{XZ}, \alpha_{YZ}$	Sidewash, upwash, and crossflow angles with respect to the store longitudinal axis, respectively positive inboard (left wing), up, and clockwise (from $-Z_B$ axis) as seen by the pilot, deg
γ	Simulated aircraft dive angle, positive for decreasing altitude, deg
ϵ	Indicated angle (in pitch; calculated using $C_{p,\epsilon}$) between the projection of the local flow velocity vector onto the probe X_B-Z_B plane and the probe X_B axis, positive for a velocity vector component in the negative Z_B direction, deg
η	Angle between the store longitudinal axis and its projection in the X_F-Z_F plane, positive when the store nose is to the right as seen by the pilot, deg
$\Delta\eta$	Angle between the store longitudinal axis and its projection in the X_P-Z_P plane, positive when the store nose is to the right as seen by the pilot, deg
η_I	Angle between the store longitudinal axis and its projection in the X_I-Z_I plane, positive when the store nose is to the right as seen by the pilot, deg
$\eta_{I,o}$	Initial input angle between the store longitudinal axis and its projection in the X_I-Z_I plane, positive when the store nose is to the right as seen by the pilot, deg (postlaunch only)
η_o	Initial calculated angle between the store longitudinal axis and its projection in the X_I-Z_I plane, positive when the store nose is to the right as seen by the pilot, deg

η_R — CTS rig yaw angle, deg

η_t — Angle between the store longitudinal axis and its projection in the X_t-Z_t plane, positive when the store nose is to the right as seen by the pilot, deg

θ — Angle between the store longitudinal axis and its projection in the X_F-Y_F plane, positive when the store nose is raised as seen by the pilot, deg

$\Delta\theta$ — Angle between the store longitudinal axis and its projection in the X_P-Y_P plane, positive when the store nose is raised as seen by the pilot, deg

$\Delta\theta_{CK}$ — Value of $\Delta\theta$ during pivot restrained motion, deg (see Appendix I)

θ_I — Angle between the store longitudinal axis and its projection in the X_I-Y_I plane, positive when store nose is raised as seen by the pilot, deg

θ_p — Rotation angle of the aircraft (flight-axis system) during a pullup/pushover maneuver, deg (see Fig. 10)

$\Delta\theta_R$ — For restricted motion, pitch angle through which store must rotate before release, deg

θ_S — Prebend angle of the CTS support sting in the pitch plane, deg

θ_T — Angle between the local flow velocity vector and the negative X_B axis, deg

λ — Aircraft model scale factor

ν — Angle between the projection of the store longitudinal axis in the X_F-Z_F plane and the X_F axis, positive when the store nose is raised as seen by the pilot, deg

$\Delta\nu$ — Angle between the projection of the store longitudinal axis in the X_P-Z_P plane and the X_P axis, positive when the store nose is raised as seen by the pilot, deg

ν_I — Angle between the projection of the store longitudinal axis in the X_I-Z_I plane and the X_I axis, positive when the store nose is raised as seen by the pilot, deg

$\nu_{I,o}$	Initial input angle between the projection of the store longitudinal axis in the X_I-Z_I plane and the X_I axis, positive when the store nose is raised as seen by the pilot, deg (postlaunch only)
ν_o	Initial calculated angle between the projection of the store longitudinal axis in the X_I-Z_I plane and the X_I axis, positive when the store nose is raised as seen by the pilot, deg
ν_R	CTS rig pitch angle, deg
ν_t	Angle between the projection of the store longitudinal axis in the X_t-Z_t plane and the X_t axis, positive when the store nose is raised as seen by the pilot, deg
ϱ_A	Density at the simulated altitude, slug/ft^3
σ	Indicated angle (in yaw; calculated using $C_{p,\sigma}$) between the projection of the local flow velocity vector onto the probe X_B-Y_B plane and the probe X_B axis, positive for a velocity-vector component in the positive Y_B direction, deg
ϕ	Angle between the store lateral (Y_B) axis and the intersection of the Y_B-Z_B and X_F-Y_F planes, positive clockwise looking upstream, deg
$\Delta\phi$	Angle between the store lateral (Y_B) axis and the intersection of the Y_B-Z_B and X_P-Y_P planes, positive clockwise looking upstream, deg
$\phi_{A/C}$	Simulated aircraft bank (roll) angle, positive clockwise looking upstream, deg
ϕ_I	Angle between the store lateral (Y_B) axis and the intersection of the Y_B-Z_B and X_I-Y_I planes, positive clockwise looking upstream, deg
ϕ_S	Separation model roll orientation with respect to the X_B-Z_B plane, positive clockwise looking upstream, deg
$\Delta\phi_{T\ R}$	For nonrolling sting applications, the calculated angle between the true and simulated roll orientation in the Euler sequence, deg (see Appendix L)
ψ	Angle between the projection of the store longitudinal axis in the X_F-Y_F plane and the X_F axis, positive when the store nose is to the right as seen by the pilot, deg

$\Delta\psi$	Angle between the projection of the store longitudinal axis in the X_P-Y_P plane and the X_P axis, positive for store nose to the right as seen by the pilot, deg
ψ_I	Angle between the projection of the store longitudinal axis in the X_I-Y_I plane and the X_I axis, positive for store nose to the right as seen by the pilot, deg
ψ_S	Prebend angle of the CTS support sting in the yaw plane, deg
ω	Angle between the store vertical (Z_B) axis and the intersection of the Y_B-Z_B and X_F-Z_F planes, positive for clockwise rotation when looking upstream, deg
$\Delta\omega$	Angle between the store vertical (Z_B) axis and the intersection of the Y_B-Z_B and X_P-Z_P planes, positive for clockwise rotation when looking upstream, deg
ω_I	Angle between the store vertical (Z_B) axis and the intersection of the Y_B-Z_B and X_I-Z_I planes, positive clockwise looking upstream, deg
$\omega_{I,o}$	Initial input angle between the store vertical (Z_B) axis and the intersection of the Y_B-Z_B and X_I-Z_I planes, positive for clockwise rotation when looking upstream, deg (postlaunch only)
ω_m	Angle of the simulated ejector force with respect to the store X_B-Z_B plane, deg
ω_o	Initial calculated angle between the store vertical (Z_B) axis and the intersection of the Y_B-Z_B and X_I-Z_I planes, positive for clockwise rotation when looking upstream, deg
ω_R	CTS rig roll angle, deg
$\Delta\omega_{TR}$	For nonrolling sting applications, the calculated angle between the true and simulated roll orientation for a pitch, yaw, roll sequence, deg (see Appendix L)
ω_t	Angle between the store vertical (Z_B) axis and the intersection of the Y_B-Z_B and X_t-Z_t planes, positive for clockwise rotation when looking upstream, deg
$(\ )_i$	Represents the ith point

$(\dot{\ })$ A single dot denotes the first derivative of a parameter with respect to time

INERTIAL-AXIS SYSTEM DEFINITIONS

Coordinate Directions

X_I Parallel to the aircraft flight path direction at store release, positive forward as seen by the pilot

Y_I Perpendicular to the X_I and Z_I directions, positive to the right as seen by the pilot

Z_I Parallel to the aircraft plane of symmetry and perpendicular to the aircraft flight path direction at store release, positive downward as seen by the pilot

Origin

The inertial-axis system origin is coincident with the store cg at release and translates along the initial aircraft flight path direction at the free-stream velocity. The coordinate axes do not rotate with respect to the initial aircraft flight path direction.

FLIGHT-AXIS SYSTEM DEFINITIONS

Coordinate Directions

X_F Parallel to the current aircraft flight path direction, positive forward as seen by the pilot

Y_F Perpendicular to the X_F and Z_F directions, positive to the right as seen by the pilot

Z_F Parallel to the aircraft plane of symmetry and perpendicular to the current aircraft flight path direction, positive downward as seen by the pilot

Origin

The flight-axis system origin is coincident with the store cg at release. The origin is fixed with respect to the aircraft and thus translates along the current aircraft flight path at the free-stream velocity. The coordinate axes rotate to maintain alignment of the X_F axis with the current aircraft flight path direction.

PYLON-AXIS SYSTEM DEFINITIONS

Coordinate Directions

X_P	Parallel to the store longitudinal axis at release and at constant angular orientation with respect to the current aircraft flight path direction, positive forward as seen by the pilot
Y_P	Perpendicular to the X_P direction and parallel to the X_F-Y_F plane, positive to the right as seen by the pilot
Z_P	Perpendicular to the X_P and Y_P directions, positive downward as seen by the pilot

Origin

The pylon-axis system origin is coincident with the flight-axis system origin and the store cg at release. It is fixed with respect to the aircraft and thus translates along the current aircraft flight path at the free-stream velocity. The coordinate axes rotate to maintain constant angular orientation with respect to the current aircraft flight path direction.

STORE BODY-AXIS SYSTEM DEFINITIONS

Coordinate Directions

X_B	Parallel to the store longitudinal axis, positive direction is upstream at store release
Y_B	Perpendicular to X_B and Z_B directions, positive to the right looking upstream when the store is at zero yaw and roll angles
Z_B	Perpendicular to the X_B direction and parallel to the aircraft plane of symmetry when the store and aircraft are at zero yaw and roll angles, positive downward as seen by the pilot when the store is at zero pitch and roll angles

Origin

The store body-axis system origin is coincident with the store cg at all times. The X_B, Y_B, and Z_B coordinate axes rotate with the store in pitch, yaw, and roll so that mass moments of inertia about the three axes are not time-varying quantities.

TUNNEL-AXIS SYSTEM DEFINITIONS

Coordinate Directions

X_t	Parallel to the tunnel centerline, positive direction is upstream
Y_t	Perpendicular to the X_t direction and parallel to the tunnel top and bottom walls, positive to the left when looking upstream.
Z_t	Perpendicular to the X_t and Y_t directions, positive up

Origin

The tunnel-axis system origin is located on the tunnel centerline at the midpoint of axial travel of the CTS pitch center (Tunnel Station 133.26)

AIRCRAFT-AXIS SYSTEM DEFINITIONS

Coordinate Directions

X_A	Parallel to the aircraft longitudinal axis at store release and at constant angular orientation with respect to the current aircraft flight path direction, positive forward as seen by the pilot
Y_A	Perpendicular to the X_A direction and parallel to the X_F-Y_F plane, positive to the right as seen by the pilot
Z_A	Perpendicular to the X_A and Y_A directions, positive downward as seen by the pilot

Origin

The aircraft-axis system origin is coincident with the flight-axis system origin and the store cg at release. It is fixed with respect to the aircraft and thus translates along the current aircraft flight path at the free-stream velocity. The coordinate axes rotate to maintain constant angular orientation with respect to the current aircraft flight path direction.

REFERENCE-AXIS SYSTEM DEFINITIONS

The reference-axis system is a right-hand, orthogonal coordinate system whose coordinate directions (X_{REF}, Y_{REF}, and Z_{REF}) and origin may be arbitrarily selected on a test-by-test basis. The most common alignment of the coordinate directions is parallel to the pylon- or aircraft-axis system coordinate directions, and the most common origin locations are coincident with the store cg at carriage or at the aircraft fuselage station, waterline, and buttock line zero location.